

QUALITY PARAMETER MODELS FOR STRATIFIED  
IMPOUNDMENTS

By

PRASERT CHUAPHANICH

Bachelor of Engineering  
Chulalongkorn University  
Bangkok, Thailand  
1969

Master of Science  
Oklahoma State University  
Stillwater, Oklahoma  
1972

Submitted to the Faculty of the Graduate College  
of the Oklahoma State University  
in partial fulfillment of the requirements  
for the Degree of  
DOCTOR OF PHILOSOPHY  
May, 1975

MAY 12 1976

QUALITY PARAMETER MODELS FOR STRATIFIED  
IMPOUNDMENTS

Thesis Approved:

*Richard N. DeVries*  
\_\_\_\_\_  
Thesis Adviser

*Don F. Kincannon*  
\_\_\_\_\_

*D. F. Maudy Jr.*  
\_\_\_\_\_

*Robert D. Morrison*  
\_\_\_\_\_

*Charles E. Rice*  
\_\_\_\_\_

*D. D. Stanton*  
\_\_\_\_\_

Dean of the Graduate College

938884

## ACKNOWLEDGEMENTS

I would like to express my sincere indebtedness to Dr. Richard N. DeVries, my major adviser, for his valuable advice and constant encouragement throughout my duration of graduate studies and during the preparation of this thesis.

My deep appreciation is also extended to Dr. Robert D. Morrison, Dr. Don F. Kincannon, Dr. Anthony F. Gaudy, Jr., and Dr. Charles E. Rice, members of the advisory committee, for their valuable suggestions during the course of study and their careful evaluation of this manuscript.

Special thanks are extended to the Royal Thai Government for her financial assistance during my graduate studies, and to Mrs. Janet Sallee for her careful typing of this manuscript.

Finally, to my wife, Chanpen, for her constant love and patience, who not only helped with the preparation of this manuscript, but also made many sacrifices without uttering a discouraging word throughout, and to my parents in Thailand for their continuous affectionate concern and encouragement, the author cannot thank them sufficiently.

This work was supported in part by the Oklahoma Water Resources Research Institute project A-058, and the Oklahoma State University, College of Engineering's System Science Center.

## TABLE OF CONTENTS

Chapter	Page
I. INTRODUCTION. . . . .	1
A. Introduction . . . . .	1
B. Objectives of the Study. . . . .	5
II. LITERATURE REVIEW . . . . .	6
A. Temperature Model. . . . .	6
B. Water Quality Model. . . . .	18
III. THEORETICAL CONSIDERATIONS. . . . .	24
A. Classification of Reservoirs . . . . .	24
B. Reservoir Hydrodynamics. . . . .	26
1. Temperature Stratification Mechanics. . . . .	28
2. Reservoir Currents. . . . .	29
3. Withdrawal Layer Thickness. . . . .	33
4. Factors Influencing Water Quality . . . . .	35
C. General Governing Equations. . . . .	37
IV. DEVELOPMENT OF THE MODELS . . . . .	41
A. Development and Solution of the Temperature Model. . . . .	41
1. Schematization of the Reservoir . . . . .	43
2. Determination of Parameters . . . . .	46
3. Derivation of Governing Equations . . . . .	57
4. Solution of the Temperature Model . . . . .	60
B. Development and Solution of Water Quality Model. . . . .	69
1. Determination of Parameters . . . . .	71
2. Derivation of Governing Equations . . . . .	74
3. Solution of the Water Quality Model . . . . .	76
C. Application of the Models. . . . .	84
V. RESULTS . . . . .	86
A. Description of Reservoir . . . . .	86

TABLE OF CONTENTS (Continued)

Chapter	Page
B. Inputs to the Mathematical Models . . . . .	86
C. Results of the Temperature Model . . . . .	89
D. Results of the Water Quality Model . . . . .	100
VI. DISCUSSION. . . . .	124
A. The Temperature Model. . . . .	124
B. The Water Quality Model. . . . .	126
VII. CONCLUSIONS . . . . .	131
VIII. SUGGESTIONS FOR FUTURE STUDY. . . . .	133
SELECTED BIBLIOGRAPHY . . . . .	134
APPENDIX A. . . . .	140
APPENDIX B. . . . .	149
APPENDIX C. . . . .	152
APPENDIX D. . . . .	154

LIST OF TABLES

Table	Page
I. Reservoir Classifications and Froude Numbers. . . . .	27
II. Effects of Mixing Coefficients on Outflow Temperatures. . .	99
III. Effects of Mixing Coefficients on Outflow D.O. Concentra- tions for $D.O._{sur} = 0.8 D.O._{sat}$ . . . . .	150
IV. Effects of Mixing Coefficients on Outflow D.O. Concentra- tions for $D.O._{sur} = D.O._{sat}$ . . . . .	151

## LIST OF FIGURES

Figure	Page
1. Graphical Temperature Prediction Model of Wunderlich. . . . .	10
2. Graphical D.O. Prediction Model of Wunderlich . . . . .	23
3. Three Basic Types of Inflows. . . . .	31
4. Idealization of a Reservoir Water Body. . . . .	44
5. Control Volumes for Mass and Heat Balance . . . . .	45
6. Dye Concentration Profiles in Fontana Reservoir . . . . .	53
7. Conservation of Heat of the Surface Layer . . . . .	62
8. Conservation of Heat of the Internal Element. . . . .	65
9. Conservation of Heat of the Bottom Layer. . . . .	67
10. Control Volume for Dissolved Oxygen Balance . . . . .	72
11. Conservation of BOD of the Surface Layer. . . . .	78
12. Conservation of D.O. of the Internal Element. . . . .	80
13. Conservation of D.O. of the Bottom Layer. . . . .	83
14. Map of Fontana Reservoir and Watershed. . . . .	87
15. Measured and Predicted Temperature Profiles, Fontana Reservoir, April 27, 1966. . . . .	91
16. Measured and Predicted Temperature Profiles, Fontana Reservoir, June 22, 1966 . . . . .	92
17. Measured and Predicted Temperature Profiles, Fontana Reservoir, July 20, 1966 . . . . .	93
18. Measured and Predicted Temperature Profiles, Fontana Reservoir, August 17, 1966 . . . . .	94
19. Measured and Predicted Temperature Profiles, Fontana Reservoir, September 15, 1966. . . . .	95

LIST OF FIGURES (Continued)

Figure	Page
20. Measured and Predicted Temperature Profiles, Fontana Reservoir, October 26, 1966. . . . .	96
21. Measured and Predicted Temperature Profiles, Fontana Reservoir, November 16, 1966 . . . . .	97
22. Outflow Temperatures for Fontana Reservoir, 1966. . . . .	98
23. D.O. Profiles for $k_1 = 0.10 \text{ Day}^{-1}$ , Constant $\text{BOD}_{in}$ , Fontana Reservoir, April 20, 1966 . . . . .	101
24. D.O. Profiles for $k_1 = 0.10 \text{ Day}^{-1}$ , Constant $\text{BOD}_{in}$ , Fontana Reservoir, May 20, 1966 . . . . .	102
25. D.O. Profiles for $k_1 = 0.10 \text{ Day}^{-1}$ , Constant $\text{BOD}_{in}$ , Fontana Reservoir, July 19, 1966. . . . .	103
26. D.O. Profiles for $k_1 = 0.10 \text{ Day}^{-1}$ , Constant $\text{BOD}_{in}$ , Fontana Reservoir, August 12, 1966. . . . .	104
27. D.O. Profiles for $k_1 = 0.10 \text{ Day}^{-1}$ , Constant $\text{BOD}_{in}$ , Fontana Reservoir, September 7, 1966. . . . .	105
28. D.O. Profiles for $k_1 = 0.10 \text{ Day}^{-1}$ , Constant $\text{BOD}_{in}$ , Fontana Reservoir, October 3, 1966. . . . .	106
29. D.O. Profiles for $k_1 = 0.10 \text{ Day}^{-1}$ , Constant $\text{BOD}_{in}$ , Fontana Reservoir, November 29, 1966. . . . .	107
30. Outflow D.O. Concentrations for $k_1 = 0.10 \text{ Day}^{-1}$ , Constant $\text{BOD}_{in}$ , Fontana Reservoir, 1966. . . . .	108
31. D.O. Profiles for $k_1 = 0.10 \text{ Day}^{-1}$ , Variable $\text{BOD}_{in}$ , Fontana Reservoir, September 7, 1966. . . . .	109
32. D.O. Profiles for $k_1 = 0.10 \text{ Day}^{-1}$ , Variable $\text{BOD}_{in}$ , Fontana Reservoir, October 3, 1966. . . . .	110
33. D.O. Profiles for $k_1 = 0.10 \text{ Day}^{-1}$ , Variable $\text{BOD}_{in}$ , Fontana Reservoir, November 29, 1966. . . . .	111
34. Effect of Inflow $\text{BOD}_{in}$ on the Outflow D.O. Concentrations for $k_1 = 0.10 \text{ Day}^{-1}$ , Fontana Reservoir, 1966. . . . .	112



LIST OF FIGURES (Continued)

Figure	Page
35. D.O. Profiles for $k_1 = 0.10 \text{ Day}^{-1}$ , $D.O._{sur} = 0.8 D.O._{sat}$ , Fontana Reservoir, September 7, 1966. . . . .	113
36. D.O. Profiles for $k_1 = 0.10 \text{ Day}^{-1}$ , $D.O._{sur} = 0.8 D.O._{sat}$ , Fontana Reservoir, October 3, 1966. . . . .	114
37. D.O. Profiles for $k_1 = 0.10 \text{ Day}^{-1}$ , $D.O._{sur} = 0.8 D.O._{sat}$ , Fontana Reservoir, November 29, 1966. . . . .	115
38. Effect of Surface Boundary Condition for D.O. on Outflow D.O. Concentrations for $k_1 = 0.10 \text{ Day}^{-1}$ , Fontana Reser- voir, 1966. . . . .	116
39. D.O. Profiles for $k_1 = 0.10 \text{ Day}^{-1}$ , $D.O._{sur} = 0.6 D.O._{sat}$ , Fontana Reservoir, September 7, 1966. . . . .	117
40. D.O. Profiles for $k_1 = 0.10 \text{ Day}^{-1}$ , $D.O._{sur} = 0.6 D.O._{sat}$ , Fontana Reservoir, October 3, 1966. . . . .	118
41. D.O. Profiles for $k_1 = 0.10 \text{ Day}^{-1}$ , $D.O._{ur} = 0.6 D.O._{sat}$ , Fontana Reservoir, November 29, 1966. . . . .	119
42. Effect of Surface Boundary Condition for D.O. on Outflow D.O. Concentrations for $k_1 = 0.10 \text{ Day}^{-1}$ , Fontana Reser- voir, 1966. . . . .	120
43. D.O. Profiles for $k_1 = 0.05 \text{ Day}^{-1}$ , Constant $BOD_{in}$ , Fontana Reservoir, May 20, 1966 . . . . .	141
44. D.O. Profiles for $k_1 = 0.05 \text{ Day}^{-1}$ , Constant $BOD_{in}$ , Fontana Reservoir, July 19, 1966. . . . .	142
45. D.O. Profiles for $k_1 = 0.05 \text{ Day}^{-1}$ , Constant $BOD_{in}$ , Fontana Reservoir, August 12, 1966. . . . .	143
46. D.O. Profiles for $k_1 = 0.05 \text{ Day}^{-1}$ , Constant $BOD_{in}$ , Fontana Reservoir, September 7, 1966. . . . .	144
47. D.O. Profiles for $k_1 = 0.05 \text{ Day}^{-1}$ , Constant $BOD_{in}$ , Fontana Reservoir, October 3, 1966. . . . .	145
48. Outflow D.O. Concentrations for $k_1 = 0.05 \text{ Day}^{-1}$ , Constant $BOD_{in}$ , Fontana Reservoir, 1966. . . . .	146

LIST OF FIGURES (Continued)

Figure	Page
49. D.O. Profiles for $k_1 = 0.05 \text{ Day}^{-1}$ , Variable $\text{BOD}_{in}$ , Fontana Reservoir, October 3, 1966 . . . . .	147
50. Effect of Inflow $\text{BOD}_1$ on the Outflow D.O. Concentrations for $k_1 = 0.05 \text{ Day}^{-1}$ , Fontana Reservoir, 1966 . . . . .	148

## CHAPTER I

### INTRODUCTION

#### A. Introduction

The effects of reservoir impoundment on water quality have been under investigation for many years (10,27,53), and there are still many unanswered questions and challenging problems to be solved. The first step in the development of a mathematical model to predict the influence of reservoir hydrodynamics on water quality is the understanding of the essential processes when the hydrodynamics of the reservoir is governed by thermal stratification. The basic laws governing the movements of water in stratified bodies of water have been known for some time (25, 72). However, it was not until recent years that, with the growing interest in water quality management, the application of these laws to specific problems became necessary.

The dominant quality factors that control the hydrodynamics of a reservoir are water temperature and temperature-related water quality constituents. Considerable progress has been made in understanding the mechanics of reservoir stratification, but a great deal of development is still required for an adequate solution of water resource development problems involving reservoir stratification. The prediction of such changes in a reservoir and in its discharge is important in the planning, design, and operation stages of any project which must meet water quality requirements. Optimal use of water can be achieved only if the various

processes influencing water quality are understood.

The operation of multipurpose reservoirs and the need to predict changes in water quality in the planning stage of proposed reservoirs requires the knowledge of the processes to which the natural water is subjected after entering an impoundment (71). The construction of a large reservoir on a river and thermal energy sources can induce major changes in the hydrodynamic behavior of the water environment within the reservoir and in the river downstream and, consequently, in its quality (10). Changes that occur, either in the temperature of the water or in temperature-related water quality constituents, may importantly affect beneficial uses to be served. These changes reflect modifications of the physical, chemical, and biological systems and hydraulic factors which are associated with the change in depth, surface area, reservoir operation, hydrology of the drainage basin, and the reduction of velocity.

The primary causes of the thermal stratification process are the low thermal conductivity of water, the limited penetration of radiant heat and light, surface cooling by evaporation and conduction, and the convective transfer of inflows and outflows. Thermal stratification occurs in almost all lakes and reservoir impoundments. It may assume many patterns, dependent on geometry of the reservoir, geographical location, reservoir operation and climatological conditions. In shallow reservoirs, the stratification may be relatively weak and in certain seasons the isotherms tend to be tilted in the downstream direction. In deep reservoirs in which the storage volume is large compared to the annual throughflow, the isotherms are horizontal during most of the year and strong stratification may develop during certain seasons.

The problem of predicting the variation of temperature and concentration of a particular water quality parameter at any point within a stratified reservoir and in the outlet is difficult because of the complexity of the mechanisms which govern heat and mass transfer within a waterbody and heat and mass transfer between the waterbody and its surrounding environment. Many water quality factors other than temperature are important in a reservoir. The majority of these are affected by the distribution, dilution, and detention time in the reservoir. Principal factors are seasonal variation, the quality of inflowing water, flow rate, thermal stratification, chemical and biological activities in the impounded water, and the decomposition of organic debris. The traditional methods of analysis, in which the concentration is assumed to depend on only the longitudinal coordinate, is inappropriate in a stratified reservoir because the localized horizontal currents may restrict the particular water quality parameter to a certain level within the reservoir for a long period of time.

A primary consideration in water quality of a reservoir is the dissolved oxygen within the reservoir because the ecological balance in a reservoir is very sensitive to dissolved oxygen levels. The dissolved oxygen is not only essential to the aquatic life, but also a good indicator of the overall quality of water and the degree of the presence of pollutants which utilize oxygen. The usefulness of lakes or impoundments can be substantially reduced by the depletion of dissolved oxygen from the deeper portions of these water bodies. In addition, when water containing low D.O. (dissolved oxygen) concentration is released from the impoundments, it may harm the receiving streams.

The amount of dissolved oxygen in a reservoir depends on numerous

physical and biological factors which include convective transport by internal current, atmospheric reaeration at the surface, photosynthetic oxygen sources associated with plant life, oxygen demands of river inflows, bottom deposits, respiration and decomposition of aquatic organisms. Under thermally stratified conditions, the surface layer, called "epilimnion," is often rich in oxygen while the lower layers, called "hypolimnion," are often deficient in oxygen because the oxygen demand of internal organic material exceeds the oxygen transfer from the surface layer. This can lead to anaerobic conditions and low water quality and, during the overturn, the mixing of this bottom water with the rest of the reservoir may pollute all of the water in the reservoir for a short period of time.

The biological and mass transfer processes are sensitive to temperature and thus the oxygen balance will depend on the thermal structure of the reservoir. For these reasons, some techniques are necessary for predicting the thermal profiles and the quality of water within the reservoir and the temperature and quality of water in the outlet for water quality control, proper design of the outlet works and a systematic approach to water quality management. At the present state of the art, the most effective approach to the design of the reservoirs for quality control is to specify reservoir characteristics, the operation of the reservoir and output requirements and, then, simulate to examine the results. To do this, it is necessary to construct a mathematical model or models based on reasonable assumptions and simple enough for application purposes.

## B. Objectives of the Study

The primary objective of this study is to develop mathematical models for deep lakes or reservoirs in which the storage volume is large compared to the annual throughflow, the isotherms are horizontal during most of the year, and strong stratification is developed during certain seasons. The models developed will use only data that is available before the reservoir exists, and will be able to predict temperature variation and concentration distribution of a particular pollutant in a stratified reservoir, and also the outflow temperature and concentration of the particular pollutant. The specific objectives of the study can be stated as follows:

- 1) to develop a mathematical model to predict internal temperature distributions in a horizontally stratified reservoir and the outflow temperature,

- 2) to develop a mathematical model which will be coupled with the temperature model to predict the variation of concentration distribution of dissolved oxygen in a horizontally stratified reservoir and the outflow dissolved oxygen.

In the following chapter, there is a review of literature about the temperature and water quality models. Some theoretical considerations concerned with the classification of reservoirs and reservoir hydrodynamics will be covered in Chapter III. In the fourth chapter, the temperature and water quality models will be developed, and the results will be presented in Chapter V. Following in Chapters VI, VII, and VIII, are the discussion of the results, conclusions, and recommendations for future work.

## CHAPTER II

### LITERATURE REVIEW

#### A. Temperature Model

Mathematical representation of the physics of the reservoir thermal problems was early attempted by Hutchinson (27), who computed heat transfer coefficients from assumed temperature profiles in lakes. The early effort identified the thermocline as limiting the transfer of energy into the water body. Munk and Anderson (36) suggested that relative changes in the mixing properties of water masses could be made functions of fluid density which, in turn, could be related to thermal energy levels. Dutton and Bryson (18), who considered the unsteady development of the temperature distribution in Lake Mendota, assumed that vertical thermal eddy diffusivity is independent of depth. To agree with measured temperature data, they found it necessary to assign values of eddy diffusivity to the epilimnion that were fifty times greater than for the hypolimnion. As pointed out by the authors, this method is unsatisfactory because of the assumption of constant eddy diffusivity in the basic development. However, none of these early studies took complete account of the coupling of hydrometeorological phenomena controlling the disposition of energy at the water surface with the mechanisms that are responsible for distributing energy internally throughout the fluid mass.

Raphael (45), et al. were among the first who proposed a practical means of linking energy relationships to impoundments. He presented a



procedure applying the energy budget equation to predict the temperatures in reservoirs from the inflow and outflow characteristics, the surface area and volume of the reservoirs, and meteorological records. The method is applicable to any reservoirs in which temperatures are essentially uniform. The mathematical representation of the rate of change of temperatures in reservoirs can be expressed as

$$\frac{dt_w}{d\theta} = \frac{Q_t A + m_i (t_i - t_w)}{m_w} \quad (2.1)$$

in which

$m_w$  = mass of water in the reservoir

$t_w$  = mean temperature of water in the reservoir

$m_i$  = mass of inflowing water

$t_i$  = temperature of inflowing water

$A$  = surface area of the reservoir

$Q_t$  = total surface heat transfer per unit of time acting on the entire surface area,  $A$

$\theta$  = time

The energy budget for any body of water is expressed in the following form:

$$Q_t = Q_s - Q_r - Q_b - Q_h - Q_e \quad (2.2)$$

where

$Q_s$  = solar radiation incident to water surface

$Q_r$  = reflected solar radiation

$Q_b$  = back radiation

$Q_h$  = the energy conducted from the body of water to the atmosphere

$Q_e$  = energy used for evaporation

The method developed is based on the assumption that the temperature of water in the reservoir is uniform, and mass outflow is very small in comparison with mass of the water in the reservoir. Because of the limiting assumptions, the model can be applied to only shallow reservoirs with uniform temperatures--not to deep reservoirs with thermal stratification.

Elder and Wunderlich (22) also proposed a mathematical model for predicting temperature of water in a fully mixed reservoir. The model is similar to that of Raphael (45), but it was written in differential form and each term was made consistent in units. The model can be expressed as

$$\frac{\partial \theta}{\partial t} + u \frac{\partial \theta}{\partial x} = \frac{q_H}{\rho C Y_0} \quad (2.3)$$

where

$\theta$  = water temperature in the reservoir

$t$  = time

$u$  = flow velocity

$x$  = distance in flow direction

$q_H$  = heat exchange per unit area and unit time through the water surface

$\rho$  = density of water

$C$  = specific heat of water

$Y_0$  = mean depth of water body

Orlob (39) proposed a mathematical model for predicting water temperatures in reservoirs based on the Fickian laws of diffusion. The model was developed in discretized form and assuming that the diffusion coefficient is a function of depth below the reservoir surface. His model leads to values of eddy diffusivity at a depth of 100 meters, which is of the order of 1600 times the molecular diffusivity.

Wunderlich (67) developed a graphical temperature prediction model based on simplified assumptions of flow in stratified reservoirs. The assumptions were:

- 1) the water temperature is assumed to be the only factor responsible for the density of the water;

- 2) it is assumed that on January 1 the reservoir is thermally homogeneous;

- 3) the surface temperature can be computed from meteorological data and is assumed to correspond to the equilibrium temperature of a well-exposed body of water;

- 4) the inflowing water, upon its arrival in the reservoir, spreads out over the whole horizontal area corresponding to its own temperature level;

- 5) there is no mixing between inflow water and reservoir water,

- 6) the temperature in the outlet corresponds to the temperature at the level of the outlet.

The graphical scheme is outlined in Figures 1a and 1b. The method starts with the plotting of the monthly mean values of inflow temperature and reservoir surface temperatures for the year under investigation and connected by a continuous curve as shown in Figure 1a.

Referring to Figure 1b, the integrated inflow volume curve is drawn

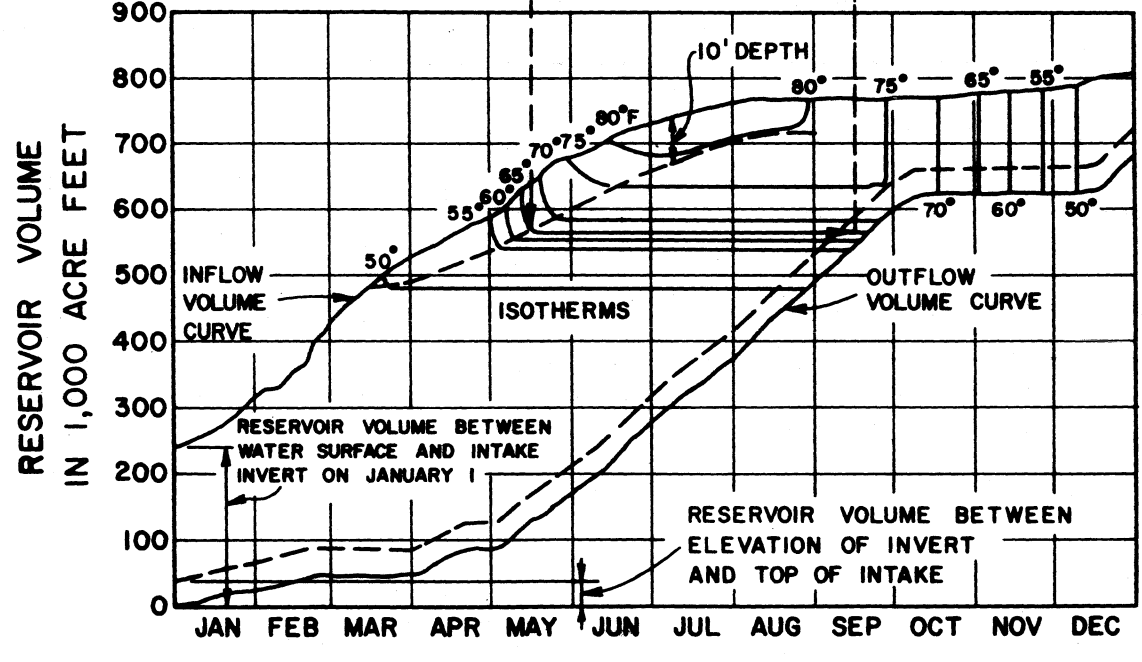
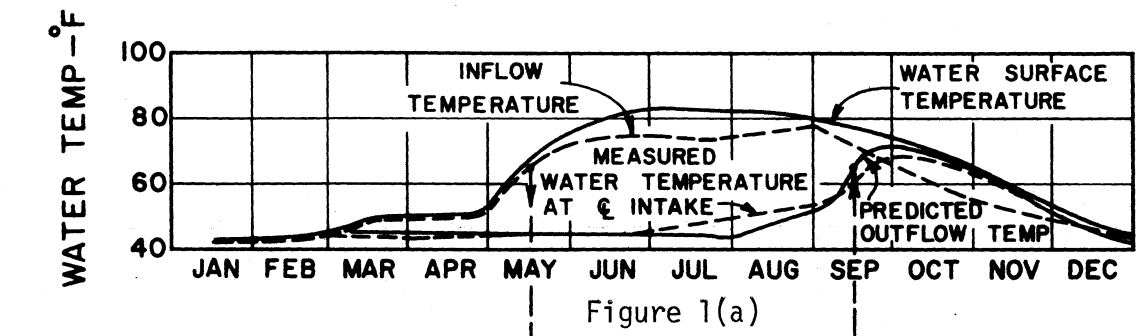


Figure 1. Graphical Temperature Prediction Model of Wunderlich

starting with the initial volume of the reservoir above the intake invert at the beginning of the year. As it is assumed that the outflow takes place at the elevation of the intake invert, the integrated outflow volume curve is plotted starting at zero on January 1. The volume band thus created between the inflow and outflow volume curves represents the stored volume between reservoir surface and the intake invert at any time of the year.

Since it is assumed that the temperature of water below the 10-foot surface layer will remain at its inflow temperature, and that the development of the warm surface layer will start during the month of March, the outflow temperature after this time is assumed to correspond to the value of the isotherm intersecting the centerline of the outflow volume band and the bottom of an assumed 10-foot thick uniform surface layer. These predicted outflow temperatures are projected upward and plotted in Figure 1a.

The model developed is based on several simplified assumptions, such as no mixing occurs between inflow water and reservoir water, and the withdrawal of water is assumed to affect only a layer between the bottom and top of the intake. Use of this model to predict water temperature in the reservoir and in the outlet is very questionable.

Dake and Harleman (14) developed an analytical study on the time dependent vertical distribution of temperature in a body of water for which analytical solution to the heat transfer equation can be obtained. The study is based on the one-dimensional heat transfer equation for heat flux in the vertical direction, neglecting the convective motion of the fluid. The applicability of the model is limited to two specific conditions:

1. Deep lakes whose area change with depth is small.
2. Simple time dependent functions for insolation and surface heat losses.

Under these assumptions, the temperature distribution in the vertical direction is governed by the differential equation

$$\frac{\partial T}{\partial t} = \alpha \frac{\partial^2 T}{\partial z^2} + \frac{H}{\rho C} \quad (2.4)$$

in which

$T$  = temperature

$t$  = time

$z$  = vertical coordinate measured downward from the water surface

$H$  = rate of heat generated per unit volume by internal absorption of solar radiation

$\alpha$  = thermal molecular diffusivity

$\rho$  = density of the fluid

$C$  = specific heat of the fluid.

The rate of internal radiant energy absorption per unit volume is

$$\begin{aligned} H &= - \frac{\partial \Phi}{\partial z} \\ &= \eta(1-\beta) \Phi_0 \exp(-\eta z) \end{aligned} \quad (2.5)$$

where

$\Phi$  = heat flux per unit horizontal area

$\Phi_0$  = net solar radiation per unit area reaching the water surface

$\eta$  = absorption coefficient

$\beta$  = proportion of  $\Phi_0$  absorbed at the water surface.

The solution of Equation (2.4) for  $T = f(z, t)$  requires that an initial condition and two boundary conditions be specified and  $\phi_0$  must be known function of time.

The heat transfer equation used by Dake has ignored the advective transfer term. For many reservoirs, inflows from tributaries and outflows at various outlet elevations will generate advective transfers along the principal axis of concern of both water and heat and, in most situations, advective heat flow may be roughly an order of magnitude larger than any imputed diffusional transfer.

Therefore, under the assumptions used to develop the model, the model can be used only to predict the temperature distribution in the vertical direction of reservoir with no inflow and outflow.

Beard and Willey (2) suggested that a practical model for analyzing reservoir temperature stratification should use generalized data that are readily available, such as average air temperature and average radiation, and the generalized model should be capable of selecting the outlets that will maintain outflow temperatures within a desired range as long as possible and leave the temperature of the remaining stored water at an optimum value.

Beard and Willey developed a model based on the basic computation interval in the order of one month and also based on a greatly simplified energy budget computation. The model has six coefficients, each associated with an energy exchange function. In developing the model, the reservoir is divided into horizontal layers of uniform thickness. The model accounts for the energy in each layer and for the energy and water transferred into and out of each layer of the reservoir. The exchange of energy between the reservoir and the atmosphere is assumed to affect

only the top ten meters of water. The exchange is considered to affect water temperature linearly, with maximum effect at the surface and zero effect at ten meters' depth. Three factors are considered in the energy exchange computation; they are solar radiation, evaporation, and a combination of conduction and long wave radiation. All are expressed as a function of the difference between air temperature and water temperature. Although it is known that water released from a particular outlet comes from both above and below the outlet, releases as computed in the model are made from the lowest water above the intake invert of the outlet.

The use of this model for studying temperature variation of proposed reservoirs requires an estimate of the model calibration coefficients. These coefficients are associated with energy exchange functions which vary from one region to the other, and can be estimated only by using existing reservoirs with observed temperature profile data. So the use of this model as a predictive tool for studying temperature variation of proposed reservoirs is questionable.

Goodling and Arnold (23) presented a model to predict the yearly behavior of the strong temperature gradients typically found in deep impoundments. The model makes use of a single vertical diffusion coefficient coupled with average monthly meteorological and hydrological data and reservoir characteristics to predict monthly one-dimensional thermal profiles of a reservoir. The model is based on the following assumptions:

- 1) Inflow is assumed to be at a temperature at or above the surface temperature of the reservoir;
- 2) Water outflow temperature is taken to be the average temperature across the face of the outflow control structure;



3) The surface heat flux,  $Q$ , is taken to be the product of the surface area, surface heat exchange coefficient, and the difference between actual surface temperature and the equilibrium temperature.

The energy balance presented by the authors is

$$mcT_i + KA(T_s - T_e) = mcT_o + \frac{d}{dt} \int_v \rho c T dv \quad (2.6)$$

which, when integrated over a time period, yields

$$(mcT_i) \Delta t + KA(T_s - T_e) \Delta t = (mcT_o) \Delta t + \int_v \rho c T dv \Big|_{t_1}^{t_2} \quad (2.7)$$

where

$m$  = mass flow in or out

$c$  = specific heat

$T_i, T_o$  = inlet and outlet water temperatures, respectively

$\Delta t$  = time increment

$K$  = surface heat exchange coefficient

$T_s$  = surface temperature

$T_e$  = equilibrium temperature

$T$  = water temperature

$v$  = reservoir volume

$A$  = reservoir surface area

The solution of the last term in Equation (2.7) is given as

$$T(z,t) = T_i + Ct \left[ 1 + 2z^2 - \frac{4}{\sqrt{\pi}} \sum_{n=1}^{\infty} \frac{(-1)^{n+1} z^{2n-1} (z^2 + n)}{(n-1)! (2n-1)} \right] \quad (2.8)$$

in which

$$Z = \frac{z}{2} \sqrt{D_V t} \quad (2.9)$$

$z$  = depth from the bottom of the epilimnion

$D_V$  = diffusion coefficient

$t$  = time

$C$  = slope of the linear dependent boundary condition

The above equation implied that the properties related to the problem remain constant during the time period of integration and the mass inflow and outflow are equal - but having different temperature. However, the assumption that the inflow temperature is at or above the surface temperature of the reservoir can be true only for some period of time.

Orlob and Selna (41) developed a model for studying the thermal energy variation in time and space of deep reservoirs which experience thermal stratification during seasonal exposure to changing environmental conditions. The general heat flow equation for deep reservoirs developed is based on the advection of inflows and outflows, direct solar insolation, convective mixing and effective diffusion. The basic assumptions of the model are:

1) Water will enter the reservoir at an elevation at which the resident water has the same temperature and will affect only the water above this level;

2) In like manner, when water is withdrawn from the reservoir, it will affect only the water above the outlet;

3) The effective diffusion coefficient is a variable in both time and space and can be approximated by an exponential variation with a maximum value at the water surface.

The resulting general equation is

$$a\theta_{,t} = a\left[\frac{h'}{c\rho} + (\phi_i\theta_i - \phi_o\theta)\right] + [aA\theta_{,z}]_{,z} - [a\phi_v\theta]_{,z} \quad (2.10)$$

in which

$\theta$  = water temperature

$\theta_i$  = temperature of inflowing water

$h'$  = heat flux per unit volume

$a$  = area of water plane at elevation  $z$

$A(z,t)$  = coefficient of effective diffusion

$\phi_i, \phi_o$  = inflow and outflow velocity, respectively

$\phi_v$  = vertical velocity

$c$  = heat capacity of water

$\rho$  = density of water

$$\theta_{,t} = \frac{\partial\theta}{\partial t}$$

$$[aA\theta_{,z}]_{,z} = \frac{\partial}{\partial z} (aA \frac{\partial\theta}{\partial z})$$

$$[a\phi_v\theta]_{,z} = \frac{\partial}{\partial z} (a \phi_v\theta)$$

The values of  $A(z,t)$  in the epilimnion can be expressed as

$$A(z,t) = A_o(t)e^{-\delta z} \quad (2.11)$$

where

$A_o(t)$  = maximum diffusion coefficient

$$\delta = A(z_T, t)/A_o(t)$$

$z_T$  = depth at which the thermocline is located.

As pointed out by the authors, the values of  $A(z_T, t)$  and  $A_o(t)$  are

likely to be the characteristic of a particular reservoir and to be dependent on other factors which, at the present time, can be represented only empirically, and whenever possible, they should be derived from experience with the reservoir being studied. In verifying the model, the authors employ an effective diffusion coefficient which is in the order of  $10^4$  times the molecular value. This would tend to indicate a high degree of turbulence, and invalidate the assumption of stratified flow.

### B. Water Quality Model

Although much work has been done on predicting dissolved oxygen in streams (5,17,51), very little work has been done on the development of methods for predicting the effects of thermally stratified reservoirs on water quality. In the earliest attempts to predict D.O. concentration in reservoirs, many investigators tried to apply the methods developed for stream D.O. prediction to the reservoir impoundments. In view of the oxygen stratification in reservoirs, the classical Streeter-Phelps (51) analysis for streams, which assumes vertically mixed conditions, is not applicable in stratified reservoirs. The oxygen balance should include the vertical variation of dissolved oxygen as influenced by internal flow patterns and the vertical distribution of oxygen sources and sinks.

O'Connell, et al. (38) developed a mathematical model used to describe the change of D.O. concentrations within the impoundments, where sedimentation is not an important factor. The model could be represented by

$$\frac{dD}{dt} = k_1(L - y) - k_2D + (R - P) \quad (2.12)$$

which, when integrated over a time period, yields

$$D = \frac{k_1 L}{k_2 - k_1} (e^{-k_1 t} - e^{-k_2 t}) + \frac{(R - P)}{k_2} (1 - e^{-k_2 t}) + D_a e^{-k_2 t} \quad (2.13)$$

in which

$D$  = D.O. deficit at any time  $t$

$t$  = time

$k_1$  = deoxygenation rate constant

$y$  = biochemical oxygen demand (BOD) at any time  $t$

$L$  = total organic BOD

$k_2$  = atmospheric reaeration rate constant

$R$  = rate of oxygen demand by the algal population

$P$  = rate of oxygen produced by the algal population

$D_a$  = initial D.O. deficit

Since the model does not consider any advection of BOD by the inflow to the reservoir or any variation of D.O. in the vertical direction, the model can be used only in a well-mixed body of water with no inflow or outflow.

Churchill and Nicholas (11) used a statistical approach to develop a mathematical model to predict D.O. concentration in the outflow of reservoirs. Churchill, et al. suggested that D.O. concentration in the outflow from a storage impoundment might be expressed as a function of retention time (measured from April 1), the temperature of the outflow, and some factors which consider reservoir operation. The model is based on the assumption that there is no mixing at the reservoir entrance, and water is drawn from the pool at the elevation of the intake, only. The mathematical model, obtained through a multiple regression analysis by

relating these three basic factors mathematically to the change in D.O. concentrations observed in the outflows, is

$$Y = a + b_1 X_1 + b_2 X_2 + b_3 X_3 + b_4 X_1^2 + b_5 X_2^2 + b_6 X_3^2 \quad (2.14)$$

where

$Y$  = decrease in D.O. concentration in the outflow, mg/l, between April 1 and the date for which a D.O. prediction is desired

$a, b_1, b_2, b_3, b_4, b_5, b_6$  = constants determined from the regression analysis

$$X_1 = T/10 \quad (2.15)$$

$T$  = time in days from April 1 to the date for which a D.O. prediction is desired

$$X_2 = \sum_{i=1}^n [(T/10)_i \Delta Te_i] \quad (2.16)$$

$n$  = number of 10-day time increments after April 1

$\Delta Te$  = increase in temperature of the outflow,  $^{\circ}\text{C}$ , between April 1 and the date for which a D.O. prediction is desired.

$$X_3 = \sum_{i=1}^n (T/10H)_i \quad (2.17)$$

$H$  = distance, in feet, above the centerline of the intake at which the April 1 inflow exists on the date of interest

Because of the assumptions in the basic development of the model, the model might be suitable for a reservoir already in existence and with several years of data are available.

Wunderlich (67) developed a graphical D.O. prediction model using

the same assumptions as the graphical temperature prediction model already developed. The model, like that of Churchill and Nicholas (11), related the changes in dissolved oxygen concentration in reservoir waters to residence time of water in the reservoir. The residence time is a variable which for a given day's input is determined from a graphical temperature prediction model. The residence time for a selected input is defined by Wunderlich as the time period between which a given input temperature appears on the inflow volume curve and the time at which this temperature appears at the center of the outflow volume band. In addition, the model also considered the depth and location of the impounded water and the biological and chemical activities in the impounded water.

Wunderlich suggested that the change of D.O. concentration in a reservoir is a function of the water quality of the inflow and the complicated interplay of surface and bottom D.O. and BOD production and consumption. He assumed that the bulk depletion factor,  $k$ , could be calculated from

$$C = C_0 e^{-kt_d} \quad (2.18)$$

in which

$C$  = D.O. concentration at any time,  $t$

$C_0$  = the initial concentration of the inflow

$t_d$  = residence time in days of that inflow

$k = k(T)$  = bulk depletion for D.O. in  $\text{day}^{-1}$

The outflow D.O. concentration can be found by using the initial inflow concentration, the residence time of a certain layer as deter-

mined from the temperature prediction model and the empirical depletion function. The intersection of the exponential D.O. decay curve with a vertical line, marking the end of the residence time, indicates the outflow D.O. as shown in Figure 2.

Because of the assumptions of no mixing at the entrance, the simplified withdrawal profile, and the bulk depletion factor must be determined empirically from the internal reservoir measurements. The outflow D.O. concentration predicted by this method is questionable.



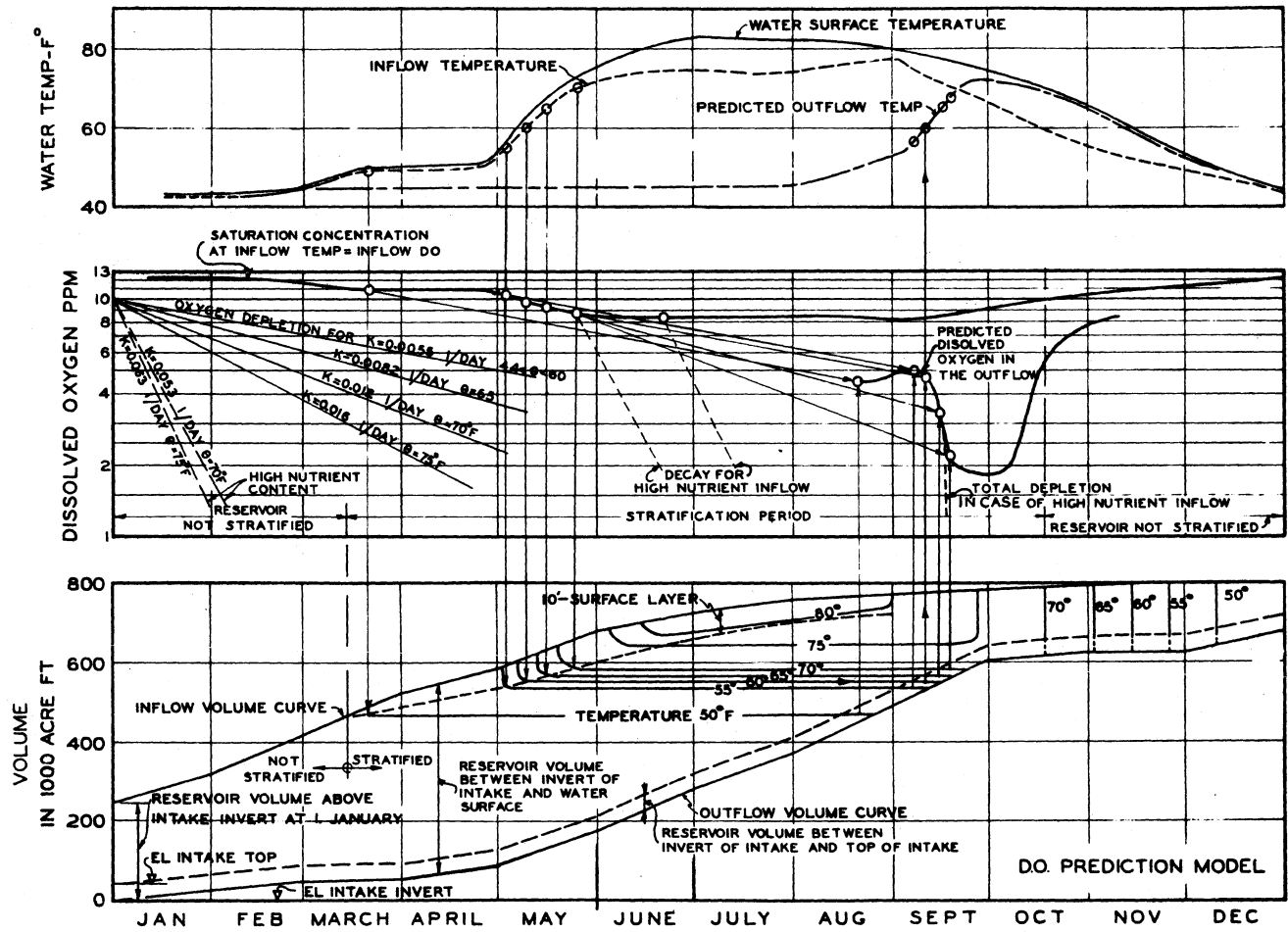


Figure 2. Graphical D.O. Prediction Model of Wunderlich

## CHAPTER III

### THEORETICAL CONSIDERATIONS

#### A. Classification of Reservoirs

There are three distinct types of reservoirs, each of which requires a different type of solution for the determination of its temperature and water quality distribution. These types are:

- 1) a deep reservoir in which the storage volume is large compared to the annual through-flow, and the isotherms are horizontal during most of the year;
- 2) shallow or weakly-stratified reservoir, characterized by isotherms which are tilted along the longitudinal axis of the reservoir;
- 3) completely mixed reservoir whose isotherms are vertical.

From the description of these three types of reservoirs, it is apparent that the deep reservoir solution and the completely mixed reservoir solution are one-dimensional because their thermal properties vary in one direction only. The difference is that the solution is taken along the vertical axis for the deep reservoir, while the completely mixed reservoir solution is taken along the longitudinal axis. In contrast, the solution of the weakly-stratified reservoir requires that both dimensions be considered.

The best criterion for determining into which type a reservoir will fall and hence the type of solution required is that of Orlob (40), who introduces a densimetric Froudenumber which is a function of the flow

through rate, the reservoir geometry and density gradient. The densimetric Froude number can be written for the reservoir as

$$F = \frac{LQ}{dV} \sqrt{\frac{1}{g\epsilon}} \quad (3.1)$$

where

$L$  = length of reservoir, m

$Q$  = flow through rate, m<sup>3</sup>/sec

$d$  = mean reservoir depth, m

$V$  = reservoir volume, m<sup>3</sup>

$\epsilon$  = average density gradient in the reservoir, m<sup>-1</sup>

$g$  = gravitational constant, m/sec<sup>2</sup>

Substituting the values of  $\epsilon$  and  $g$  in Equation (3.1), the equation will reduce to

$$F = 320 \frac{L}{d} \frac{Q}{V} \quad (3.2)$$

This number is the ratio of the inertia force of the horizontal flow to the gravitational forces within the stratified impoundment. It is a measure of the success with which the horizontal flow can alter the internal thermal structure of the reservoir from that of its gravitational static equilibrium state.

In deep reservoirs the isotherms are horizontal, which indicates that the inertia of the longitudinal flow is insufficient to disturb the overall gravitational static equilibrium state of the reservoir except possibly for local disturbances in the vicinity of the reservoir outlets and at points of inflow,  $F$  would be expected to be small for such reservoirs. In completely mixed reservoirs, the inertia of the flow is suffi

cient to completely upset the gravitational structure and destratify the reservoirs.  $F$  would be expected to be large for reservoirs of this class. In between these two extreme classes lies the weakly-stratified reservoir in which the longitudinal flow has enough inertia to disturb the reservoir isotherms from their gravitational static equilibrium state configuration but not enough to completely mix the reservoir.

Theoretical and experimental works in stratified flow (73,15) indicate that flow separation occurs in a stratified fluid when the Froude number is less than about  $\frac{1}{\pi}$ . Thus, in deep reservoirs,  $F$  would be expected to be at values of  $F \ll \frac{1}{\pi}$  and  $F \gg \frac{1}{\pi}$  for completely mixed reservoirs. The values of  $F$  for the weakly-stratified reservoir would fall between these two limits. Classification and the densimetric Froude numbers of six reservoirs are presented in Table I. The illustrations shown in Table I tend to confirm the validity of using the densimetric Froude number to classify reservoirs. However, the values that should be used to distinguish the transition points between the individual reservoir classes require further investigation.

## B. Reservoir Hydrodynamics

Reservoirs can cause considerable alterations of water quality characteristics such as temperature, dissolved oxygen, and others in comparison to the water quality regime of the original streams. These effects are strongly related to the water movements into, within, and out of the reservoirs in the presence of a density stratification. Therefore the prediction of water quality in a reservoir and in its discharge must be based on a sound understanding of the reservoir hydrodynamics.

The hydrodynamics of a density-stratified reservoir is characterized

TABLE I  
RESERVOIR CLASSIFICATIONS AND FROUDE NUMBERS

Reservoir	Length $\times 10^4$ (meters)	Average Depth (meters)	Discharge to Volume Ratio $\times 10^{-7}$ ( $\text{sec}^{-1}$ )	F	Type
Hungry Horse	4.7	70	0.12	0.0026	Deep
Fontana	4.6	107	0.25	0.0029	Deep
Detroit	1.5	56	0.35	0.0030	Deep
Lake Roosevelt	20.0	70	5.0	0.46	Weakly-stratified
Priest Rapid	2.9	18	46.0	2.4	Completely mixed
Wells	4.6	26	67.0	3.8	Completely mixed

by the simultaneous presence of a complex system of currents. Due to strong reduction of vertical turbulent exchanges in the presence of a density gradient, water movements in the horizontal become very persistent and effective. Such water movements or reservoir currents may be caused by inflow, withdrawal, wind, and others (70). Stratification which occurs in reservoirs due to temperature and other factors at various seasons of the year is mainly responsible for the movements and the quality changes of the impounded water. The investigation of the path followed by a water parcel upon entering an impoundment and of the location from where the discharge is withdrawn is at the base of any prediction of water quality within a reservoir and in the discharge from a reservoir.

#### 1. Temperature Stratification Mechanics

The transfer of heat from the atmosphere to a body of water leads to an unequal distribution of temperatures with high temperatures in the layers near the surface and decreasing temperatures with depth. Thus, warm and less dense water is accumulated at the surface, and heavier, cooler water in the layer below. This leads to a remarkably stable placement of the water particles with the lighter ones on top of the heavier, and is known as temperature stratification.

The principal factors involved in the heating of reservoir water (27) are:

- 1) absorption and transmission of solar radiation,
- 2) convection due to surface cooling by evaporation and conduction,
- 3) thermal advection into and out of the reservoir by inflows

and outflows.

The absorption of solar energy and particularly the distribution of absorbed energy are a function of the transmissivity of the water, which varies with season and location. Algae growth during the summer months and suspended particles during the flood season are the principal causes for the variation.

Convection due to surface cooling is a very important means of heat transfer. Surface losses due to evaporation, back radiation, etc., are generally greater than the surface absorbed energy due to solar radiation and atmospheric long wave radiation, so as soon as the outgoing energy from the water surface exceeds the incoming heat, a thin surface film begins to cool. The cooled water is of higher density than the warmer underlying layer, and starts to gather in shallow dips in the surface from where it eventually plunges into the deeper layers, while warmer water from beneath the surface film emerges to be cooled in turn in the same way (71). The plunging water will drop until it meets water at the same density, where it will stop. This leads to a mixed zone at the surface in most cases, although in spring and early summer this mixed zone may be rather shallow.

Thermal advection due to inflow and outflow is also very important in heat transport calculations. It may vary within wide limits--from completely stagnant pools without any appreciable inflow and outflow to run-of-the-river reservoirs with large water volumes moving continuously through the entire depth of the reservoir.

## 2. Reservoir Currents

Various types of currents are present in an impoundment. They are

inflow, outflow, balancing, convective, and wind-induced currents. A knowledge of these currents is essential for the prediction of water quality changes in most impoundments, since they usually have a marked influence on the development of the stratification pattern. Of particular interest are the inflow, withdrawal, and balancing currents. The interrelationship between these currents and the stratification patterns is a function not only of the flow rates, but also their temporal distribution, temperature and density of the inflow, the physical shape of the reservoir, and the location and size of the release structures (11, 68). In stratified bodies of water with the lighter particles located on top of the heavier ones, there is a greater resistance against movement in the vertical than in a homogeneous fluid. Whenever a particle is dislocated vertically by an external force, buoyancy or weight immediately becomes active, restoring it to its initial position. There are no such restoring forces in the horizontal direction.

Types of inflow water movements are controlled largely by the density difference between inflowing water and reservoir water, which vary with seasons of the year. Three basic types of inflow water movements, as shown in Figure 3, are overflow, interflow, and underflow.

An overflow takes place when the inflow water density is less than reservoir water surface density; the inflowing stream water spreads over the surface of the reservoir. The overflow may travel for a considerable distance and then mix with water near the surface by action of wind and waves. The overflow water remains in contact with the atmosphere and in the well insulated and aerated zone. Oxygen is replenished in this zone by reaeration of the surface film which is carried into the water below by forced and free convective mixing processes, and photosynthetic oxygen



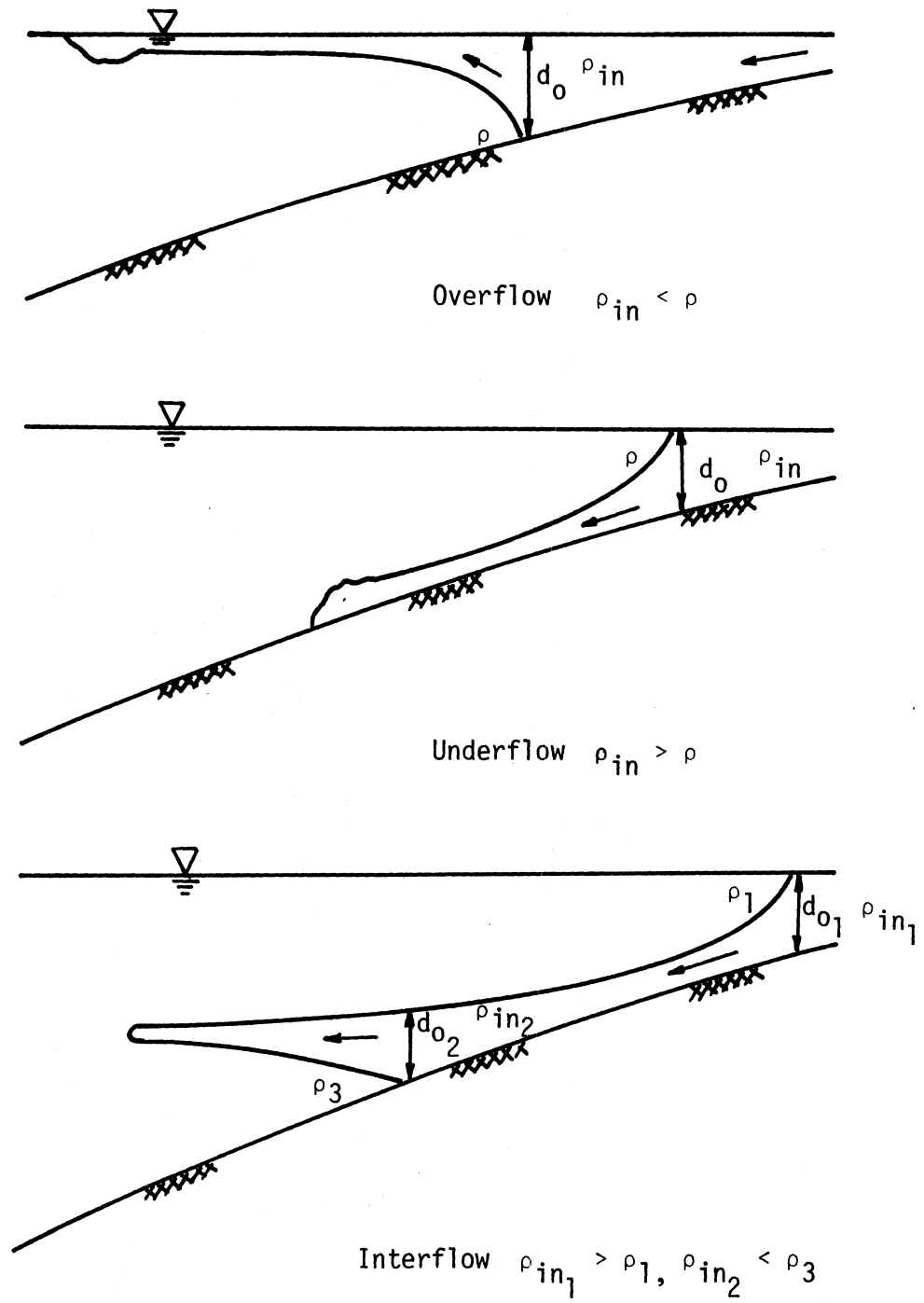


Figure 3. Three Basic Types of Inflows

production also occurs in the surface layer.

An interflow takes place when the density of the inflowing water is greater than that of water on the surface of the reservoir but less than that of deep water. The inflowing water sinks to its own density level in the reservoir and then spreads out laterally downstream.

An underflow takes place when the density of the inflowing water is greater than that of the water at any level in the reservoir. The inflowing water sinks to the reservoir bottom and travels downstream at or near the bottom. The inflow water becomes separated from contact with the atmosphere. In most impoundments, solar radiation penetration is restricted to the upper water layer, so in deep reservoirs underflow may enter rather quickly into hypolimnetic zones. From there on, waste loads in such waters depend, for their assimilation, exclusively on oxygen available in the inflow or on dilution of the underflow by entrainment at the entrance. Rapid depletion of the original D.O. concentration in the inflow water may result.

The location of the withdrawal structures has a dominant influence on the water quality development in most reservoirs. When water is withdrawn from a stratified body of water, the pressure gradient imposed on the water body by opening the outlet structures affects the water particles in the very first moment as if no density gradient were present (31). Restoring forces become immediately active in the layers above and below the intake. After steady state is established, primarily particles of the density layer at the level of the outlet and its immediate vicinity are withdrawn. So, due to the suppression of vertical movements in the presence of density stratification, all withdrawal water comes from a selective layer around the level of the intake. The thick-

ness of this layer in an incompressible, steady viscous flow depends on the density gradient and the height of the intake (31). Since all flow is concentrated in a layer of well-defined limits, the velocity is much higher than it would be in a homogeneous fluid for the same amount of withdrawal.

In a natural reservoir, balancing currents are generated whenever there are dislocations of water particles or the rise of pressure gradients, tending to restore equilibrium. When the cool inflow plunges through the warm surface water into its density layer, drag is exerted on the adjacent warm water particles so that they are entrained in a downward movement. The water which is carried away by this process is replaced by an upstream-directed current at the surface toward the plunge point. Another cause for the creation of balancing currents are changes in inflow and outflow. If a large amount of inflow reaches the reservoir, warm water which originally occupied this space is pushed out and moves into a new location corresponding to its density. If the inflow stops, reservoir water will move back into these areas at the head of the reservoir.

### 3. Withdrawal Layer Thickness

When water is withdrawn from a stratified impoundment, it does not necessarily follow that the entire fluid bulk will contribute to the outflow, as is the case for a nonstratified body. Density stratification in reservoirs causes water to be withdrawn from a layer near the level of the intake. Therefore, the prediction of the outflow temperature and water quality requires the knowledge of the thickness and the internal flow distribution of the withdrawal layer. Theoretical labora-

tory experiments and field investigations have been conducted in recent years to develop formulas which relate the withdrawal layer thickness to flow rate, density gradient, distance from the dam, viscosity, and heat diffusivity.

On the basis of the theoretical analysis of Yih (73) and experimental analysis of Debler (15) for the inviscid nondiffusive flow, the theory for a steady two-dimensional case involving both viscosity and molecular diffusion by Koh (31), the modification of Koh's solution by Brooks and Koh (7) for the high flow rate, and the field investigation of Cherokee and Fontana Reservoirs by Wunderlich (60), the withdrawal layer thickness in reservoirs with linear density distribution can be estimated by using the following formulas:

Surface and bottom intakes

$$\delta = 4.5a \quad (3.3)$$

Intermediate intakes

$$\delta = 5.0a \quad (3.4)$$

in which

$\delta$  = thickness of withdrawal layer, ft

$a$  = scale length =  $\left(\frac{q}{\sqrt{g\varepsilon}}\right)^{1/2}$ , ft

$q$  = outflow per unit width, ft<sup>2</sup>/sec

$g$  = acceleration due to gravity, ft/sec<sup>2</sup>

$\varepsilon$  = average density gradient in the reservoir, ft<sup>-1</sup>

$$= \frac{1}{\rho} \frac{d\rho}{dy}$$

$\rho$  = density, gm/cm<sup>3</sup>

$y$  = depth, ft

The density gradient in the reservoir can be related to the temperature gradient through the expression

$$\frac{d\rho}{dy} = \frac{d\rho}{dT} \cdot \frac{dT}{dy} \quad (3.5)$$

By using the least square fit of density vs. temperature (26) for the range of 4°C to 26°C, yielded

$$\rho = 1.0 - 6.63 \times 10^{-6} (T - 4)^2 \quad (3.6)$$

where

$\rho$  = density of water, gm/cm<sup>3</sup>

$T$  = water temperature, °C

Thus,

$$\epsilon = \frac{2(T - 4)}{151000 - (T - 4)^2} \frac{dT}{dy} \quad (3.7)$$

#### 4. Factors Influencing Water Quality

The governing factor in reservoir water quality development is the temporal and spatial variation of the density and quality of the water which enters, is temporarily stored, and finally withdrawn from the reservoir. In most reservoirs, water temperature plays the dominant role in determining density. In special cases, however, other factors may be of importance. The main factors influencing the temporal and spatial distribution of temperature and water quality are the geometry of the reservoir, storage management over the yearly cycle, outlet works design, hydrology of the drainage basin, water quality of the inflow,

biological and chemical activities in the impounded water, optical properties of the impounded water, and climate of the environment.

The geometry of a reservoir can be characterized by surface area, volume, length and cross-sectional shape--all being functions of the water surface elevation. The surface area together with the climate of the environment controls the heat exchange through the water surface and the water volume affected by surface heating.

The types of outlet works, the densities of inflow and reservoir water, and the geometry of the reservoir determine the flow patterns which may develop in a stratified reservoir. If only the elevation of the outlet is changed and all other factors are kept constant, there is always an elevation at which inflow would move straight through the reservoir into the outlet. Spilling over an overfall spillway during the stratification season would cause warm water to leave the reservoir, keeping the cool winter water in untouched storage. Spilling through deep sluices in late spring when stratification has already developed would cause a loss of cool winter water and lead to the accumulation of warmer water with a possible increasing of nutrient content in the upper layer of the reservoir. It follows that the improper use of an outlet structure at a certain time may have noxious consequences for the reservoir water quality during the rest of the year. So, the operation of the reservoir is very important, because a change in the operating pattern will result in a change in the discharge water quality.

The hydrology of the drainage basin of a reservoir governs the discharge characteristics of the natural inflow and is an important factor in the development of the thermal and water quality structure of the receiving impoundment. The water quality of the inflow also has an

influence on the thermal stratification and on other water quality parameters, such as dissolved oxygen concentration in the impoundment and in the outflow.

The climate of the environment governs the intensity of the heat exchange through the water surface as well as the temperature of the inflow. The optical properties of the impounded water influence the physical as well as the biological character of the reservoir water. The heating of the lake surface layers by absorption of solar energy depends largely on the transparency of the water. The penetration of solar radiation into deep layers of the water is a very direct process in heating reservoir water in addition to the heat transferred from the surface downward by conduction and mixing, and clear water is more conducive to oxygen exchange in the upper layers due to biological activity than that of turbid water.

### C. General Governing Equations

The prediction of the temporal and spatial distribution of temperature and concentration of a particular pollutant in a stratified reservoir requires the knowledge of density distribution, flow pattern, conservation of heat and conservation of mass for all the substances under consideration. Mathematically, the hydrodynamics, thermal behavior, and pollutant concentration can be completely described by the simultaneous solution of the Navier-Stokes equation (equation of motion), the continuity equation, the conservation of heat equation, and conservation of mass equation for each pollutant under investigation .

The equation of motion:

$$\rho \left( \frac{\partial u_i}{\partial t} + u_j \frac{\partial u_i}{\partial x_j} \right) = -\rho g_i - \frac{\partial p}{\partial x_i} + \mu \frac{\partial^2 u_i}{\partial x_j^2} - \left[ \rho \frac{\partial}{\partial x_j} (u_i' u_j') \right] \quad (3.8)$$

The continuity equation:

$$\frac{\partial \rho}{\partial t} + u_j \frac{\partial \rho}{\partial x_j} + \rho \frac{\partial u_j}{\partial x_j} = 0 \quad (3.9)$$

The conservation of heat equation:

$$\frac{\partial T}{\partial t} + u_j \frac{\partial T}{\partial x_j} = D_t \frac{\partial^2 T}{\partial x_j^2} - \frac{\partial}{\partial x_j} (u_j' T') + \frac{\text{sources}_t}{\rho C_h} - \frac{\text{sinks}_t}{\rho C_h} \quad (3.10)$$

The conservation of mass equation:

$$\frac{\partial C}{\partial t} + u_j \frac{\partial C}{\partial x_j} = D_m \frac{\partial^2 C}{\partial x_j^2} - \frac{\partial}{\partial x_j} (u_j' C') + \frac{\text{sources}_m}{\rho} - \frac{\text{sinks}_m}{\rho} \quad (3.11)$$

in which

$u_i, u_j$  = velocity in the  $i^{\text{th}}$  and  $j^{\text{th}}$  direction at time  $t$ , respectively ( $i, j = 1, 2, 3$ )

$p$  = pressure

$\rho$  = density

$g$  = acceleration due to gravity

$\mu$  = dynamic viscosity, mass/length-time

$u_i', u_j'$  = turbulent velocity fluctuation in the  $i^{\text{th}}$  and  $j^{\text{th}}$  direction, respectively

$T$  = temperature at time  $t$

$T'$  = turbulent temperature fluctuation at time  $t$



$D_t$  = molecular diffusivity of heat, area/time

$C_h$  = specific heat of water, heat/mass-degree

$\text{sources}_t$  = sources of heat per unit volume per unit time

$\text{sinks}_t$  = sinks of heat per unit volume per unit time

$C$  = concentration of a particular pollutant at time  $t$

$C'$  = turbulent concentration fluctuation

$D_m$  = molecular diffusivity of mass, area/time

$\text{sources}_m$  = sources of mass per unit volume per unit time

$\text{sinks}_m$  = sinks of mass per unit volume per unit time

The initial turbulence of inflow dies down as the water enters into the reservoir and the water will become quiescent. This is because stratified flows are remarkably stable and persistent due to the fact that the existence of a horizontal density stratification in a gravitational field tends to inhibit vertical motion in the fluid. A reason for the stability of stratified flow as proposed by Koh (31) can be explained as follows: The amount of work, other than that required to overcome the viscous forces, required to move a fluid particle from level  $y_1$  to  $y_2$  in a stably stratified flow is given by

$$w = \int_{y_1}^{y_2} F dy = V \int_{y_1}^{y_2} [\rho(y_1) - \rho(y)] g dy \quad (3.12)$$

where

$w$  = work required to move a fluid particle

$F$  = force required to move the fluid particle

$V$  = volume of the fluid particle

$\rho(y_1)$  = density of fluid particle at level  $y_1$

$\rho(y)$  = density of fluid particle at any level

$g$  = acceleration due to gravity

This work is always positive, regardless of whether  $y_1 > y_2$  or  $y_1 < y_2$ , provided that the density increases with depth, which in the nature of density stratifications it must, with the exceptions of the entrance mixing and surface layer instability caused by evaporative cooling which results in an unstable density gradient. So, a total amount of work equal to  $2w$  must be carried out if two fluid particles, each of volume  $V$  and at levels  $y_1$  and  $y_2$  are interchanged. In other words, any vertical motion requires an addition of energy. For a homogeneous fluid in which  $\rho$  is a constant, this work equals to zero, and a fluid particle may move freely from one position to another except for the viscous force. Therefore, the existence of a horizontal density stratification in a gravity field tends to inhibit vertical motion in the fluid to the extent that turbulent transport of momentum, heat, and mass in Equations (3.8), (3.10), and (3.11), respectively, can be neglected.

## CHAPTER IV

### DEVELOPMENT OF THE MODELS

#### A. Development and Solution of the Temperature Model

Water temperature has assumed an important role in water resources planning and management because of its influence on the physical, biological, and chemical characteristics of the water itself and its wide ranging effects on aquatic life, particularly on various parts of their life cycle. In addition, the water temperature, through its influence on density, affects the hydrodynamic characteristics of the waterbody, particularly in impoundments which are subject to thermal stratification. Through its influence on the hydrodynamic characteristics, the temperature can exert a profound influence on the temporal and spatial variation of water quality characteristics.

In lakes and reservoirs, stable density stratification is caused primarily by the temperature variation with depth, and secondarily by a variable concentration of pollutants. The upper layers of the reservoir are generally heated by the sun, while wind and surface evaporation cause mixing in a surface zone, called the epilimnion, which is fairly uniform in temperature. Below this is the thermocline through which the temperature decreases rapidly to that of the lower zone, the hypolimnion, which feels a negligible effect of the surface heating. Thermal regimes of the reservoirs are affected by the substantial inflows and outflows

which contribute to the heat and mass balance of the reservoir. Both the inflows and outflows produce a continuing alteration of the density profiles because of the vertical displacements of water masses due to inflows pushing into certain levels and outflows vacating other layers.

In terms of an overall heat balance, a reservoir receives heat convectively from the river inflow and by solar radiation on the reservoir water surface. Both the inflow and solar radiation are governed by the climate conditions and the hydrology of the drainage basin. Heat is removed from the reservoir by surface losses which are largely due to evaporation, and by withdrawal from the reservoir which is governed by the operation of the reservoir and the design of the outlet structures. Within the reservoir, heat is distributed by diffusion and vertical advection. Therefore, in developing a model to predict temperature in a stratified reservoir, the model must account for heat transfer through the surface, internal absorption of solar radiation, heat transported by diffusion and vertical advection, and horizontal advection into and out of the reservoir.

In developing the temperature model, the assumptions upon which the model is based are as follows:

- 1) The basic assumption underlying the temperature model is the existence of horizontal isotherms, and hence thermal gradients exist in the vertical direction only. This assumption implies that the horizontal variations in temperatures are very small compared to the vertical variations and has the effect of reducing the problem from a three-dimensional to a one-dimensional problem. This will be a reasonable assumption in the case of deep reservoirs with a low discharge to volume ratio and densimetric Froude number  $\ll \frac{1}{H}$ .

2) Within the range of temperatures encountered, the values of the fluid density and specific heat vary only slightly, and they are assumed to be constant, except when dealing with buoyancy and stability effects. The coefficients of molecular diffusivity of heat and mass are also assumed to be constant in all heat budget and heat transport calculations.

3) The water temperature is assumed to be the only factor responsible for the density of the water.

4) Because the existence of horizontal density stratification tends to inhibit vertical motion in the fluid, the turbulent effects can be neglected.

5) Solar radiation is assumed to be transmitted in the vertical direction only.

6) The heat crossing the boundaries, except from the surface, is through inflow and outflow. That is, the sides and bottom of the reservoir are assumed to be insulated.

Since it is assumed that all transfers of heat can be accomplished along the vertical axis, the water body must be segmented along this axis, and the necessary water and energy balance equations must be written accordingly.

### 1. Schematization of the Reservoir

The idealization of the reservoir water body is presented in Figure 4. In general, the reservoir is divided into horizontal layers of uniform thickness, extending over the entire length and width of the reservoir, the bounding planes of which are common between adjacent layers and can be determined from the reservoir's topography. In Figure 5a,

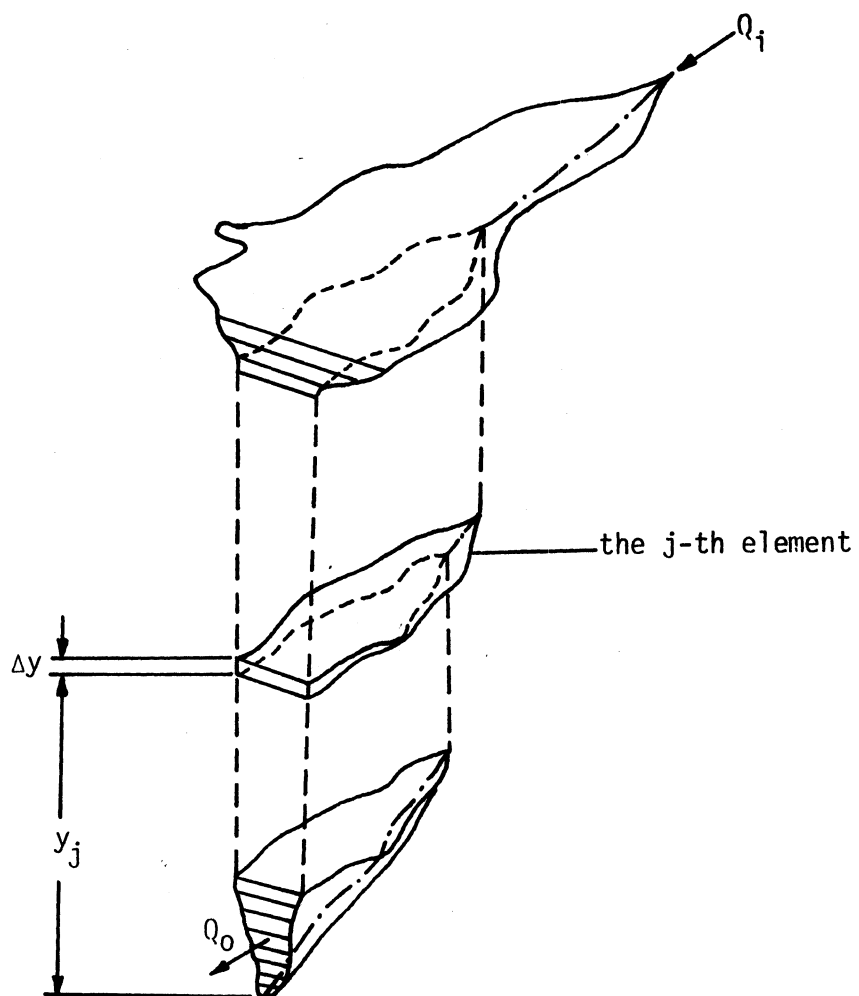
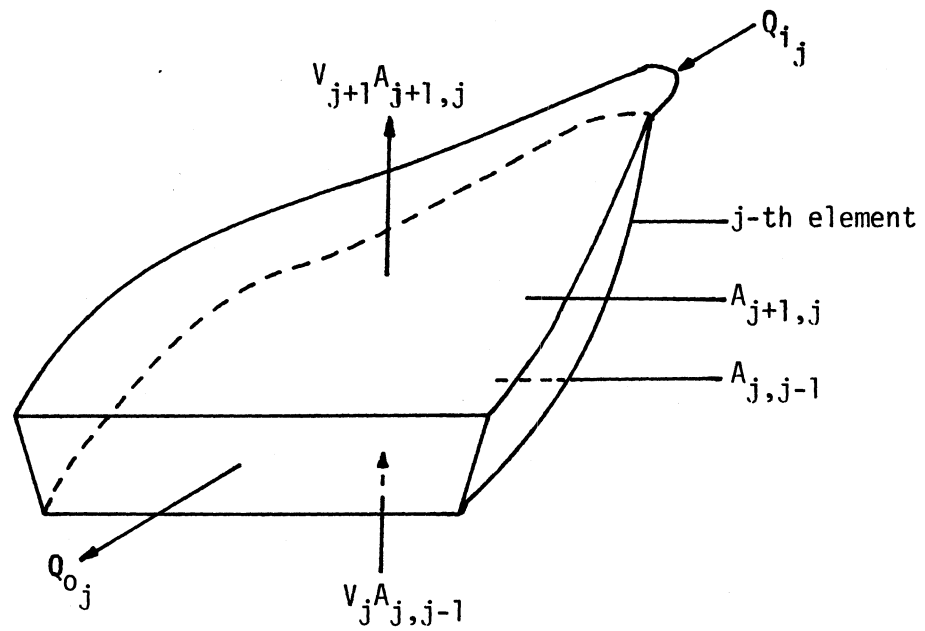
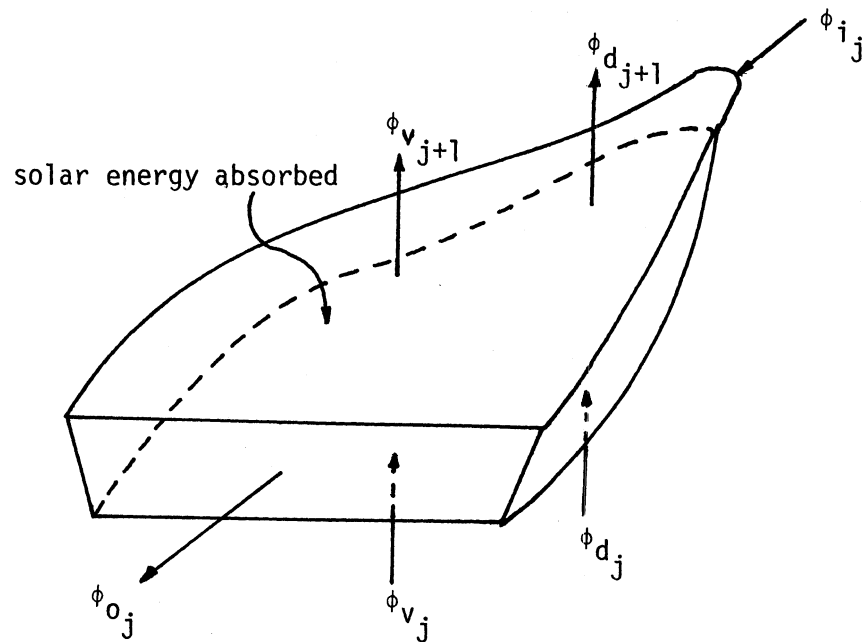


Figure 4. Idealization of a Reservoir Water Body



(a) Control Volume for Mass Balance



(b) Control Volume for Heat Balance

Figure 5. Control Volumes for Mass and Heat Balance

the  $j$ -th element which is at elevation  $y_j$  has a horizontal area  $A_j$  and thickness  $\Delta y$ . A portion of the river inflow enters the element at the upstream; a portion of the outflow through the dam leaves the element at the downstream end, and a portion of water may enter or leave the element through vertical advection depending on the amount of inflow and outflow through that element. Heat also enters the element through the horizontal surface by absorption of solar radiation, transmission, vertical advection and diffusion, and enters the element through the vertical surface by advection of the inflow and leaves the element by advection of the outflow, as shown in Figure 5b. The governing equation for the distribution of temperature in a reservoir is formulated by considering the conservation of heat within each layer and then extended to the entire reservoir. However, before this can be done, it is necessary to consider the mechanism of solar radiation absorption and transmission, heat convection, advection and diffusion. The notation used herein numbers the elements successively from the bottom to the top of the reservoir, so  $j = 1$  refers to the bottom element.

## 2. Determination of Parameters

The net heat transfer between a water body and the atmosphere is computed as the algebraic sum of the heat flux terms:

$$\phi_h = \phi_{sn} + \phi_{ar} - \phi_w - \phi_e - \phi_c \quad (4.1)$$

in which

$$\begin{aligned} \phi_h &= \text{net heat transfer across the water surface, kcal/m}^2\text{-day} \\ \phi_{sn} &= \text{net solar radiation heat flux penetrating into the water,} \\ &\quad \text{kcal/m}^2\text{-day} \end{aligned}$$



$\phi_{ar}$  = net atmospheric radiation heat flux delivered through the interface, kcal/m<sup>2</sup>-day

$\phi_w$  = water surface radiation heat flux, kcal/m<sup>2</sup>-day

$\phi_e$  = energy loss by evaporation, kcal/m<sup>2</sup>-day

$\phi_c$  = energy loss by conduction, kcal/m<sup>2</sup>-day

Several formulas are available for obtaining the net solar radiation, atmospheric longwave radiation and the water surface radiation (1,26,45), but the most up-to-date are the ones developed by Wunderlich, Gras and staff of the engineering laboratory of the Tennessee Valley Authority (62).

The net solar radiation passing the air-water interface is described as the extraterrestrial radiation flux arriving at the top of the atmosphere less losses incurred by scattering and absorption in the atmosphere and by reflection from the water surface. The formula is as follows:

$$\phi_{sn} = \phi_a \left[ \frac{a_2 + 0.5 (1 - a_1 - d)}{1 - 0.5 R_g (1 - a_1 + d)} \right] (1 - R_t)(1 - 0.65 c^2) \quad (4.2)$$

where

$\phi_a$  = extraterrestrial solar radiation flux, kcal/m<sup>2</sup>-day

$$= \frac{I_0}{r^2} \sin \alpha \quad (4.3)$$

$I_0$  = solar constant = 27936 kcal/m<sup>2</sup>-day

$r$  = relative distance earth - sun, dimensionless

$\alpha$  = solar altitude, radians

$a_1$  = mean atmospheric transmission coefficient after scattering, a function of the optical air mass and the moisture content of

the atmosphere, dimensionless

$a_2$  = mean atmospheric transmission coefficient after scattering and absorption, a function of the optical air mass and the moisture content of the atmosphere, dimensionless

$d$  = total dust depletion of the atmosphere, dimensionless

$R_g$  = reflectivity of the ground in the vicinity of the reservoir, dimensionless

$R_t$  = reflectivity of the water surface, dimensionless

$C$  = fraction of the sky covered by clouds, varying from 0 to 1

The net atmospheric longwave radiation heat flux entering the water surface may be calculated as a function of air temperature and cloud cover, and is expressed as:

$$\phi_{ar} = 0.937 \times 10^{-5} \sigma T_a^6 (1 + 0.17C^2)(1 - R_a) \quad (4.4)$$

where

$\sigma$  = Stefan-Boltzmann constant  $\approx 1.171 \times 10^{-6} \text{ kcal/m}^2\text{-day-}^\circ\text{K}^4$

$T_a$  = air temperature at 2 meters above the water surface,  $^\circ\text{K}$

$R_a$  = reflectivity of water surface for atmospheric radiation  
 $\approx 0.03$

The water surface longwave radiation emitted by the water surface layer is given by

$$\phi_w = 0.97 \sigma T_w^4 \quad (4.5)$$

in which

$T_w$  = water surface temperature,  $^\circ\text{K}$

Many formulas for calculating heat loss by evaporation are available (1,32,62). A general form of the formula is

$$\phi_e = \rho E (L + C_h T_w) \quad (4.6)$$

where

$\rho$  = water density, kg/m<sup>3</sup>

$E$  = rate of evaporation, m/day

$$= (a + bU)(e_w - \psi e_a) \quad (4.7)$$

$L$  = heat of vaporization of water, kcal/kg

$$= 595.9 - 0.54 T_w \quad (4.8)$$

$C_h$  = specific heat of water, kcal/kg - °C

$a, b$  = empirical constant

$U$  = wind speed, m/sec

$e_w$  = saturation vapor pressure at water surface temperature, mm Hg

$e_a$  = vapor pressure of the air, mm Hg

$\psi$  = relative humidity

Heat loss by conduction is considered to be a function of wind speed, pressure gradient in the air mass overlying the water surface and Bowen ratio, and is expressed as

$$\phi_c = \rho ER \quad (4.9)$$

where

$$R = N \frac{(T_w - T_a)}{(e_w - \psi e_a)} = \text{Bowen Ratio} \quad (4.10)$$

$N$  = empirical constant

In this study, heat losses by evaporation and conduction are calculated based on the values of empirical constants derived by Rohwer (46); therefore

$$a = 0.000308 \text{ m/day} - \text{mm Hg}$$

$$b = 0.000185 \text{ sec/day} - \text{mm Hg}$$

$$N = 269.1 \text{ kcal} - \text{mm Hg/kg} - ^\circ\text{C}$$

Based on Beer's law, the absorption of solar radiation in water at any elevation  $y$  can be described as

$$\phi_{sy} = \phi_{sn} \exp [-\eta(y_s - y)] \quad (4.11)$$

where

$\phi_{sy}$  = solar radiation intensity at depth  $y$ ,  $\text{kcal/m}^2\text{-day}$

$\eta$  = bulk extinction coefficient,  $\text{m}^{-1}$

$y_s$  = water surface elevation,  $\text{m}$

$y$  = elevation,  $\text{m}$  (positive upward)

The plotting of field data on solar radiation intensity variation with depth on semi-log graph show the nonlinearity of the curves near the water surface which shows that solar radiation absorption cannot be represented by Equation (4.11) over the whole depth of the reservoir. The reason of the nonlinearity of the curves at the water surface layer is that the water surface layer absorbs a very large amount of incoming solar radiation. One way of accounting for this surface absorption is to assume that a portion of the total incident solar radiation intensity is directly absorbed by the water surface (14). Therefore, the amount of solar radiation absorbed at the water surface layer is

$$\phi_{ss} = \beta\phi_{sn} \quad (4.12)$$

where

$\phi_{ss}$  = solar radiation absorbed at the water surface, kcal/m<sup>2</sup>-day  
 $\beta$  = ratio of radiation absorbed at the water surface to net incoming radiation, dimensionless

and the amount of solar radiation absorbed in water by transmission at any elevation  $y$  can be expressed as

$$\phi_{sy} = (1-\beta)\phi_{sn} \exp [-\eta(y_s - y)] \quad (4.13)$$

Thus, the amount of heat from external solar energy sources absorbed in water surface layer except by transmission is

$$\phi_s = \beta\phi_{sn} + \phi_{ar} - \phi_w - \phi_e - \phi_c \quad (4.14)$$

where

$\phi_s$  = heat from external solar energy sources, kcal/m<sup>2</sup>-day

During the fall and winter, the surface layer of a reservoir cools more rapidly than the underlying layers because the heat losses due to evaporation and water surface radiation often exceeds the heat inputs from surface absorbed solar radiation and atmospheric radiation. This cooling process causes the surface water to become more dense than the warmer water below it; the surface water begins to sink and mix with warmer subsurface water. When the model generates this type of unstable temperature distribution, convective mixing is allowed to take place in order to eliminate the instability. The mixing is accomplished by checking the temperature distribution and whenever the temperature gradient is negative, all layers from the top of the reservoir to the

level of instability are mixed. The new temperature of the mixed layer is found by taking the weighted average of volumes and temperatures of the mixed elements in order to maintain the energy balance. If an instability still exists between the mixed layer and the element below, the element below is mixed. This process is repeated until a stable temperature gradient exists.

As a stream enters a stratified reservoir, a certain amount of mixing and entrainment will take place at the entrance, then the incoming water will seek its own density level within the reservoir. If the incoming water is warmer than the surface water, it will enter and flow along the reservoir surface. If the inflowing water is cooler than the surface water, it will sink until it reaches an elevation corresponding to its own density level, at which point it will begin to move horizontally. Elder and Wunderlich (21) made dye tests for the investigation of inflow water movements in the reservoir. The results of dye concentration profiles are shown in Figure 6, which indicates that the inflow velocity profile can be approximated by a normal distribution curve. Thus, the inflow velocity can be expressed as

$$U_i(y) = U_{i_{\max}}(t) \exp \left[ -(y-y_i)^2 / 2\sigma_i^2 \right] \quad (4.15)$$

where

$U_i(y) = U_i(y,t)$  = inflow velocity at elevation  $y$ , m/day

$U_{i_{\max}}(t)$  = maximum inflow velocity at time  $t$ , m/day

$$= \frac{Q_i(t)}{\int_{y_b}^{y_s} B(y) \exp \left[ -(y-y_i)^2 / 2\sigma_i^2 \right] dy} \quad (4.16)$$

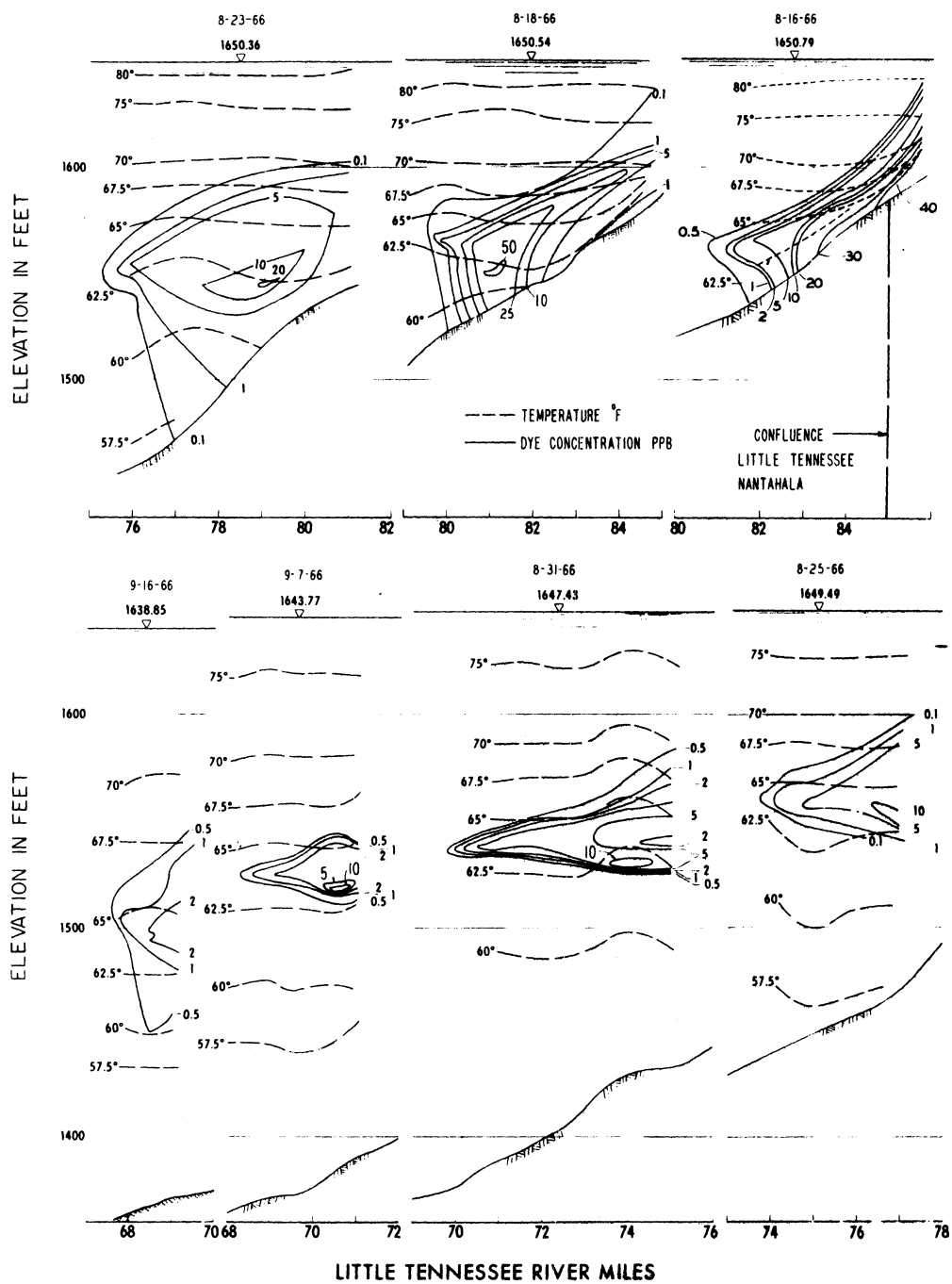


Figure 6. Dye Concentration Profiles in Fontana Reservoir

$y_i = y_i(t)$  = depth at which the reservoir density is the same as that of the incoming water, m

$\sigma_i$  = inflow standard deviation, m

$B(y)$  = width of the reservoir at elevation  $y$ , m  
 $= A(y)/L(y)$  (4.17)

$y_s$  = water surface elevation, m

$y_b$  = bottom elevation of the reservoir, m

$L(y)$  = length of the reservoir at elevation  $y$ , m

$Q_i(t)$  = total inflow rate at time  $t$ , m<sup>3</sup>/day

Therefore, heat advected in a control volume by inflow is

$$\phi_i = \rho C_h U_i B T_i \Delta y \quad (4.18)$$

where

$\phi_i$  = heat advected in by inflow, kcal/day

$T_i$  = inflow temperature, °C

When inflowing water from a river enters a reservoir, it will entrain some of the existing reservoir water. The amount of this entrainment depends on the geometry of the river entering the reservoir. Entrance mixing is accounted for in the model by the use of mixing coefficient,  $m_c$ , which is the ratio of the amount of water entrained and the inflow water. No field measurements of entrance mixing are available, and hence the choice of an entrance mixing coefficient is somewhat arbitrary. Thus, the mixed inflow rate,  $Q_{inm}$ , is given by

$$Q_{inm} = (1 + m_c) Q_i \quad (4.19)$$

and the mixed inflow temperature,  $T_{inm}$ , is represented by



$$T_{inm} = \frac{m Q_i T_e + Q_i T_i}{Q_{inm}} \quad (4.20)$$

where

$T_e$  = average temperature of the water entrained, °C

When water is withdrawn from a stratified impoundment, the water is withdrawn from a layer near the level of the intake. The thickness of the withdrawal layer can be calculated by Equation (3.3) and Equation (3.4). Based on the works of Koh (31), Brooks and Koh (7), and Wunderlich (60), the outflow velocity profile can also be approximated by a normal distribution curve. The outflow velocity can thus be represented by

$$U_o(y) = U_{o_{max}}(t) \exp [-(y-y_o)^2/2\sigma_o^2] \quad (4.21)$$

where

$U_o(y) = U_o(y,t)$  = outflow velocity at elevation  $y$ , m/day

$U_{o_{max}}(t)$  = maximum outflow velocity at  $y = y_o$ , m/day

$$= \frac{Q_o(t)}{\int_{y_b}^{y_s} B(y) \exp [-(y-y_o)^2/2\sigma_o^2] dy} \quad (4.22)$$

where

$y_o$  = elevation of outlet centerline, m

$\sigma_o$  = outflow standard deviation, m

$Q_o(t)$  = total outflow rate at time  $t$ , m<sup>3</sup>/day

The outflow standard deviation is calculated based on the 95 per-

cent confidence interval, which means that 95 percent of the outflow comes from the calculated withdrawal layer thickness  $\delta$ . Thus, the outflow standard deviation is

$$\sigma_o = \frac{\delta/2}{1.96} \quad (4.23)$$

Therefore, heat advected out of a control volume by outflow is

$$\phi_o = \rho C_h U_o B T \Delta y \quad (4.24)$$

where

$\phi_o$  = heat advected out by outflow, kcal/day

$T = T(y)$  = temperature of the control volume at elevation  $y$ ,  $^{\circ}\text{C}$

Referring to Figure 5a, a water mass balance for a control volume is represented by a continuity equation in which advected flows must be in equilibrium. The difference of vertical advected flows through a control volume must equal the net horizontal advected flow. Therefore

$$Q_i - Q_o = Q_{v_{j+1}} - Q_{v_j} = V_{j+1} A_{j+1,j} - V_j A_{j,j-1} \quad (4.25)$$

where

$Q_{v_j}$  = vertical flow rate in the  $j$ -th element,  $\text{m}^3/\text{day}$

$Q_{v_{j+1}}$  = vertical flow rate in the  $(j+1)$ -th element,  $\text{m}^3/\text{day}$

$V_j$  = vertical advective velocity in the  $j$ -th element,  $\text{m}/\text{day}$   
(positive upward)

$V_{j+1}$  = vertical advective velocity in the  $(j+1)$ -th element,  $\text{m}/\text{day}$

$A_{j,j-1}$  = horizontal area at the interface of  $j$ -th and  $(j-1)$ -th elements,  $\text{m}^2$

$A_{j+1,j}$  = horizontal area at the interface of (j+1)-th and j-th elements,  $m^2$

The vertical advective velocity is then calculated by Equation (4.25), starting at the bottom element of the reservoir in which the vertical flow across the bottom is equal to zero. Thus, the vertical advective velocity of the other elements can be obtained.

Therefore, the heat advected in a control volume by vertical advection can be given by

$$\phi_v = \rho C_h V A T \quad (4.26)$$

where

$\phi_v = \phi_v(y,t)$  = heat advected in by vertical flow at elevation  $y$ ,  
kcal/day

The diffusive heat flux into a control volume,  $\phi_d$ , is expressed as

$$\phi_d = - \rho C_h A D_t \frac{\partial T}{\partial y} \quad (4.27)$$

where

$D_t$  = molecular diffusivity of heat,  $m^2/\text{day}$

The negative sign indicates positive transport in the direction of negative gradient.

### 3. Derivation of Governing Equations

Consider the control volume in Figure 5b, the conservation of heat equation can be obtained by equating the time rate change of heat stored in the control volume to the change of heat flux through the control

volume.

The time rate change of heat stored in the control volume,  $H_t$ , is given by

$$H_t = \rho C_h A \Delta y \frac{\partial T}{\partial t} \quad (4.28)$$

The net horizontal advective heat flux through the control volume,  $H_h$ , is as follows:

$$H_h = \phi_i - \phi_o \quad (4.29)$$

The difference of heat flux through the control volume due to the transmission of solar radiation,  $H_s$ , is expressed as

$$H_s = A\phi_{sy} - (A\phi_{sy} + \frac{\partial}{\partial y} (A\phi_{sy}) \Delta y) \quad (4.30)$$

The net vertical advective heat flux through the control volume,  $H_v$ , is represented by

$$H_v = \phi_v - (\phi_v + \frac{\partial \phi_v}{\partial y} \Delta y) \quad (4.31)$$

The change of diffusive heat flux through the control volume,  $H_d$ , is obtained by

$$H_d = \phi_d - (\phi_d + \frac{\partial \phi_d}{\partial y} \Delta y) \quad (4.32)$$

Therefore, the conservation of heat equation is given by

$$H_t = H_h + H_s + H_v + H_d \quad (4.33)$$

which, when substituting the value of each term, yields

$$\rho C_h A \Delta y \frac{\partial T}{\partial t} = \phi_i - \phi_o - \frac{\partial(A\phi_{sy})}{\partial y} \Delta y - \frac{\partial\phi_v}{\partial y} \Delta y - \frac{\partial\phi_d}{\partial y} \Delta y \quad (4.34)$$

Simplifying Equation (4.34), the result is given as

$$\begin{aligned} \frac{\partial T}{\partial t} &= \frac{1}{A} (U_i B T_i - U_o B T) - \frac{1}{\rho C_h A} \frac{\partial}{\partial y} (A \phi_{sy}) - \frac{1}{A} \frac{\partial}{\partial y} (VAT) \\ &+ \frac{D_t}{A} \frac{\partial}{\partial y} (A \frac{\partial T}{\partial y}) \end{aligned} \quad (4.35)$$

In solving Equation (4.35), one initial condition which specifies the values of temperatures as functions of depth at time  $t = 0$  and two boundary conditions which give the values of heat flux as functions of time at the surface and bottom of the impoundment are required.

At the beginning of the spring, the reservoir is assumed to be in an isothermal state, so the initial condition is given by

$$T = T_{in} \text{ for all } y \text{ at } t = 0 \quad (4.36)$$

where

$$T_{in} = \text{initial temperature of water in the reservoir, } ^\circ\text{C.}$$

At the water surface of the reservoir, the extra heat sources and sinks absorbed by the surface layer are equal to the amount of heat from external solar energy sources except by transmission. Thus, the surface boundary condition is

$$\phi_s = \beta\phi_{sn} + \phi_{ar} - \phi_w - \phi_e - \phi_c \text{ at } y = y_s \quad (4.37)$$

Therefore, the conservation of heat equation for the surface layer is given as

$$\begin{aligned} \frac{\partial T}{\partial t} = & \frac{1}{A} (U_i B T_i - U_o B T) - \frac{1}{\rho C_h A} \frac{\partial (A \phi_{sy})}{\partial y} + \frac{1}{A \Delta y} (VAT) \\ & - \frac{D_t}{A \Delta y} (A \frac{\partial T}{\partial y}) + \frac{1}{\rho C_h A \Delta y} (A \phi_s) \end{aligned} \quad (4.38)$$

At the bottom of the reservoir, there is no heat flow through the bottom of the reservoir. Therefore, the bottom boundary condition is expressed as

$$\frac{\partial T}{\partial y} = 0 \text{ at } y = y_b \text{ for all } t \quad (4.39)$$

and the conservation of heat equation for the bottom layer is

$$\begin{aligned} \frac{\partial T}{\partial t} = & \frac{1}{A} (U_i B T_i - U_o B T) - \frac{1}{\rho C_h A \Delta y} (A \phi_{sy}) - \frac{1}{A \Delta y} (VAT) \\ & + \frac{D_t}{A \Delta y} (A \frac{\partial T}{\partial y}) \end{aligned} \quad (4.40)$$

The outflow temperature at any time  $t$  is obtained by the weighted average of flow rates and temperatures of all the layers within the withdrawal layer thickness.

#### 4. Solution of the Temperature Model

There is no analytical way of solving the Equation (4.35), subject to the initial and boundary conditions mentioned, so a finite difference method is used.

There are three basic finite difference methods:

- 1) explicit or forward difference scheme,
- 2) implicit or backward difference scheme,

3) a combination of the first two which also results in an implicit method.

Implicit methods are unconditionally stable for any time step used in the solution but require more complicated methods of solution. Explicit methods are subject to certain stability requirements which can restrict the time step used in the solution, but the explicit methods have the advantage of keeping separate the various terms in the equation, which facilitates alterations and corrections to the model. Therefore, the explicit scheme is used in this study.

The use of an explicit scheme causes limitations imposed on the choice of  $\Delta y$  and  $\Delta t$  if numerical stability is to be maintained. The stability criteria can be expressed as

$$V \frac{\Delta t}{\Delta y} < 1 \quad (4.41)$$

where

$V$  = vertical velocity, m/day

$\Delta t$  = time increment, day

$\Delta y$  = distance increment, m

At the beginning of the calculation, a value of  $\Delta y$  and a reasonable value of  $\Delta t$  are assumed. Since it is possible that the choice of  $\Delta y$  and  $\Delta t$  may lead to violation of Equation (4.41), thus for each time step the vertical velocities are calculated and the maximum is selected. If Equation (4.41) is violated, a new  $\Delta t$  is selected such that  $n$  times new  $\Delta t$  is less than or equal to the previous time interval chosen, where  $n$  is a positive integer number.

Referring to Figure 7, the conservation of heat equation for the surface layer can be formulated in finite difference form as follows:

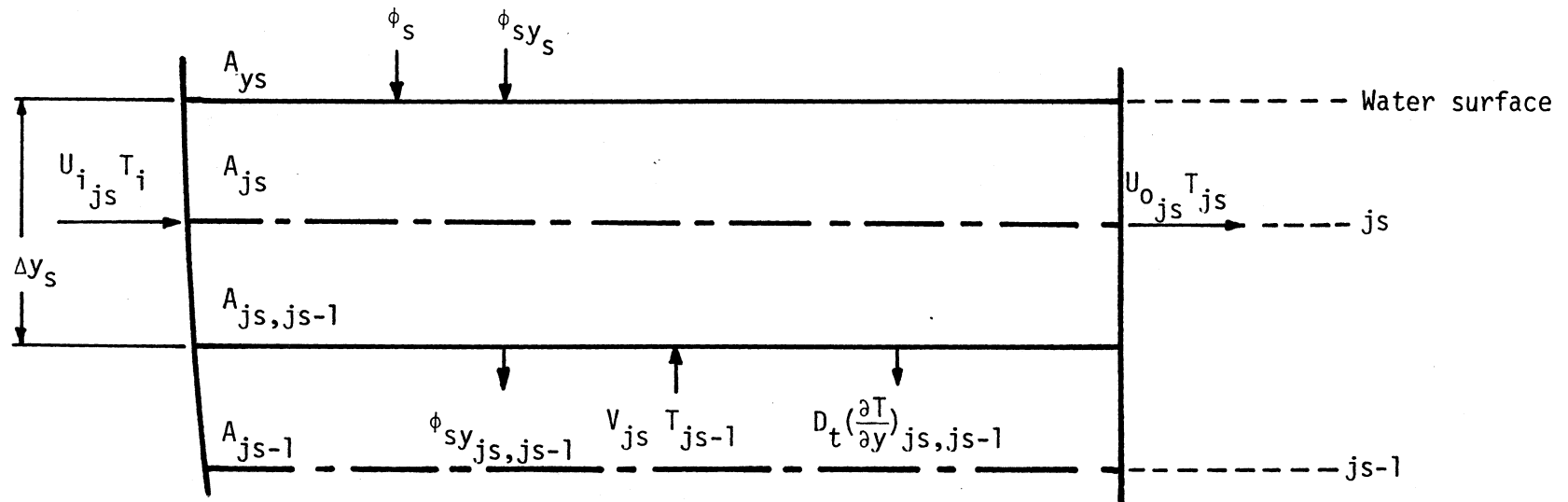


Figure 7. Conservation of Heat of the Surface Layer



The horizontal advective heat flux:

$$\Delta T_h = \frac{1}{A_{sa}} (U_{i_{js}} B_{js} T_i - U_{o_{js}} B_{js} T_{js}) \Delta t \quad (4.42)$$

where

$\Delta T_h$  = temperature change due to horizontal advective heat flux,  $^{\circ}\text{C}$

$A_{sa}$  = average horizontal area of surface layer,  $\text{m}^2$

The transmission of solar radiation:

$$\Delta T_t = \frac{1}{\rho C_h A_{sa} \Delta y_s} (A_{ys} \phi_{sy_s} - A_{js,js-1} \phi_{sy_{js,js-1}}) \Delta t \quad (4.43)$$

where

$\Delta T_t$  = temperature change due to transmission of radiation,  $^{\circ}\text{C}$

$\Delta y_s$  = thickness of surface layer, m

The vertical advective heat flux:

If  $V_{js} > 0$

$$\Delta T_v = \frac{1}{A_{sa} \Delta y_s} (V_{js} A_{js,js-1} T_{js-1}) \Delta t \quad (4.44)$$

where

$\Delta T_v$  = temperature change due to vertical advective heat flux,  $^{\circ}\text{C}$

If  $V_{js} < 0$

$$\Delta T_v = \frac{1}{A_{sa} \Delta y_s} (V_{js} A_{js,js-1} T_{js}) \Delta t \quad (4.45)$$

The diffusive heat flux:

$$\Delta T_d = - \frac{D_t}{A_{sa} \Delta y_s} (A_{js,js-1} \frac{(T_{js} - T_{js-1})}{\Delta y}) \Delta t \quad (4.46)$$

where

$\Delta T_d$  = change of temperature due to diffusion of heat,  $^{\circ}\text{C}$

The heat from external solar energy sources:

$$\Delta T_s = \frac{1}{\rho C_h A_{sa} \Delta y_s} (A_{ys} \phi_s) \Delta t \quad (4.47)$$

where

$\Delta T_s$  = change of temperature due to external solar energy sources,  $^{\circ}\text{C}$

Therefore, the total temperature change in the surface layer  $\Delta T_{sur}$ , in time increment  $\Delta t$ , is given by

$$\Delta T_{sur} = (\Delta T_h + \Delta T_t + \Delta T_v + \Delta T_d + \Delta T_s) \quad (4.48)$$

The conservation of heat equation for the internal layer can be represented in finite difference scheme, by considering the control volume in Figure 8, as follows:

The horizontal advective heat flux:

$$\Delta T_h = \frac{1}{A_j} (U_{i,j} B_j T_i - U_{o,j} B_j T_j) \Delta t \quad (4.49)$$

The transmission of solar radiation:

$$\Delta T_t = \frac{1}{\rho C_h A_j \Delta y} (A_{j+1,j} \phi_{sy_{j+1,j}} - A_{j,j-1} \phi_{sy_{j,j-1}}) \Delta t \quad (4.50)$$

The vertical advective heat flux:

If  $V_j > 0$ ,  $V_{j+1} > 0$

$$\Delta T_v = \frac{1}{A_j \Delta y} (V_j A_{j,j-1} T_{j-1} - V_{j+1} A_{j+1,j} T_j) \Delta t \quad (4.51)$$

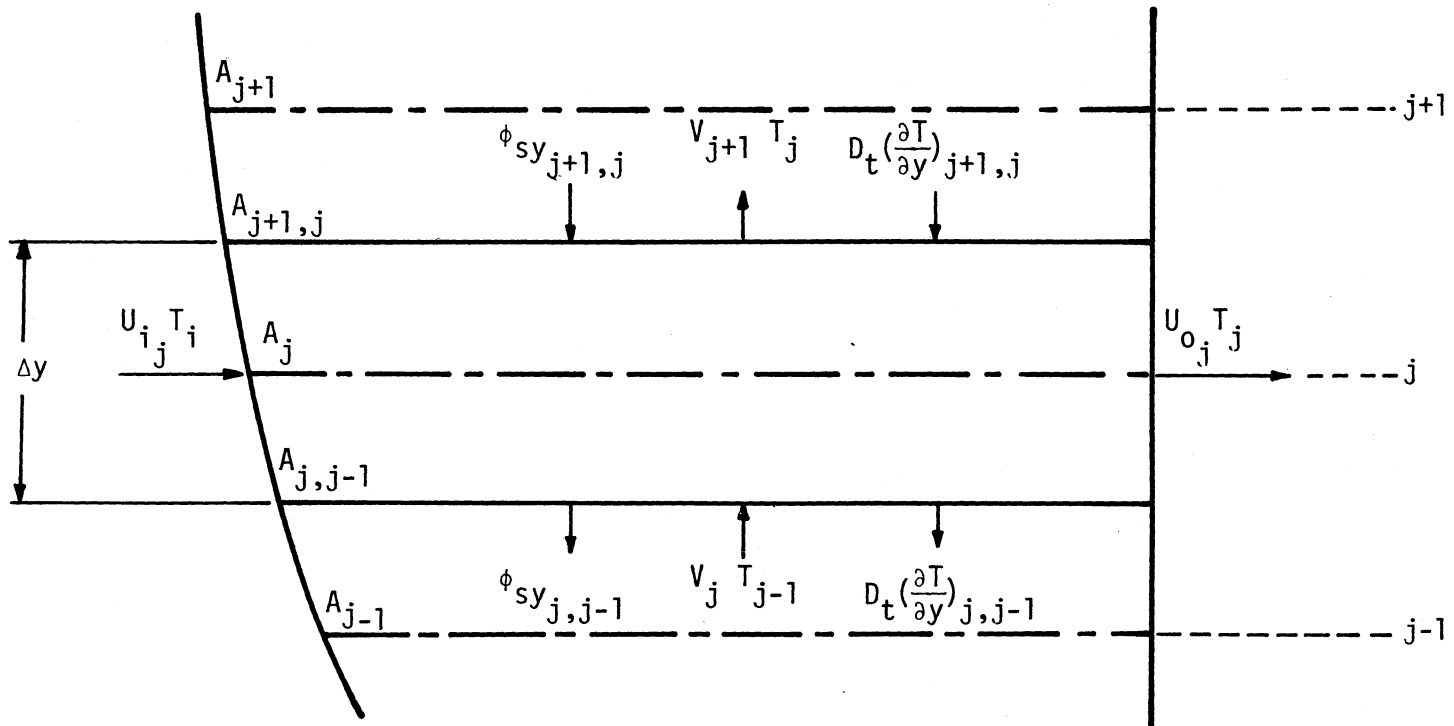


Figure 8. Conservation of Heat of the Internal Element

If  $V_j > 0$ ,  $V_{j+1} < 0$

$$\Delta T_v = \frac{1}{A_j \Delta y} (V_j A_{j,j-1} T_{j-1} - V_{j+1} A_{j+1,j} T_{j+1}) \Delta t \quad (4.52)$$

If  $V_j < 0$ ,  $V_{j+1} > 0$

$$\Delta T_v = \frac{1}{A_j \Delta y} (V_j A_{j,j-1} T_j - V_{j+1} A_{j+1,j} T_j) \Delta t \quad (4.53)$$

If  $V_j < 0$ ,  $V_{j+1} < 0$

$$\Delta T_v = \frac{1}{A_j \Delta y} (V_j A_{j,j-1} T_j - V_{j+1} A_{j+1,j} T_{j+1}) \Delta t \quad (4.54)$$

The diffusive heat flux:

$$\Delta T_d = \frac{D_t}{A_j \Delta y} (A_{j+1,j} \frac{(T_{j+1} - T_j)}{\Delta y} - A_{j,j-1} \frac{(T_j - T_{j-1})}{\Delta y}) \Delta t \quad (4.55)$$

Thus, the total temperature change of each internal layer  $\Delta T_{int}$ , in time increment  $\Delta t$ , is represented by

$$\Delta T_{int} = \Delta T_h + \Delta T_t + \Delta T_v + \Delta T_d \quad (4.56)$$

The conservation of heat equation for the bottom layer can be formulated in finite difference form as shown in Figure 9, as follows:

The horizontal advective heat flux:

$$\Delta T_h = \frac{1}{A_b} (U_{i1} B_1 T_i - U_{o1} B_1 T_1) \Delta t \quad (4.57)$$

where

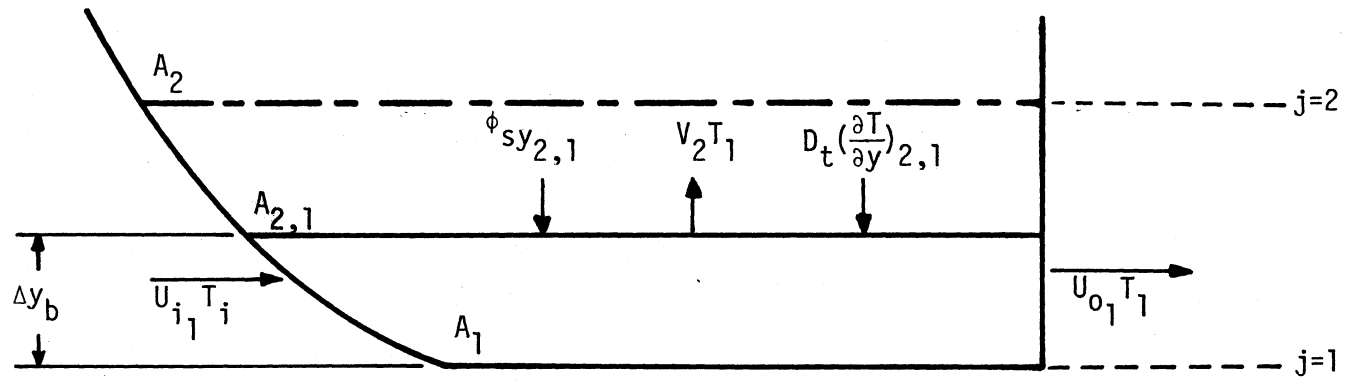


Figure 9. Conservation of Heat of the Bottom Layer

$A_b$  = average horizontal area of bottom layer,  $m^2$ .

The transmission of solar radiation:

$$\Delta T_t = \frac{1}{\rho C_h A_b \Delta y_b} (A_{2,1} \phi_{sy_{2,1}}) \Delta t \quad (4.58)$$

where

$$\Delta y_b = \Delta y / 2$$

The vertical advective heat flux:

If  $V_2 > 0$

$$\Delta T_v = - \frac{1}{A_b \Delta y_b} (V_2 A_{2,1} T_1) \Delta t \quad (4.59)$$

If  $V_2 < 0$

$$\Delta T_v = - \frac{1}{A_b \Delta y_b} (V_2 A_{2,1} T_2) \Delta t \quad (4.60)$$

The diffusive heat flux:

$$\Delta T_d = \frac{D_t}{A_b \Delta y_b} (A_{2,1} \frac{(T_2 - T_1)}{\Delta y}) \Delta t \quad (4.61)$$

The total temperature change of the bottom layer  $\Delta T_b$ , in time increment  $\Delta t$ , is given by

$$\Delta T_b = \Delta T_h + \Delta T_t + \Delta T_v + \Delta T_d \quad (4.62)$$

In using the temperature model, the data required as inputs to the model are reservoir geometry, initial reservoir temperature profile, solar radiation, atmospheric radiation, air temperatures, relative

humidities, wind speeds, streamflow rates, streamflow temperatures, outflow rates, surface elevations, inflow standard deviation, coefficient of diffusion of heat, density and specific heat of water, extinction coefficient of water, and fraction of solar radiation absorbed at the surface.

## B. Development and Solution of Water

### Quality Model

The depletion of dissolved oxygen in lakes and impoundments, especially in the deeper layers, can substantially reduce the usefulness of the impounded water. In addition, waters containing low D.O. concentrations that are released from the impoundments may harm the receiving streams.

During the periods of thermal stratification, the D.O. concentrations within the epilimnion remain high because of air-water oxygen transfer and photosynthetic oxygenation. When D.O. concentrations in the surface water fall below saturation, oxygen is transferred from the air into the water while the reverse is true when oxygen concentrations exceed the saturation value. So, D.O. concentrations at the surface often remain close to saturation. The low vertical mixing across the thermocline usually results in a small transfer of D.O. from the upper layers to the hypolimnion zone. In addition, plankton which sink from the epilimnion and other organics, exert an oxygen demand on the deeper water which results in the decline of D.O. concentrations in the hypolimnion zone.

In terms of an overall mass balance of dissolved oxygen, the D.O. balance in a reservoir is dependent on the inflows and outflows D.O.,

oxygen demands of river inflows, initial D.O. and oxygen demand in the reservoir, diffusion and vertical advection of mass, decomposition of organic matter, atmospheric reaeration at the surface, photosynthetic oxygenation, algal respiration and bottom deposits. In addition, the biological and mass transfer processes are sensitive to temperature and thus the D.O. balance is also dependent on the thermal structure of the reservoir.

The water quality model developed in this study is to predict the D.O. concentrations of the outflows and the concentration distributions of D.O. in a deep reservoir in which the isotherms are horizontal during most of the year. Because the horizontal variations of D.O. are often small when compared to the vertical variations and the variations that occur with time, therefore the assumptions used in developing the water quality model are the same as that of the temperature model. In addition, it is also assumed that, in euphotic zone, the rate of oxygen produced by photosynthesis is equal to the rate of oxygen consumed by algal respiration and the respiration of organic matter.

In this model, the reservoir is also divided into horizontal layers of uniform thickness, extending over the entire length and width of the reservoir. The governing equation for the concentration distributions of D.O. is formulated by considering the conservation of mass within each layer and it is coupled with the temperature model in such a way that the velocity distributions used in the temperature model can be used in the water quality model. However, before this can be done, it is necessary to consider the parameters involved in the D.O. balance in a reservoir such as horizontal advection of D.O. and BOD, diffusion and advection of mass in the vertical direction, and BOD removal.



## 1. Determination of Parameters

By the use of the control volume as shown in Figure 10, all the parameters involved in the conservation of D.O. and BOD equations are determined as follows:

The amount of D.O. advected in the control volume by inflow is

$$M_i = (\rho C_i U_i B \Delta y) 10^{-6} \quad (4.63)$$

where

$M_i$  = the amount of D.O. advected in by inflow, kg/day

$\rho$  = water density, kg/m<sup>3</sup>

$C_i$  = inflow D.O. concentration, ppm

$U_i$  = inflow velocity, m/day

$B$  = width of the control volume, m

$\Delta y$  = thickness of the control volume, m

The amount of D.O. advected out of the control volume by the outflow is

$$M_o = (\rho C U_o B \Delta y) 10^{-6} \quad (4.64)$$

where

$M_o$  = the amount of D.O. advected out by the outflow, kg/day

$C$  = D.O. concentration within the control volume, ppm

$U_o$  = outflow velocity, m/day

D.O. advected in the control volume by vertical advection is

$$M_v = (\rho C V A) 10^{-6} \quad (4.65)$$

where

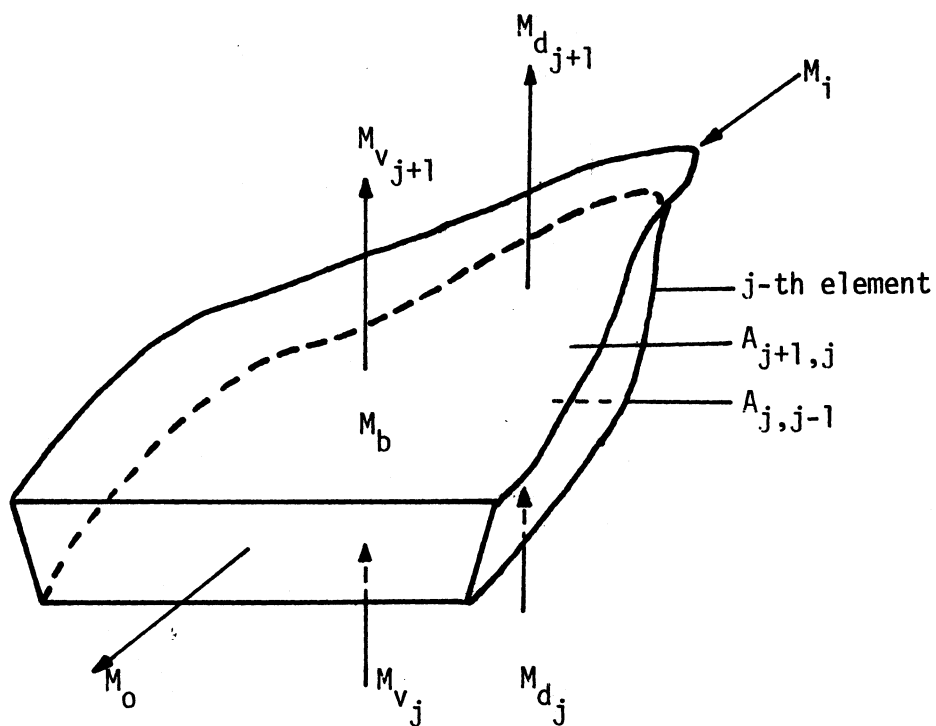


Figure 10. Control Volume for Dissolved Oxygen Balance

$M_v$  = the amount of D.O. advected in by vertical advection, kg/day

$V$  = vertical velocity, m/day (positive upward)

$A$  = horizontal area of the control volume,  $m^2$

The flux of D.O. into the control volume by diffusion is

$$M_d = - (\rho D_m A \frac{\partial C}{\partial y}) 10^{-6} \quad (4.66)$$

where

$M_d$  = the amount of D.O. diffused into the control volume, kg/day

$D_m$  = molecular diffusivity of mass,  $m^2/\text{day}$

The negative sign indicates positive transport in the direction of the negative gradient.

The amount of oxygen consumed by the removal of BOD is

$$M_b = (\rho k_1 \ell A \Delta y) 10^{-6} \quad (4.67)$$

where

$M_b$  = the amount of oxygen consumed, kg/day

$k_1$  = first order decay rate constant,  $\text{day}^{-1}$

$\ell$  = BOD concentration

Convective mixing due to surface instability because of the evaporation and water surface radiation exceeds the solar radiation and atmospheric radiation absorbed at the surface will be treated the same as that used in the temperature model. Therefore, D.O. concentration of the mixed layer is obtained by the weighted average of D.O. concentration and volume of the layers that are mixed.

All of the above formulas used to calculate the amount of D.O. can be used to calculate the amount of BOD by replacing  $C$  with  $\ell$  and no other changes are necessary.

## 2. Derivation of Governing Equations

The conservation of D.O. equation of the control volume as shown in Figure 10 can be obtained by equating the time rate of change of D.O. concentration within the control volume to the sum of all D.O. inputs and removed from that control volume.

The time rate change of D.O. concentration within the control volume,  $M_t$ , is given by

$$M_t = (\rho A \Delta y \frac{\partial C}{\partial t}) 10^{-6} \quad (4.68)$$

The net horizontal advection of D.O. through the control volume,  $\Delta M_h$ , is expressed as

$$\Delta M_h = M_i - M_o = \rho B \Delta y (C_i U_i - C U_o) 10^{-6} \quad (4.69)$$

The difference of vertical advection of D.O. through the control volume,  $\Delta M_v$ , is represented by

$$\begin{aligned} \Delta M_v &= M_v - (M_v + \frac{\partial M_v}{\partial y} \Delta y) \\ &= - \frac{\partial M_v}{\partial y} \cdot \Delta y \end{aligned} \quad (4.70)$$

The change of D.O. due to diffusion through the control volume,  $\Delta M_d$ , is obtained by

$$\begin{aligned} \Delta M_d &= M_d - (M_d + \frac{\partial M_d}{\partial y} \Delta y) \\ &= - \frac{\partial M_d}{\partial y} \Delta y \end{aligned} \quad (4.71)$$

Therefore, the conservation of dissolved oxygen equation is given by

$$\begin{aligned}
 (\rho A \Delta y \frac{\partial C}{\partial t}) 10^{-6} &= \rho B \Delta y (C_i U_i - C U_o) 10^{-6} - \frac{\partial M_v}{\partial y} \Delta y - \frac{\partial M_d}{\partial y} \Delta y \\
 &- (\rho k_1 \ell A \Delta y) 10^{-6}
 \end{aligned} \tag{4.72}$$

which, when simplified, yields

$$\frac{\partial C}{\partial t} = \frac{B}{A} (C_i U_i - C U_o) - \frac{1}{A} \frac{\partial V C A}{\partial y} + \frac{D_m}{A} \frac{\partial}{\partial y} (A \frac{\partial C}{\partial y}) - k_1 \ell \tag{4.73}$$

Because the concentration distribution of D.O. is dependent on the concentration distribution of BOD, the governing equation for the concentration distribution of BOD must be known, which can be obtained by replacing C with  $\ell$  in Equation (4.73). Therefore, the conservation of BOD equation is given by

$$\frac{\partial \ell}{\partial t} = \frac{B}{A} (\ell_i U_i - \ell U_o) - \frac{1}{A} \frac{\partial V \ell A}{\partial y} + \frac{D_m}{A} \frac{\partial}{\partial y} (A \frac{\partial \ell}{\partial y}) - k_1 \ell \tag{4.74}$$

In order to solve Equations (4.73) and (4.74), the initial conditions which specify the values of D.O. and BOD as functions of depth at time  $t = 0$  and boundary conditions which give the values of D.O. and BOD as functions of time at the surface and bottom of the reservoir are required.

The initial conditions for D.O. and BOD are the D.O. and BOD profiles at time  $t = 0$ .

The surface boundary condition for D.O. is assumed to be saturated with D.O. because D.O. concentrations at the surface often remain close

to saturation. Therefore,

$$C = C_{\text{sat}} \quad \text{at } y = y_s \quad (4.75)$$

where

$$C_{\text{sat}} = \text{D.O. saturation, ppm}$$

and the surface boundary condition for BOD is obtained by assuming that there is no transfer of BOD across the water surface. Thus,

$$\frac{\partial \ell}{\partial y} = 0 \quad \text{at } y = y_s \quad \text{for all } t \quad (4.76)$$

Since there is no transfer of mass across the bottom of the reservoir, so the bottom boundary conditions for D.O. and BOD are

$$\frac{\partial C}{\partial y} = 0 \quad \text{at } y = y_b \quad \text{for all } t \quad (4.77)$$

and

$$\frac{\partial \ell}{\partial y} = 0 \quad \text{at } y = y_b \quad \text{for all } t \quad (4.78)$$

The outflow D.O. concentration at any time  $t$  is obtained by the weighted average of D.O. concentrations and flow rates of all the layers within the withdrawal layer thickness.

### 3. Solution of the Water Quality Model

In general, analytical solutions to Equations (4.73) and (4.74) subject to the initial and boundary conditions mentioned, cannot be presently obtained except for some simplified versions such as assuming steady state condition. Therefore, the finite difference method is used in a

manner similar to that used in the temperature model.

The conservation of D.O. equation for the surface layer is

$$C = C_{sat} \quad (4.78)$$

Consider the control volume in Figure 11, the conservation of BOD equation for the surface layer can be formulated in finite difference form as follows:

The horizontal advection of BOD:

$$\Delta B_h = \frac{B_{js}}{A_{sa}} (\ell_i U_{i_{js}} - \ell_{js} U_{o_{js}}) \Delta T \quad (4.79)$$

where

$\Delta B_h$  = change of BOD due to horizontal advection, ppm

The vertical advection of BOD:

If  $V_{js} > 0$

$$\Delta B_v = \frac{1}{A_{sa} \Delta y_s} (V_{js} \ell_{js-1} A_{js,js-1}) \Delta t \quad (4.80)$$

If  $V_{js} < 0$

$$\Delta B_v = \frac{1}{A_{sa} \Delta y_s} (V_{js} \ell_{js} A_{js,js-1}) \Delta t \quad (4.81)$$

where

$\Delta B_v$  = change of BOD due to vertical advection, ppm.

The diffusion of BOD:

$$\Delta B_d = - \frac{D_m}{A_{sa} \Delta y_s} (A_{js,js-1} \frac{(\ell_{js} - \ell_{js-1})}{\Delta y}) \Delta t \quad (4.82)$$

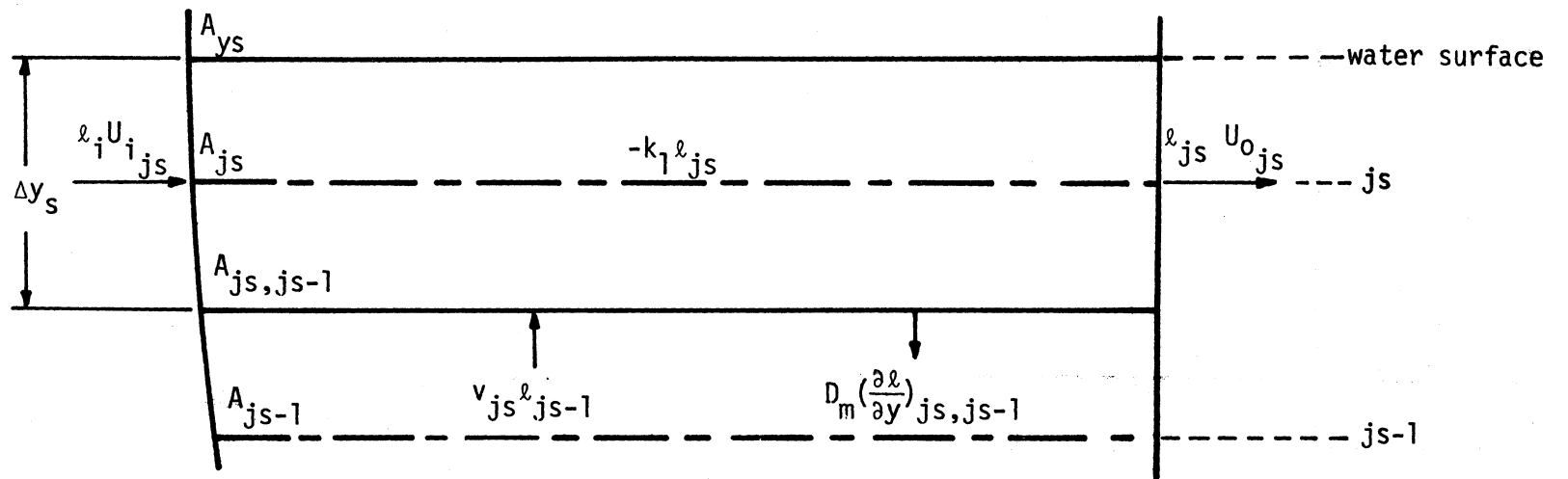


Figure 11. Conservation of BOD of the Surface Layer



where

$\Delta B_d$  = change of BOD due to diffusion, ppm.

The removal of BOD:

$$\Delta B_r = - (k_1 l_{j_s}) \Delta t \quad (4.83)$$

Therefore, the total BOD concentration change in the surface layer  $\Delta B_{sur}$ , in time increment  $\Delta t$ , is given by

$$\Delta B_{sur} = \Delta B_h + \Delta B_v + \Delta B_d + \Delta B_r \quad (4.84)$$

Referring to the control volume in Figure 12, the conservation of D.O. equation for the internal layer can be represented in finite difference scheme as follows:

The horizontal advection of D.O.:

$$\Delta C_h = \frac{B_j}{A_j} (C_i U_{i_j} - C_j U_{o_j}) \Delta t \quad (4.85)$$

where

$\Delta C_h$  = change of D.O. due to horizontal advection, ppm.

The vertical advection of D.O.:

If  $V_j > 0$ ,  $V_{j+1} > 0$

$$\Delta C_v = \frac{1}{A_j \Delta y} (V_j C_{j-1} A_{j,j-1} - V_{j+1} C_j A_{j+1,j}) \Delta t \quad (4.86)$$

If  $V_j > 0$ ,  $V_{j+1} < 0$

$$\Delta C_v = \frac{1}{A_j \Delta y} (V_j C_{j-1} A_{j,j-1} - V_{j+1} C_{j+1} A_{j+1,j}) \Delta t \quad (4.87)$$

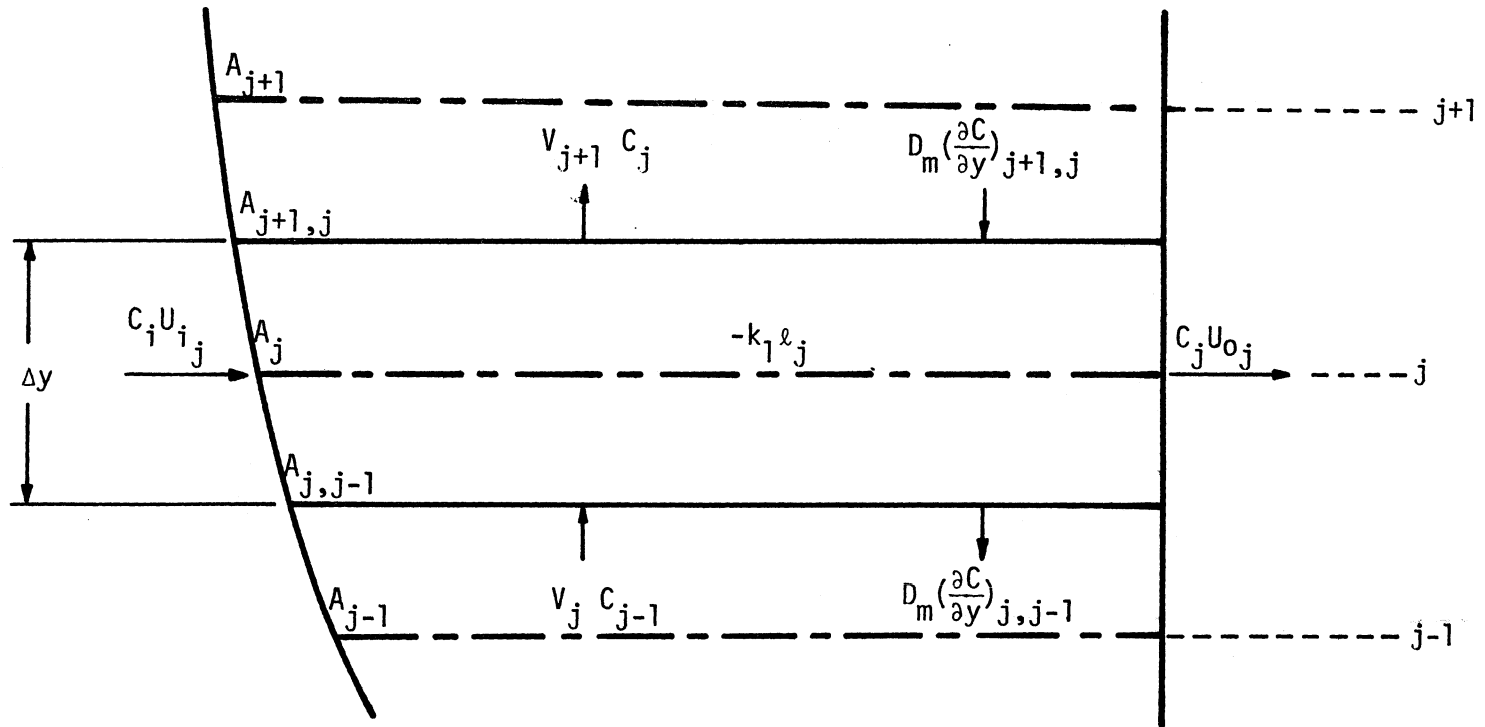


Figure 12. Conservation of D.O. of the Internal Element

If  $V_j < 0$ ,  $V_{j+1} > 0$

$$\Delta C_v = \frac{1}{A_j \Delta y} (V_j C_j A_{j,j-1} - V_{j+1} C_{j+1} A_{j+1,j}) \Delta t \quad (4.88)$$

If  $V_j < 0$ ,  $V_{j+1} < 0$

$$\Delta C_v = \frac{1}{A_j \Delta y} (V_j C_j A_{j,j-1} - V_{j+1} C_{j+1} A_{j+1,j}) \Delta t \quad (4.89)$$

where

$\Delta C_v$  = change of D.O. due to vertical advection, ppm.

The diffusion of D.O.:

$$\Delta C_d = \frac{D_m}{A_j \Delta y} (A_{j+1,j} \frac{(C_{j+1} - C_j)}{\Delta y} - A_{j,j-1} \frac{(C_j - C_{j-1})}{\Delta y}) \Delta t \quad (4.90)$$

where

$\Delta C_d$  = change of D.O. due to diffusion, ppm

The removal of BOD:

$$\Delta C_r = - (k_1 l_j) \Delta t \quad (4.91)$$

where

$\Delta C_r$  = amount of oxygen consumed by the removal of BOD, ppm.

Thus, the total change of D.O. in each internal layer  $\Delta C_{int}$ , in time increment  $\Delta t$ , is expressed as

$$\Delta C_{int} = \Delta C_h + \Delta C_v + \Delta C_d + \Delta C_r \quad (4.92)$$

The conservation of BOD equation for the internal layer can be ob-

tained by replacing  $C$  with  $\ell$  in Equations (4.85) to (4.91) with no other changes necessary.

The conservation of D.O. equation for the bottom layer can be represented in finite difference form as shown in Figure 13, as follows:

The horizontal advection of D.O.:

$$\Delta C_h = \frac{B_1}{A_b} (C_i U_{i_1} - C_1 U_{o_1}) \Delta t \quad (4.93)$$

The vertical advection of D.O.:

If  $V_2 > 0$

$$\Delta C_v = - \frac{1}{A_b \Delta y_b} (V_2 C_1 A_{2,1}) \Delta t \quad (4.94)$$

If  $V_2 < 0$

$$\Delta C_v = - \frac{1}{A_b \Delta y_b} (V_2 C_2 A_{2,1}) \Delta t \quad (4.95)$$

The diffusion of D.O.:

$$\Delta C_d = \frac{D_m}{A_b \Delta y_b} (A_{2,1} \frac{(C_2 - C_1)}{\Delta y}) \Delta t \quad (4.96)$$

The removal of BOD:

$$\Delta C_r = - (k_1 \ell_1) \Delta t \quad (4.97)$$

Therefore, the total change of D.O. for the bottom layer  $\Delta C_{bot}$  in time increment  $\Delta t$ , is given by

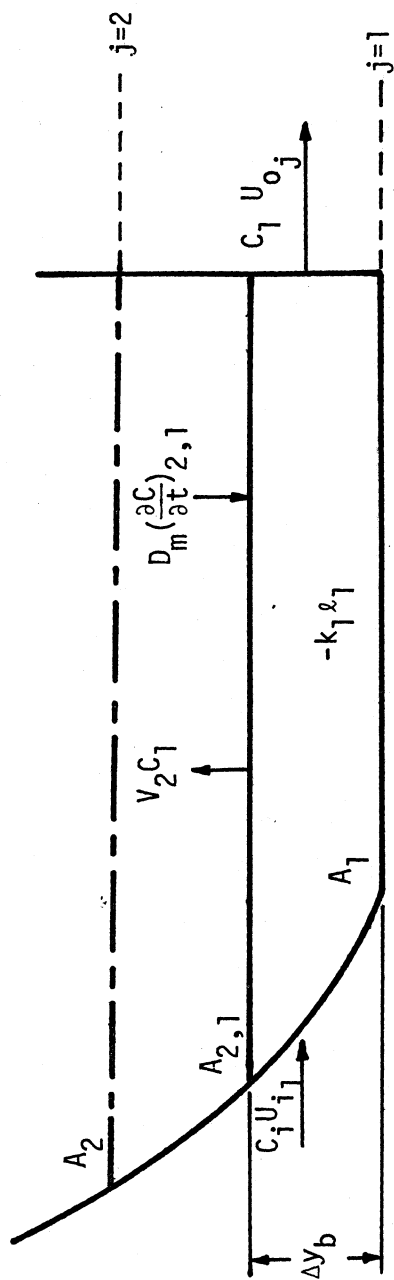


Figure 13. Conservation of D.O. of the Bottom Layer

$$\Delta C_{\text{bot}} = \Delta C_h + \Delta C_v + \Delta C_d + \Delta C_r \quad (4.98)$$

Again, the conservation of BOD equation for the bottom layer can be obtained by replacing  $C$  with  $\lambda$  in Equations (4.93) to (4.97), with no other changes necessary.

In using the water quality model, the data required as inputs to the model in addition to that required for the temperature model are initial D.O. and BOD profiles, inflows D.O. and BOD, and first order decay rate constant.

### C. Application of the Models

The models developed in this study are for predicting the temperature and D.O. variations of deep reservoirs with horizontal isotherms, low densimetric Froude number, and the hydrodynamics of the reservoirs are governed by thermal stratification.

The temperature distributions in a reservoir can be obtained by solving Equation (4.35) subject to the initial and boundary conditions mentioned, which are represented in finite difference form in Equations (4.48), (4.56), and (4.62).

The data required for solving the above equations are:

- 1) Reservoir geometry.
- 2) Meteorological data as solar radiation, air temperatures, relative humidities, wind speeds, and cloud cover.
- 3) Hydrological data as stream inflow rates and temperatures, and the desired reservoir outflow rates.
- 4) Initial temperature profile in the reservoir.
- 5) The extinction coefficient of water and the fraction of solar

radiation absorbed at the surface.

By solving Equations (4.73) and (4.74) subject to the initial and boundary conditions, which are in finite difference form in Equations (4.78), (4.84), (4.92), and (4.98), the D.O. concentration distributions in the reservoir can be obtained.

The required input data for the prediction of the D.O. concentration distributions are the data required for predicting the temperature distributions in the reservoir, and

- 1) The initial D.O. and BOD profiles in the reservoir.
- 2) The streamflow D.O. and BOD, and the first order decay rate constant.

## CHAPTER V

### RESULTS

#### A. Description of Reservoir

Fontana Reservoir, shown in Figure 14, which was selected for the verification of the mathematical models developed in this study, is located on the Little Tennessee River in western North Carolina. It is categorized as a low discharge to volume ratio type and is about 120 m. deep, narrow, approximately 46 kilometers long, and is fully stratified during the summer season. It is fed by three major rivers--the Little Tennessee, the Tuckasegee, the Nantahala, and several smaller streams and the runoff from the drainage area along the north and south bounds, which provide an average annual runoff of about  $3.69 \times 10^9$  cu. m. The drainage area is about  $4.0 \times 10^9$  m.<sup>2</sup> and the reservoir has the storage volume of  $1.78 \times 10^9$  cu. m. at elevation 513 m. above mean sea level.

#### B. Inputs to the Mathematical Models

During the year 1966, extensive field measurements were made to investigate the thermo-hydrodynamics of Fontana Reservoir (59). These data included all pertinent hydrological and meteorological parameters, temperature, and dissolved oxygen data on inflow, outflow, and the water in the reservoir. The data obtained from the field measurements at Fontana site were available either on an hourly mean or daily mean basis. The time step of one day was used in the computer program; therefore,



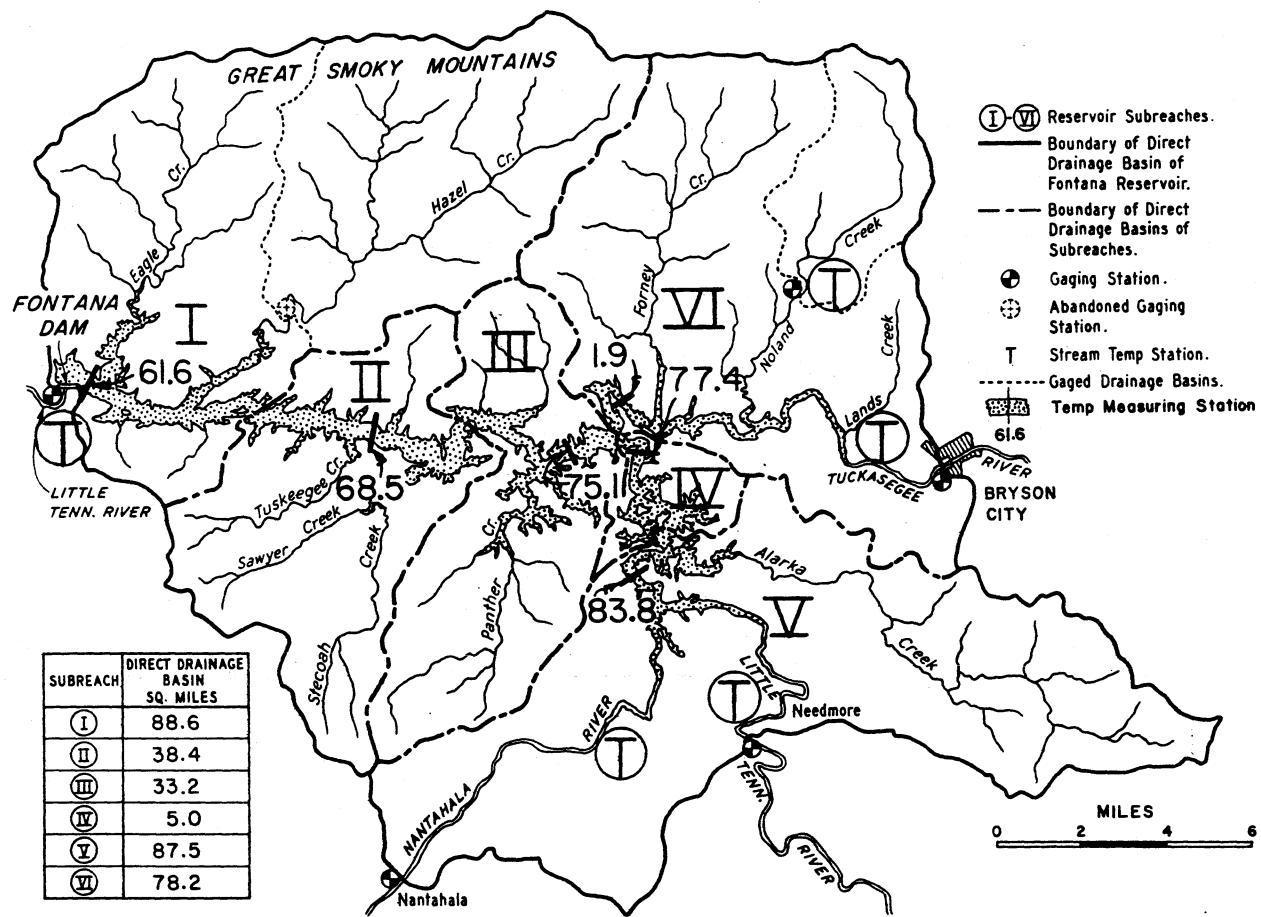


Figure 14. Map of Fontana Reservoir and Watershed

all of the hourly means data were converted to daily means.

Reservoir geometry such as lengths, widths, and areas were available at fifty foot intervals and the values of these geometric data at other elevations were obtained by linear interpolation.

The inflow rates, temperatures and dissolved oxygen of the five sources of water for the reservoir were available on a daily mean basis. The sum of the inflow rates of these sources of water were used as the inflow to the reservoir; the weighted average of the inflow temperatures and inflow rates from each of the five sources were used as the inflow temperatures, and the inflow D.O. was taken as the weighted average of the inflow D.O. and the inflow rates from each of the three rivers. The inflow standard deviation  $\sigma_i$  was estimated from dye tests which were made to investigate the inflow water movements in the Fontana Reservoir, as shown in Figure 6 in Chapter IV. The dye trace occupied in many cases, a depth of 40 ft or more. Therefore, the inflow standard deviation was assumed to be equal to 4.0 m. The inflow BOD ( $BOD_{in}$ ) during the time that the inflow D.O. was measured was not available. Some of the inflow BOD was sampled in 1965. The average values of five-day BOD of these samples were ranged from 0.8 to 1.7 ppm. However, in dealing with a reservoir, where water can be retained from several days to several months, at least a 21-day BOD should be used. Therefore, a constant inflow BOD of 8.0 ppm was at first assumed.

The outflow rates, temperatures, and D.O. were also available on a daily mean basis.

The temperature and D.O. profiles in the reservoir were measured periodically from April through November. The D.O. profile on March 1 was not available, but when considering the fact that on that day the

reservoir was isothermal and the measured outflow D.O. was 8.0 ppm. Therefore, the initial D.O. profile on March 1 would be 8.0 ppm. The BOD profile on March 1 or during the time that D.O. profiles were measured was also not available, therefore BOD values had to be assumed. Three initial BOD ( $BOD_0$ ) of 0, 1.0, and 3.0 were assumed for sensitivity analysis of the results.

The value of the first order decay rate constant,  $k_1$ , also had to be assumed. Two different values of 0.05 and 0.10  $\text{day}^{-1}$  were assumed for sensitivity analysis of the results.

The meteorological data, such as air temperatures, air vapor pressures, relative humidities, wind speeds, solar radiations, atmospheric radiations and cloudiness, obtained by the Tennessee Valley Authority, were available either on hourly means or daily means basis and all hourly means data were converted to daily means. The values of the light extinction coefficient,  $n$ , and the ratio of radiation absorbed at the water surface to net incoming radiation,  $\beta$ , were obtained from measurements in Fontana Reservoir, which were 0.7  $\text{m}^{-1}$  and 0.5, respectively.

### C. Results of the Temperature Model

Through the use of Equations (4.48), (4.56), and (4.62) in Chapter IV, the vertical temperature distributions of water in the reservoir were calculated daily from March to December, and the outflow temperatures were also calculated daily from March to December by the weighted average of the temperatures and outflow rates of all layers within the withdrawal layer thickness.

Because no field measurements of entrance mixing are available, five different values of mixing coefficients  $m_c$ , namely 0, 0.5, 1.0, 1.5,

and 2.0, were assumed for sensitivity of the results. The comparison of the predicted and measured temperature profiles for various days of the year are presented in Figures 15 through 21, and the predicted and measured outflow temperatures as functions of time are given on Figure 22. The sensitivity of the temperature profiles to the various values of mixing coefficients are also given in Figures 15 to 21, and that of the outflow temperatures are given in Figure 22 and Table II.

Considering the complex nature of the thermal stratification problem, the temperature model appeared to give a reasonable prediction of the reservoir performance over the yearly cycle of temperature change within the reservoir and in the outlet.

As shown in Figures 15 through 21, entrance mixing affects the predicted temperature profiles since the early stages of stratification through the end of the cooling period. Increasing the value of mixing coefficient from 0 to 1.0 has the effect of increasing the predicted temperatures of water in the reservoir. During the early stages of warming period, the effect of increasing the mixing coefficient from 0 to 1.0, as shown in Figures 15 and 16, was found to be insignificant. However, after the reservoir was well established in the stratification state and during the cooling period, the effect of increasing the values of the mixing coefficients was quite significant, as shown in Figures 17 to 21. In general, the overall pattern of the temperature profiles for both  $m_c = 0$  and 1.0 predicted by the model, agreed well with those measured; however, by using  $m_c = 1.0$ , better results were obtained.

The predicted outflow temperatures are also increased as the value of the mixing coefficient is increased, as shown in Figure 22 for the cases of  $m_c = 0, 1.0, \text{ and } 2.0$ , and in Table II, except during the early

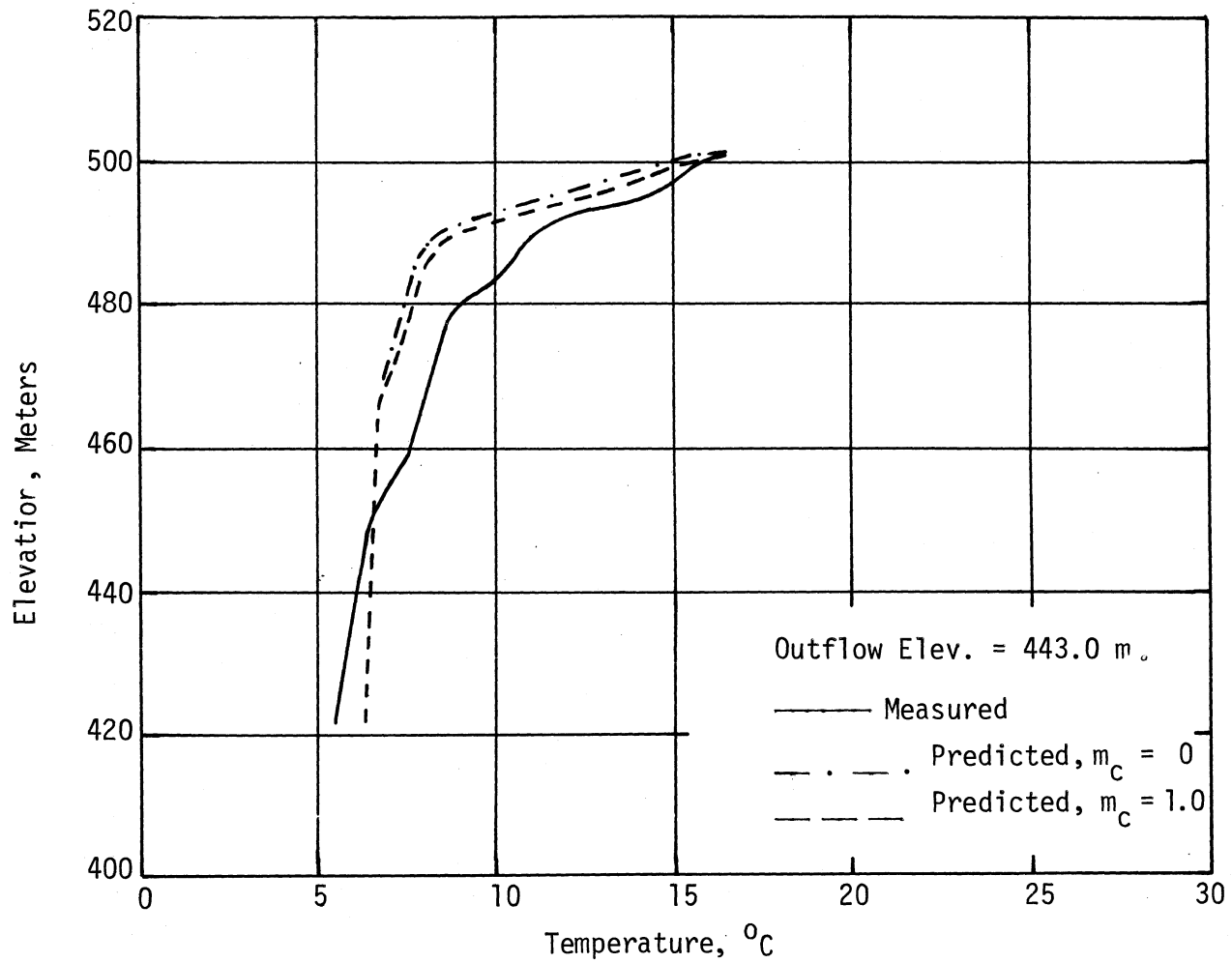


Figure 15. Measured and Predicted Temperature Profiles, Fontana Reservoir, April 27, 1966

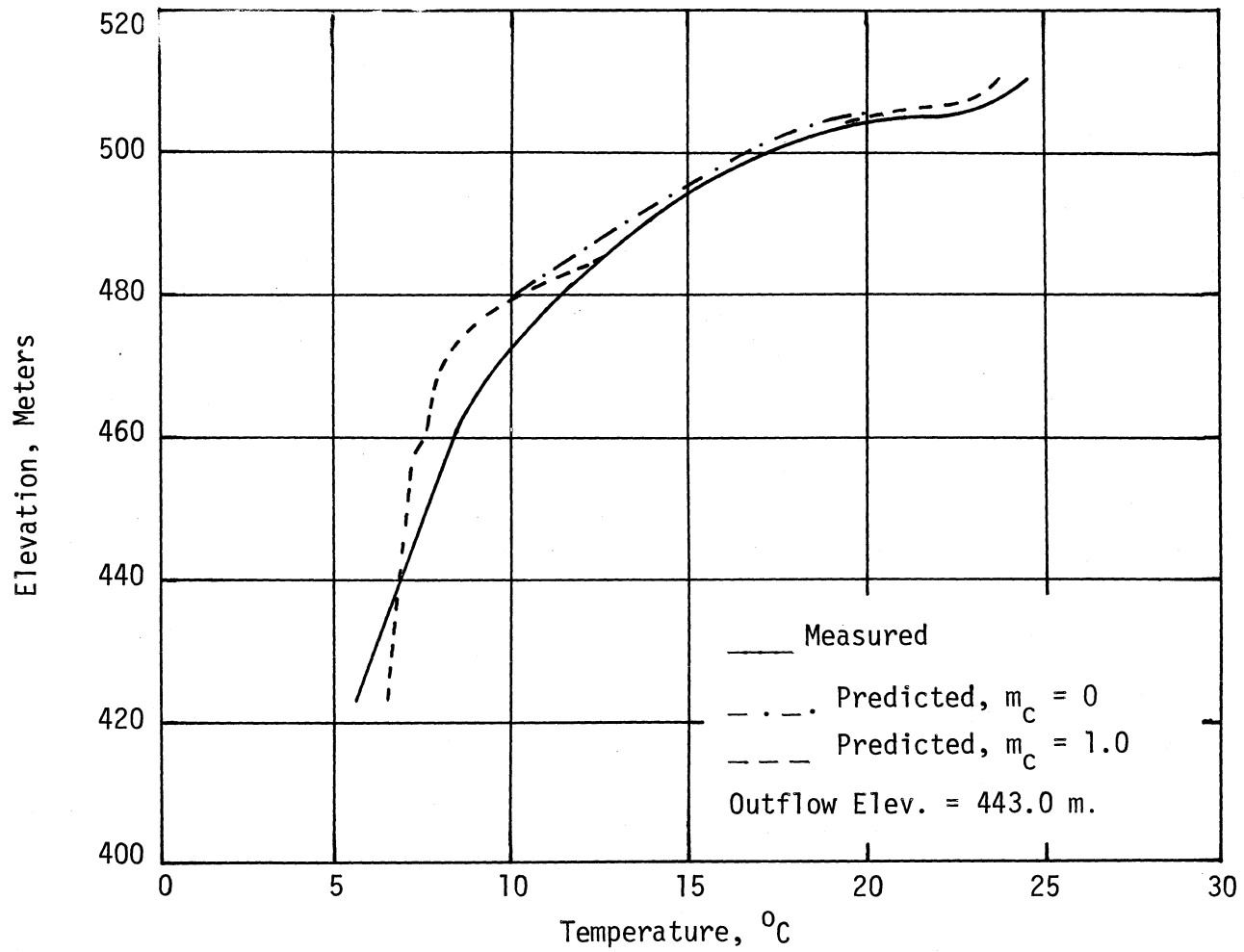


Figure 16. Measured and Predicted Temperature Profiles, Fontana Reservoir, June 22, 1966

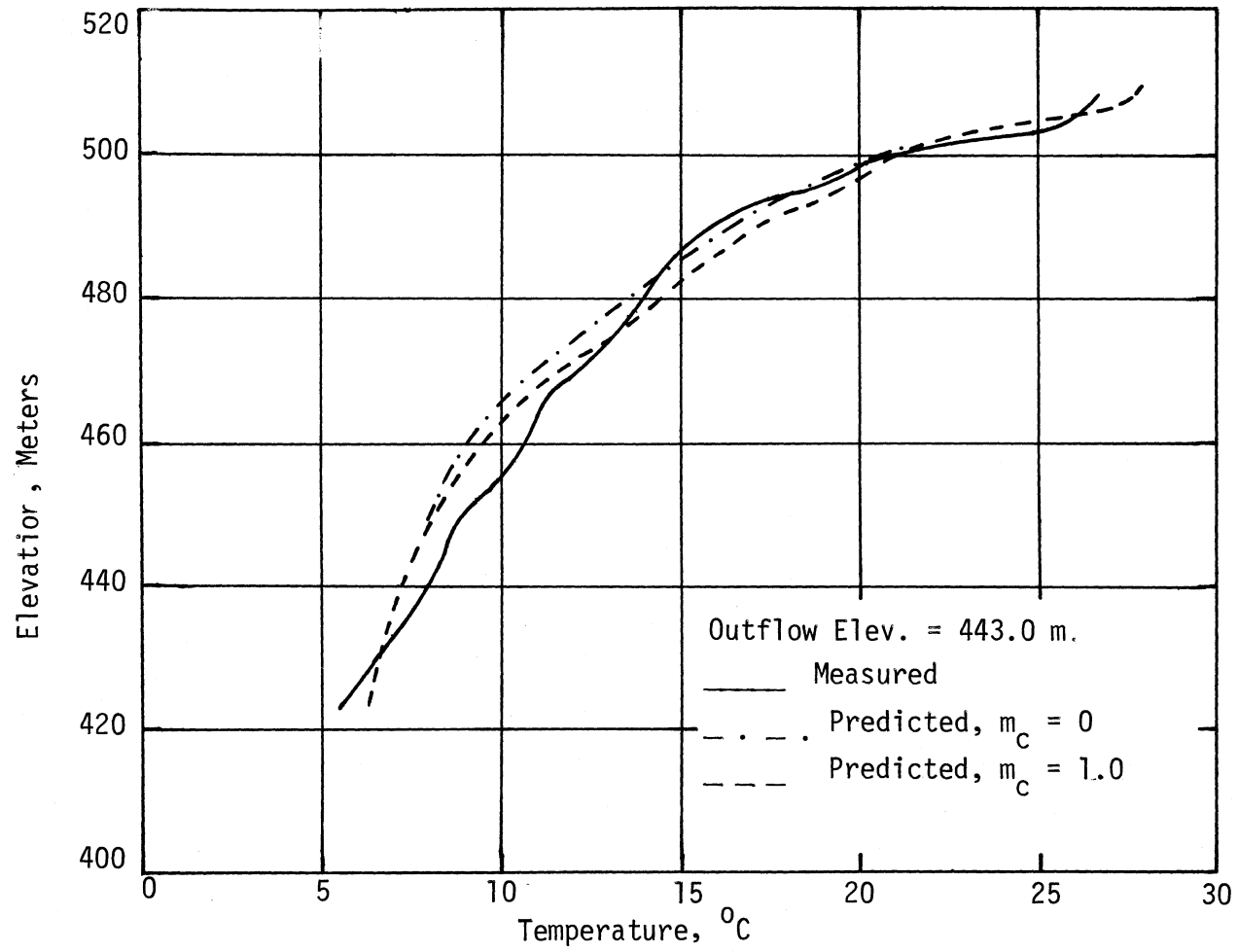


Figure 17. Measured and Predicted Temperature Profiles, Fontana Reservoir, July 20, 1966

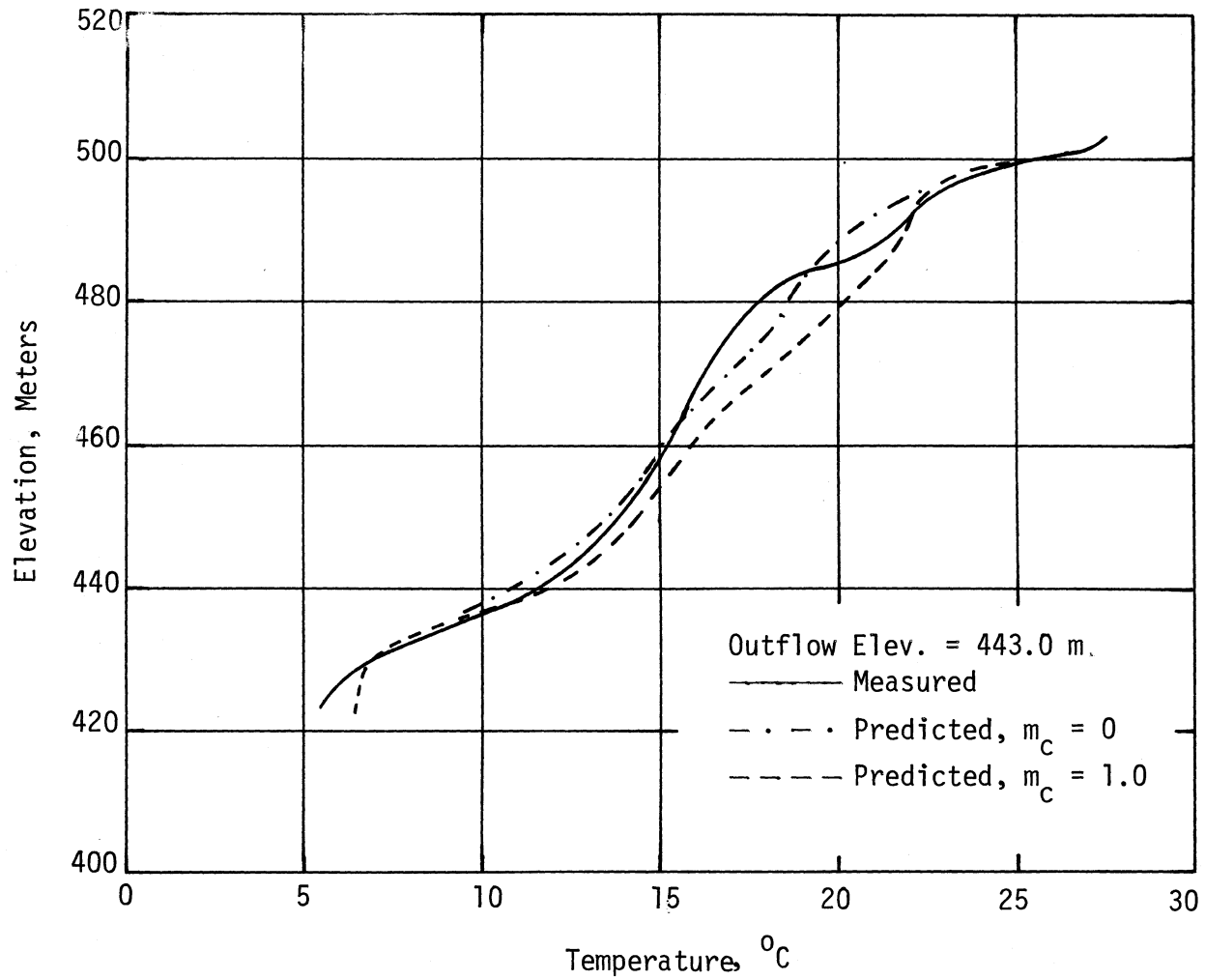


Figure 18. Measured and Predicted Temperature Profiles, Fontana Reservoir, August 17, 1966



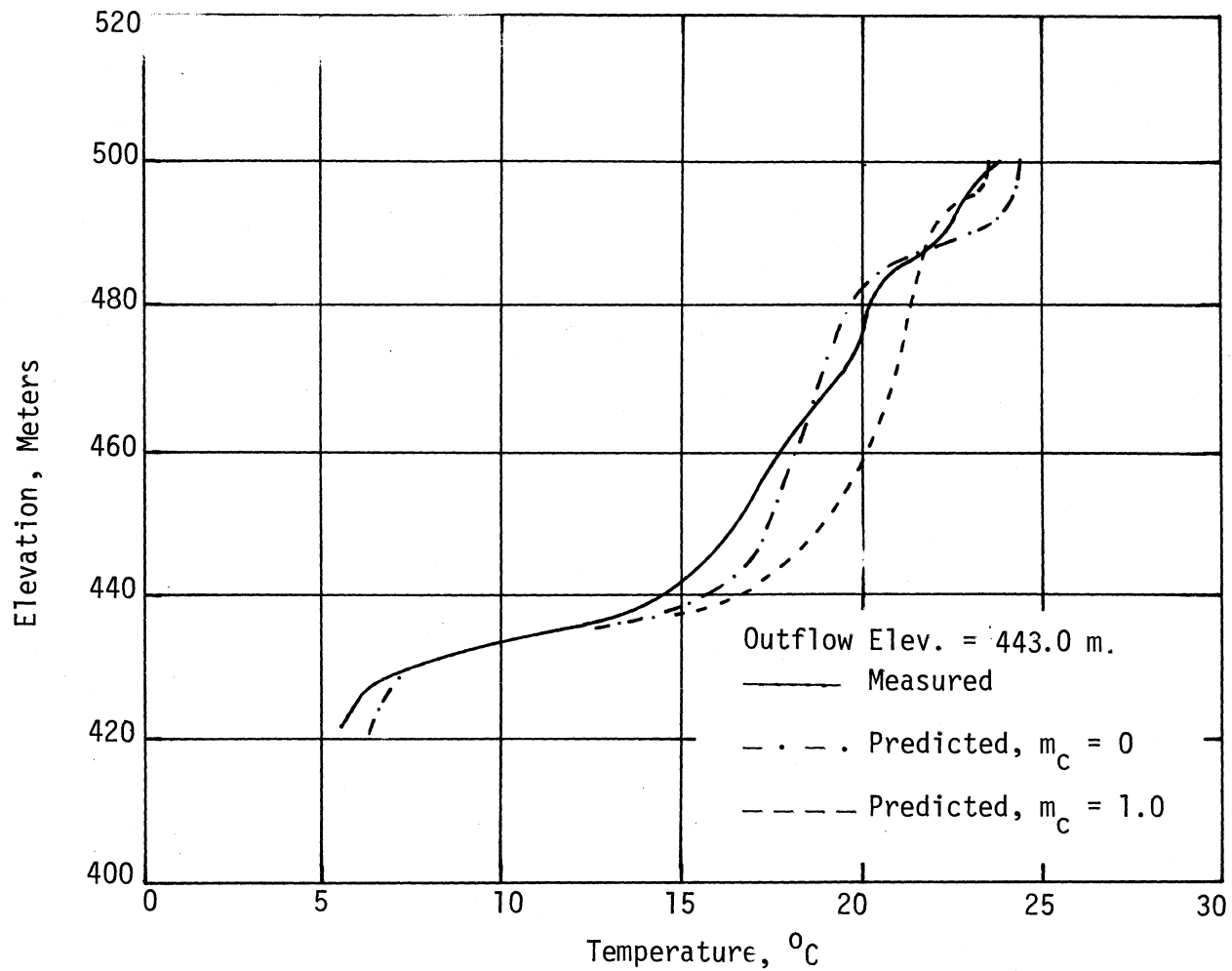


Figure 19. Measured and Predicted Temperature Profiles, Fontana Reservoir, September 15, 1966

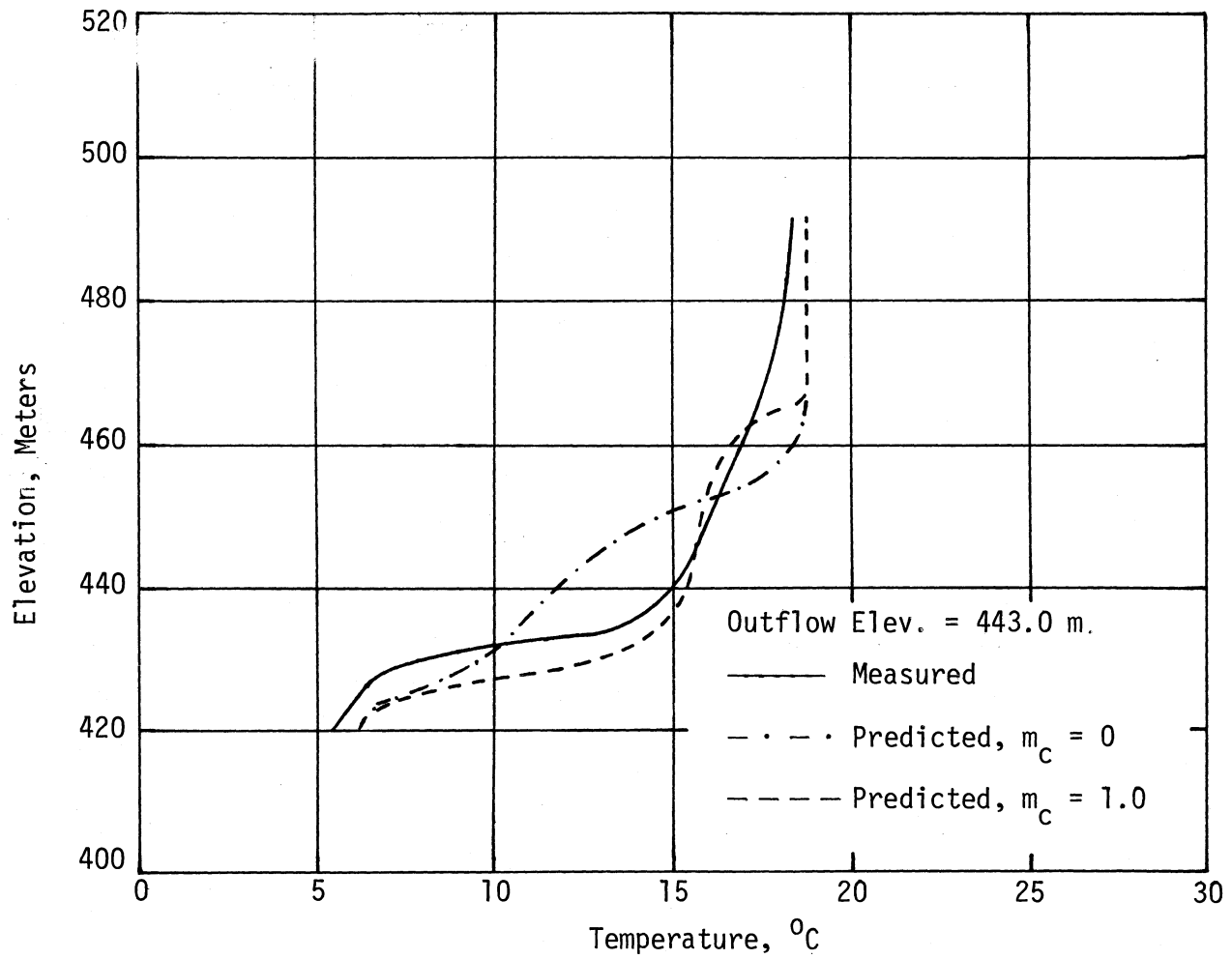


Figure 20. Measured and Predicted Temperature Profiles, Fontana Reservoir, October 26, 1966

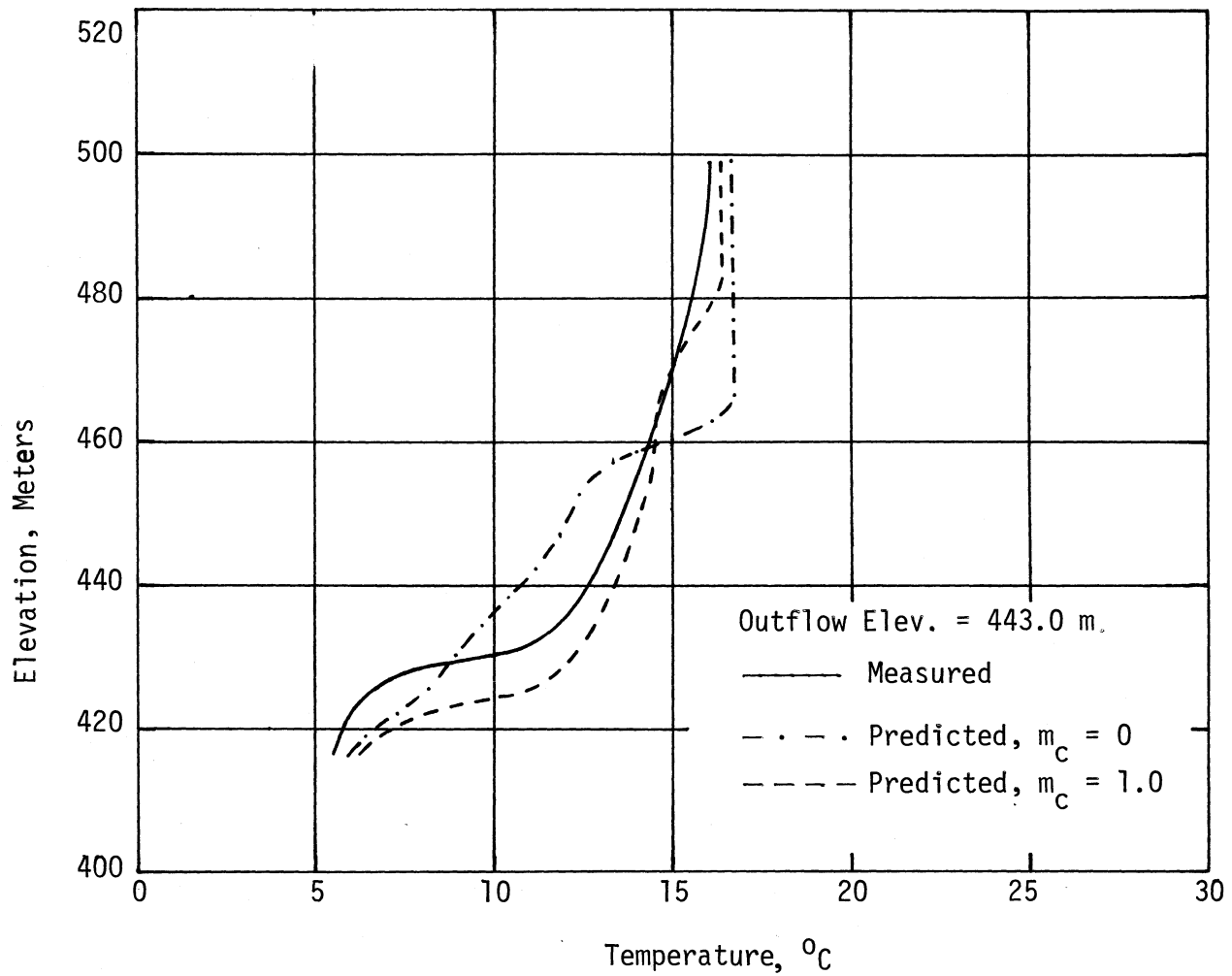


Figure 21. Measured and Predicted Temperature Profiles, Fontana Reservoir, November 16, 1966

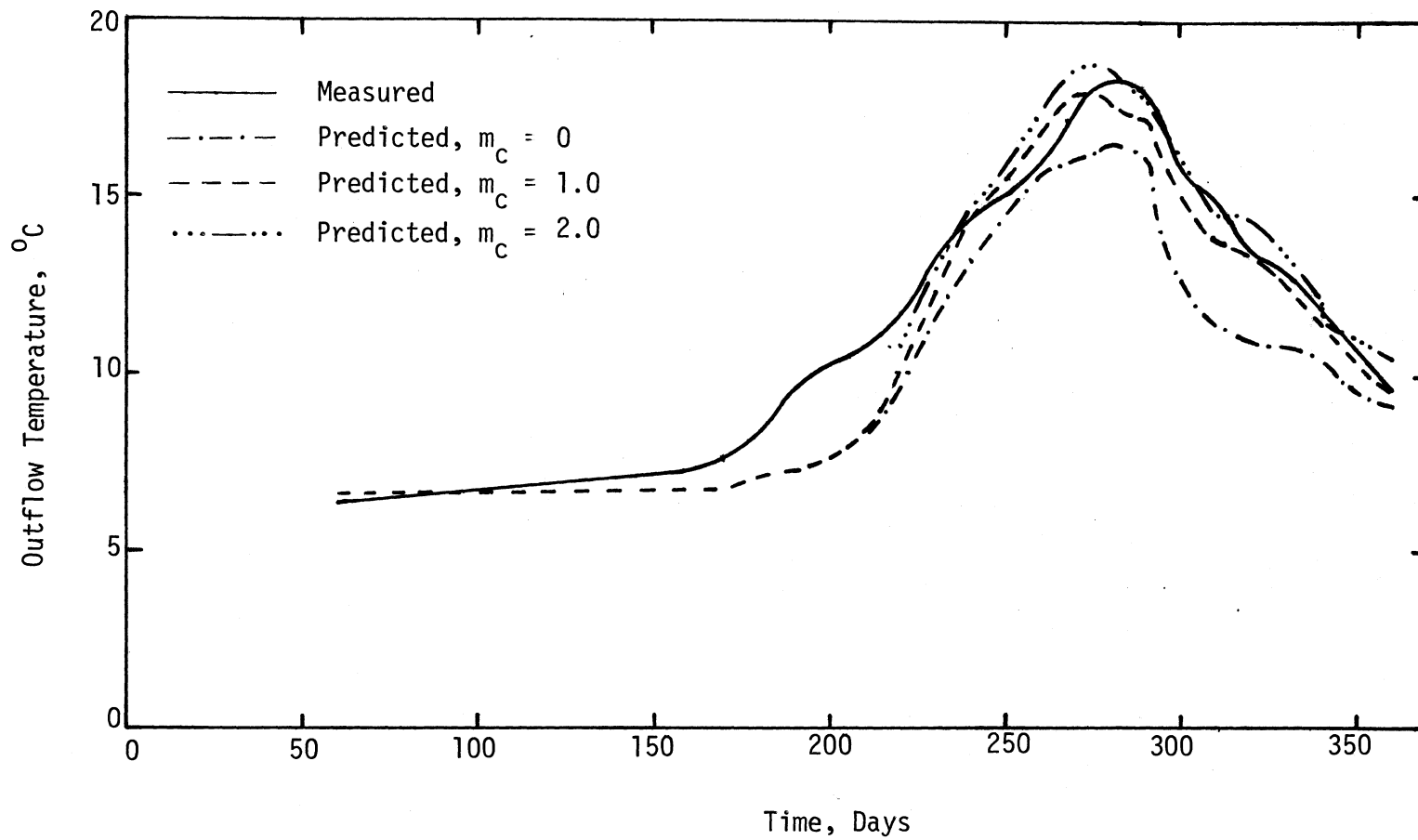


Figure 22. Outflow Temperatures for Fontana Reservoir, 1966

TABLE II  
EFFECTS OF MIXING COEFFICIENTS ON OUTFLOW TEMPERATURES

No. of days since March 1	Outflow Temperatures ( $^{\circ}\text{C}$ )					
	Measured	Predicted				
		$m_c$				
		0	0.5	1.0	1.5	2.0
1	6.1	6.7	6.6	6.7	6.6	6.6
11	6.4	6.3	6.5	6.5	6.5	6.5
21	6.1	6.6	6.6	6.6	6.6	6.5
31	6.7	6.6	6.6	6.6	6.6	6.6
41	6.7	6.6	6.6	6.6	6.6	6.6
51	6.7	6.6	6.6	6.6	6.6	6.6
61	7.2					
71	6.7	6.6	6.6	6.6	6.6	6.6
81	7.2	6.6	6.7	6.6	6.6	6.6
91	7.2	6.7	6.7	6.6	6.6	6.6
101	7.2	6.7	6.7	6.7	6.7	6.7
111	7.8	6.8	6.8	6.7	6.7	6.8
121	8.3	7.1	7.1	7.1	7.1	7.2
131	9.7	7.2	7.3	7.3	7.3	7.3
141	10.3	7.5	7.5	7.6	7.6	7.7
151	10.6	8.2	8.3	8.4	8.4	8.5
161	11.6	9.9	10.2	10.4	10.6	10.7
171	13.3	11.7	12.2	12.5	12.7	12.9
181	14.4	13.3	13.8	14.2	14.5	14.7
191	15.0	14.6	15.1	15.5	15.7	16.0
201	16.1	15.9	16.7	17.0	17.3	17.6
211	17.7	16.1	17.3	18.0	18.5	18.9
221	18.3	16.4	17.3	17.8	18.2	18.4
231	18.0	16.2	16.9	17.3	17.5	17.7
241	15.8	13.0	14.3	15.1	15.6	16.0
251	15.0	11.7	13.0	13.9	14.3	14.6
261	13.3	11.1	12.8	13.6	14.0	14.3
271	13.0	11.0	12.2	12.8	13.2	13.4
281	11.9	10.8	11.2	11.5	11.7	11.8
291	10.8	9.6	10.1	10.5	10.8	11.0
301	9.7	9.2	9.5	9.8	10.1	10.3

stages of stratification that the entrance mixing does not have any effect on the predicted outflow temperatures. For  $m_c = 0$ , the predicted outflow temperatures were low, especially during the high temperature period and during the cooling period, but for  $m_c = 2.0$ , the predicted outflow temperatures were higher than those measured. Again, by using  $m_c = 1.0$ , as shown on Figure 22 and in Table II, better results were obtained. However, the overall pattern of the predicted outflow temperature curves were in good agreement with those measured.

#### D. Results of the Water Quality Model

As stated, the value of  $m_c = 1.0$  gave the better results for both the temperature profiles and the outflow temperatures. Therefore, the value of  $m_c = 1.0$  would be used in the water quality model.

The D.O. profiles of water in the reservoir were calculated daily from March to December through the use of Equations (4.78), (4.92), and (4.98), and the equations for calculating BOD concentrations in the reservoir in Chapter IV. The outflow D.O. concentrations were also obtained daily from March to December by the weighted average of the D.O. concentrations and the outflow rates of all layers within the withdrawal layer thickness.

The results of the D.O. profiles for various days of the year and the outflow D.O. concentrations for  $k_1 = 0.10 \text{ day}^{-1}$  are shown in Figure 23 through 42, and those for  $k_1 = 0.05 \text{ day}^{-1}$  are presented in Appendix A and the effect of mixing coefficients on the predicted outflow D.O. concentrations are found in Appendix B.

Although there were some deviations between the predicted and the measured D.O. profile, the overall pattern predicted by the water quality

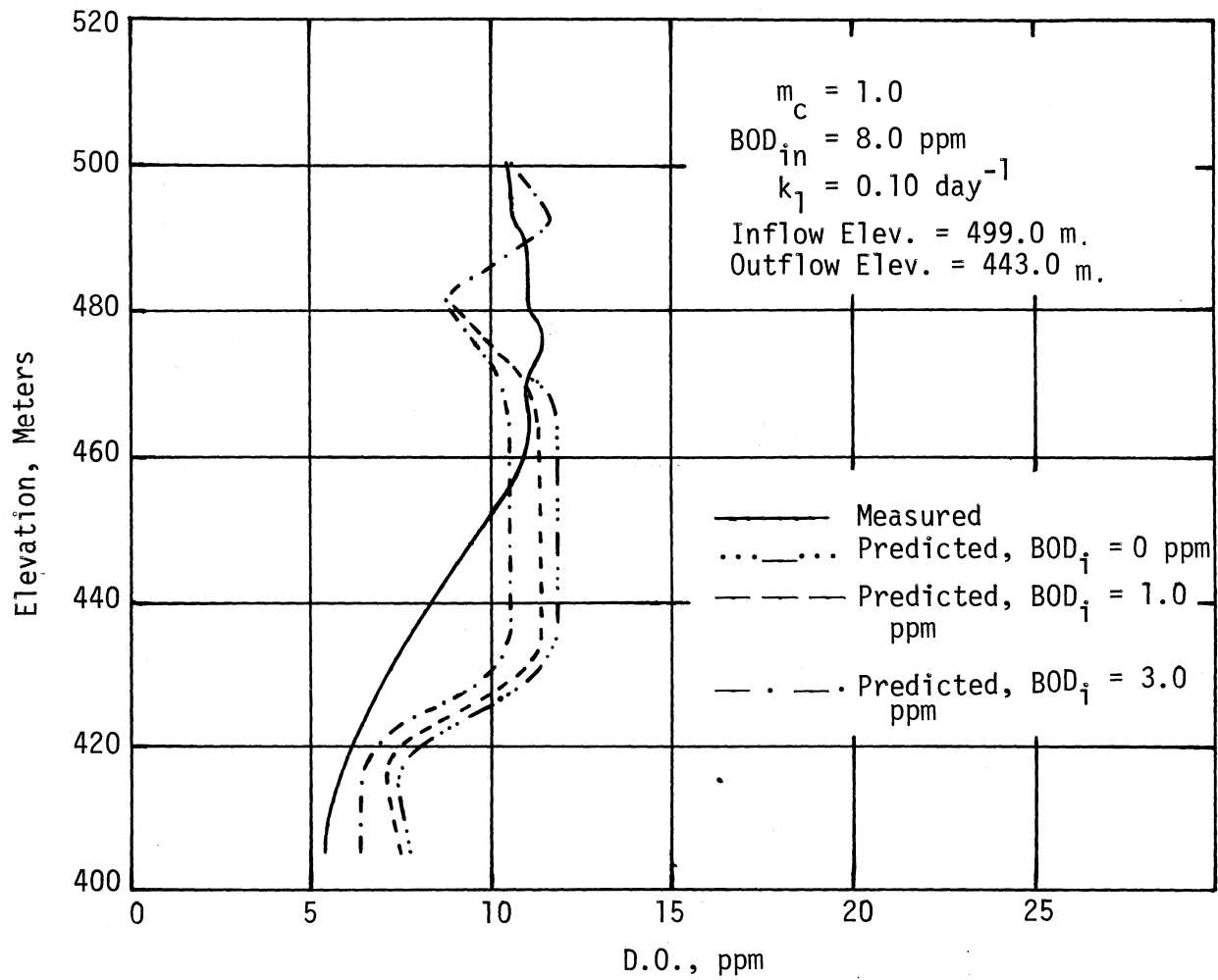


Figure 23. D.O. Profiles for Fontana Reservoir, April 20, 1966

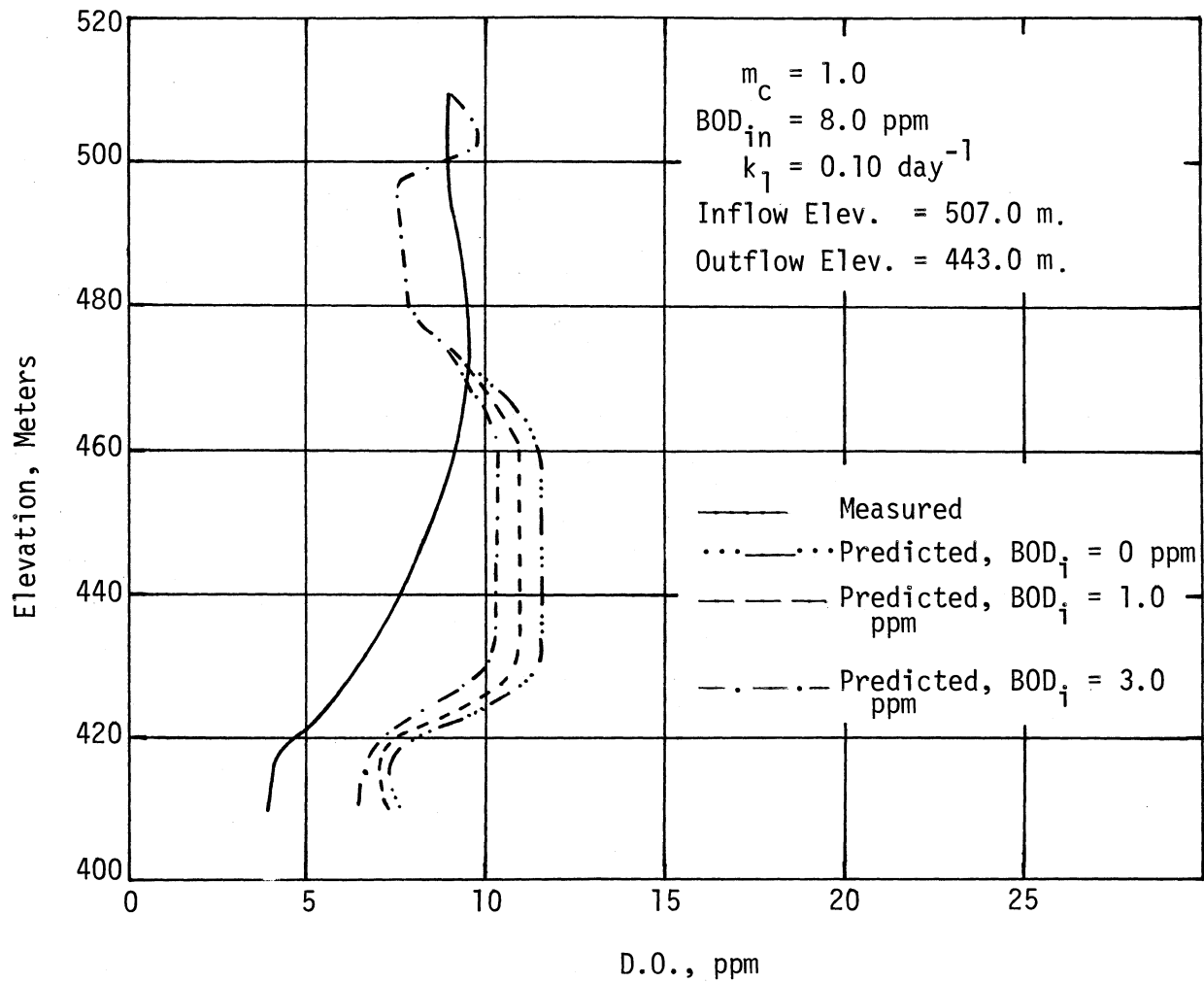


Figure 24. D.O. Profiles for Fontana Reservoir, May 20, 1966



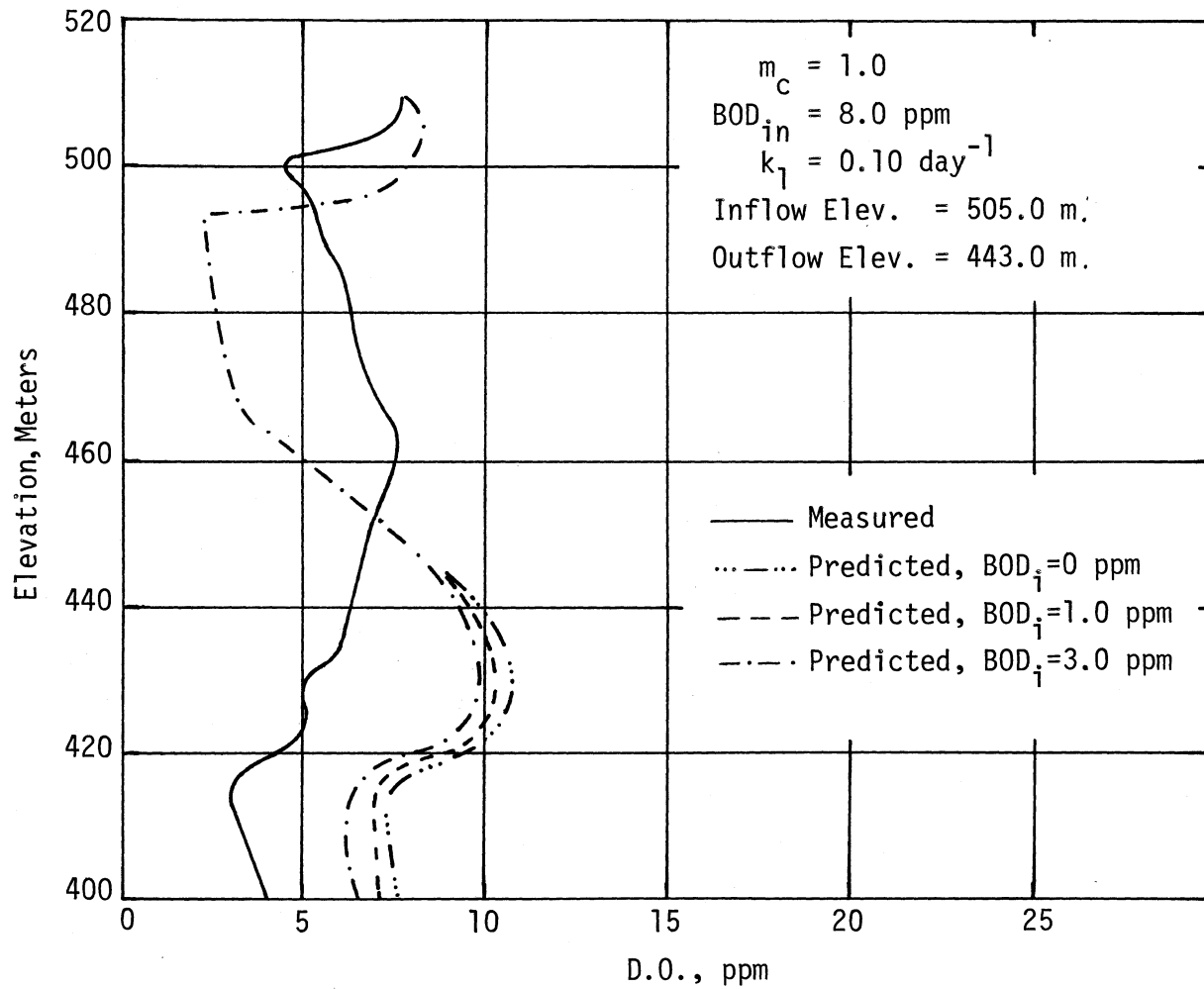


Figure 25. D.O. Profiles for Fontana Reservoir, July 19, 1966

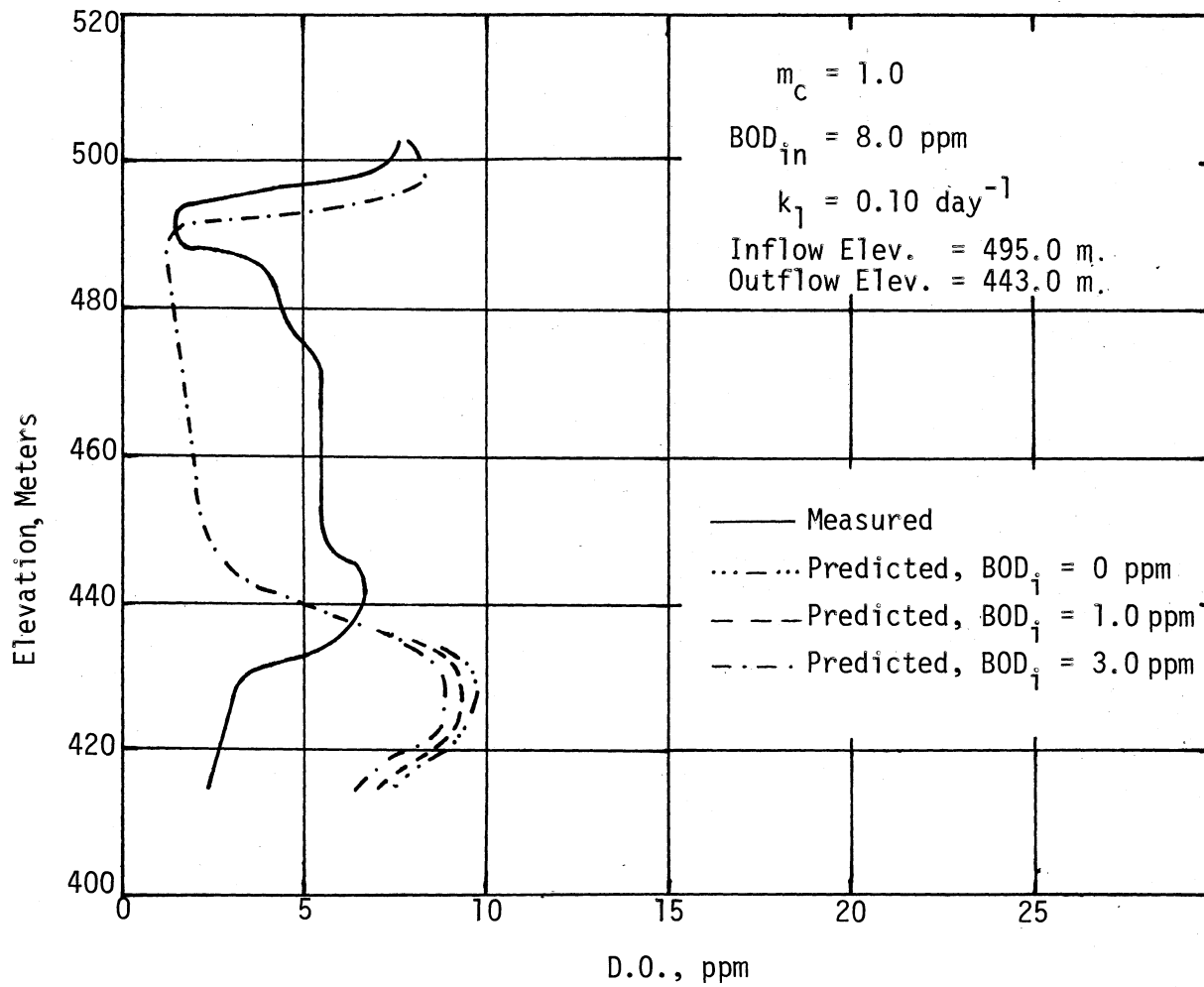


Figure 26. D.O. Profiles for Fontana Reservoir, August 12, 1966

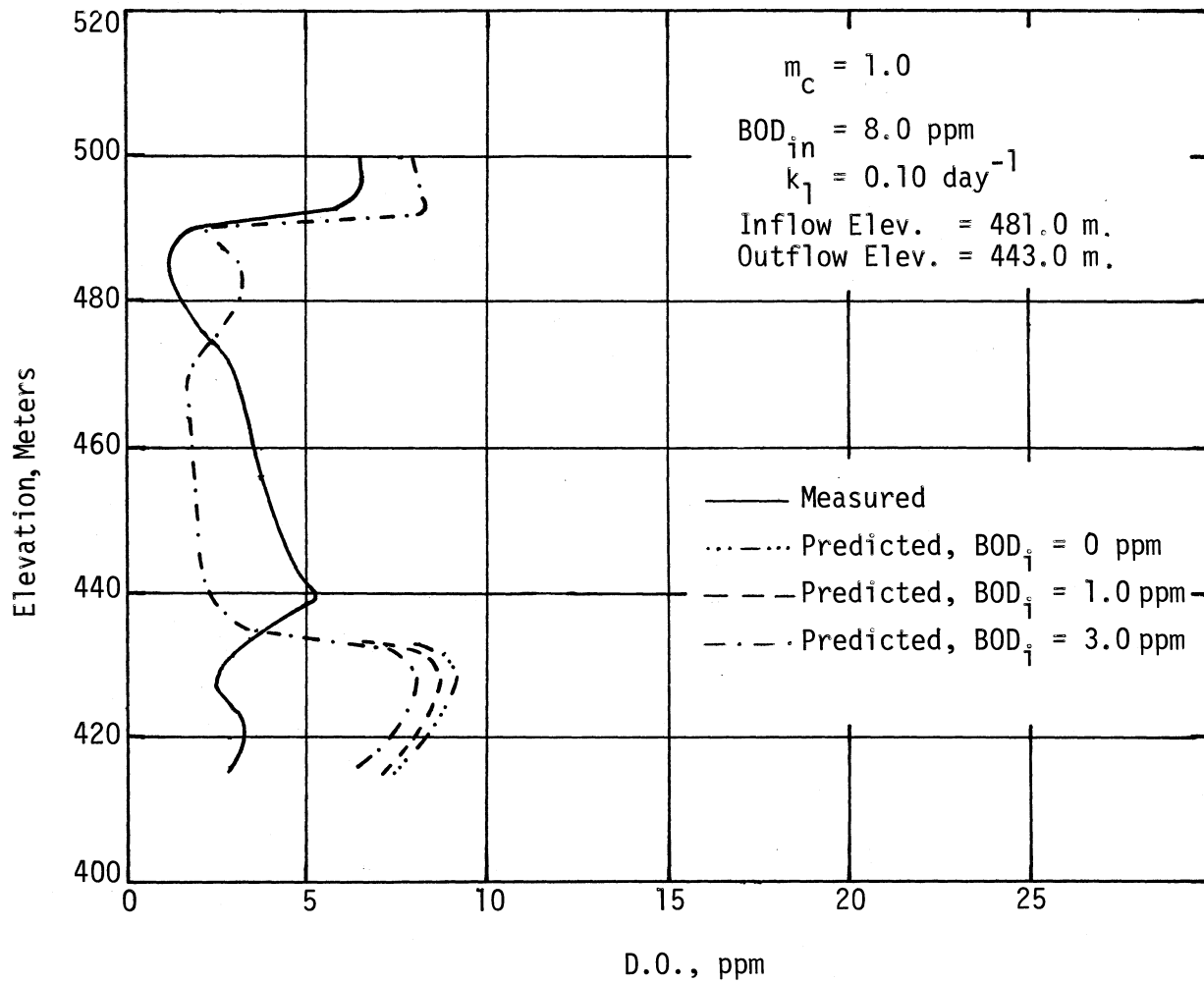


Figure 27. D.O. Profiles for Fontana Reservoir, September 7, 1966

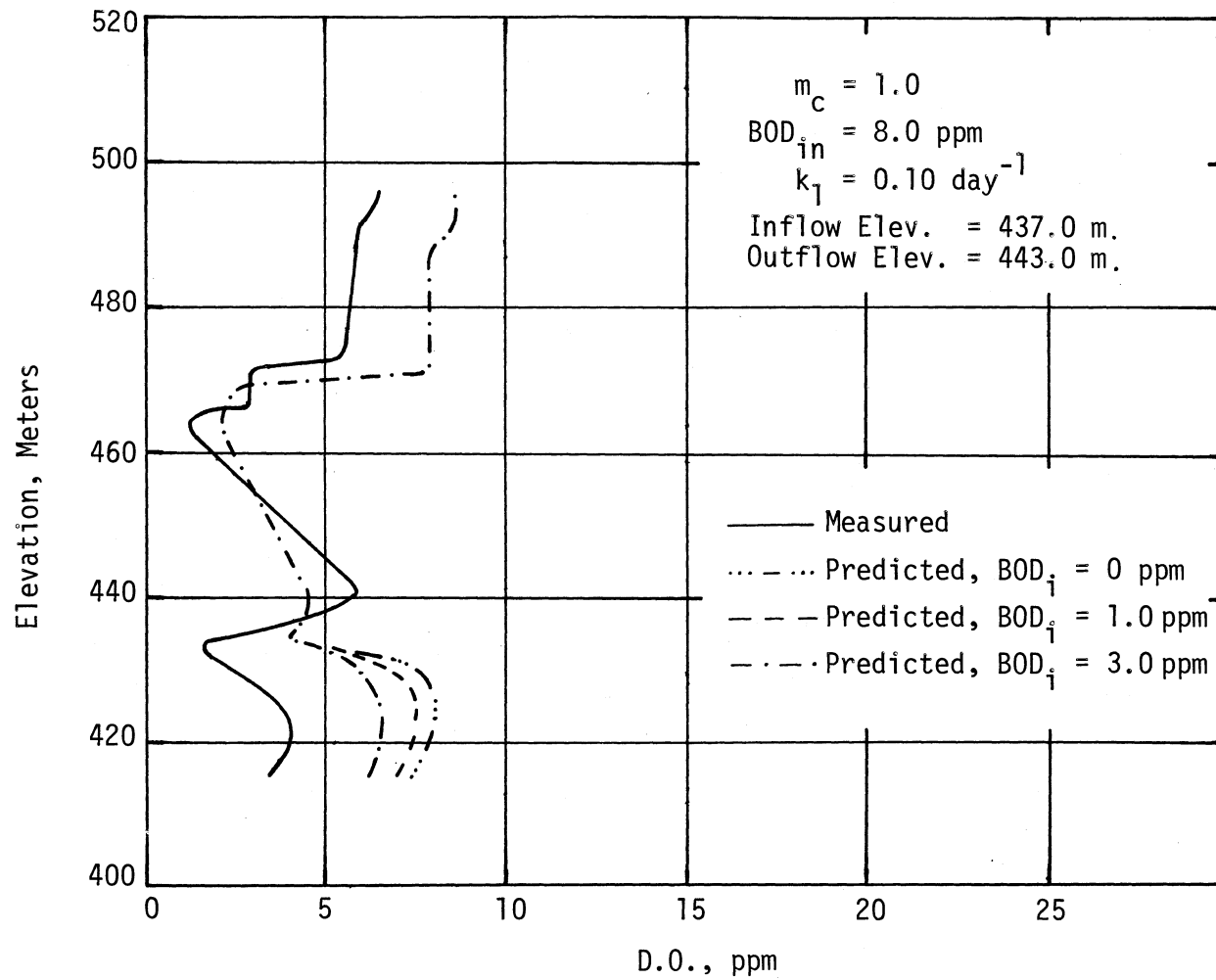


Figure 28. D.O. Profiles for Fontana Reservoir, October 3, 1966

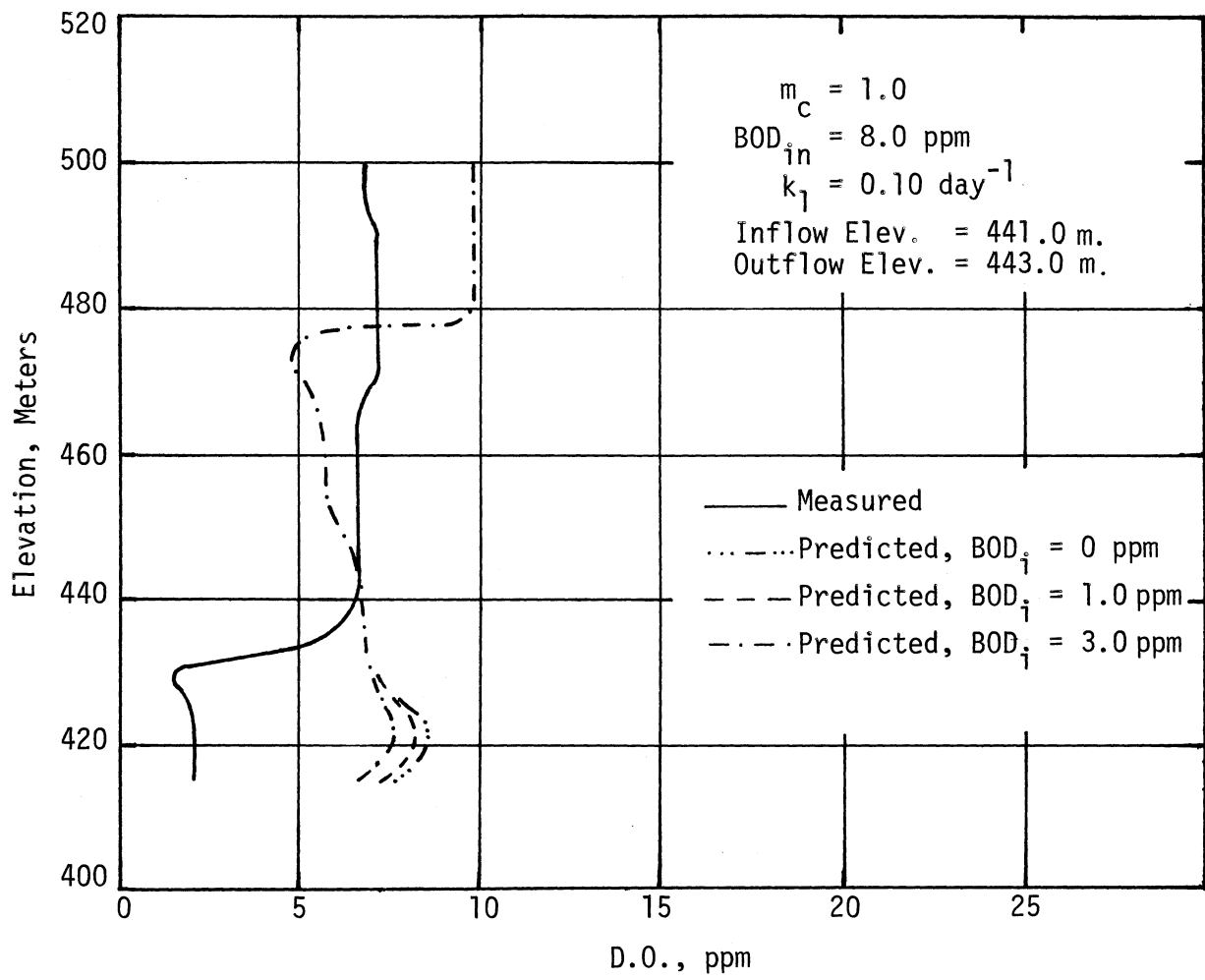


Figure 29. D.O. Profiles for Fontana Reservoir, November 29, 1966

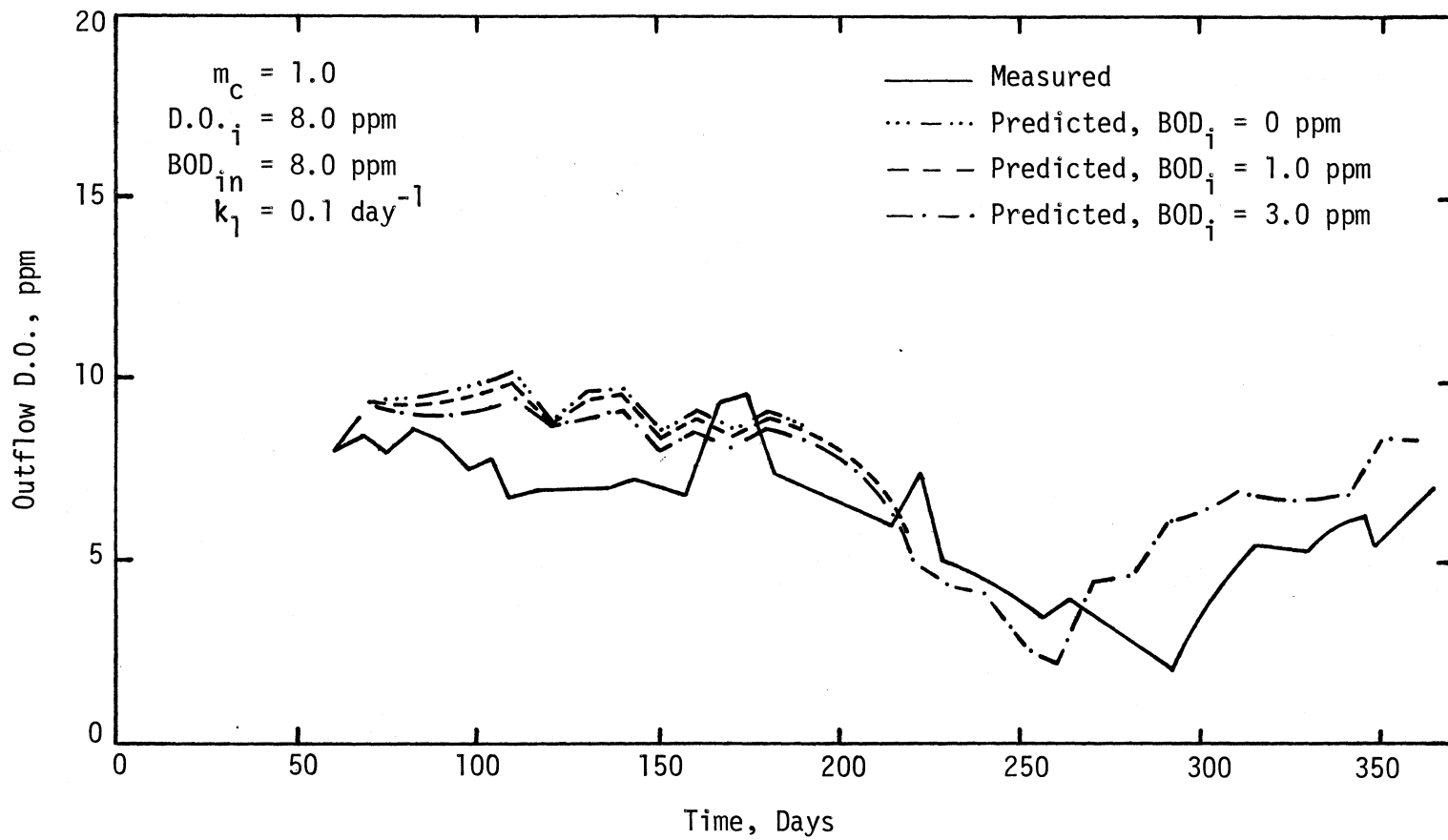


Figure 30. Outflow D.O. Concentrations, Fontana Reservoir, 1966

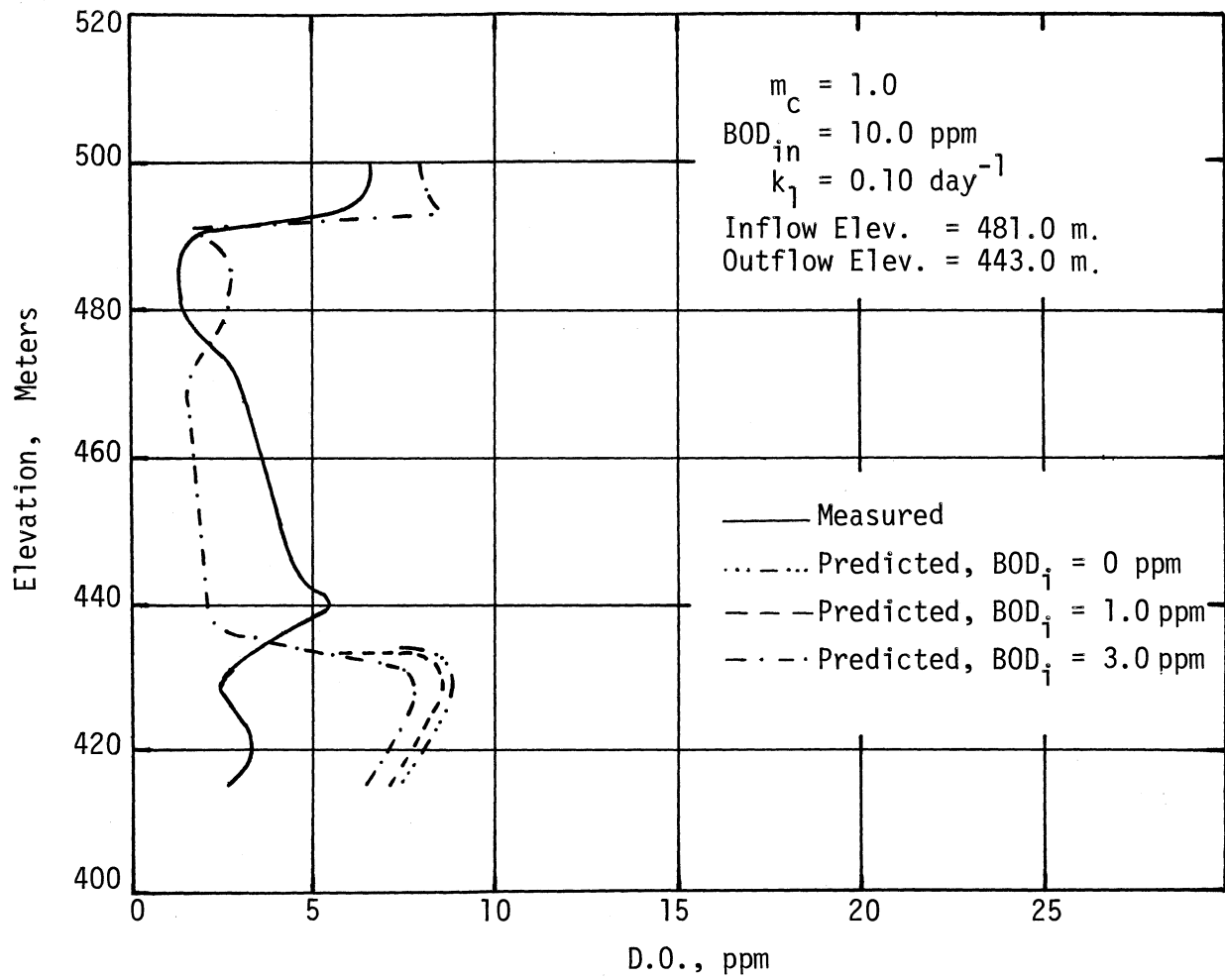


Figure 31. D.O. Profiles for Fontana Reservoir, September 7, 1966

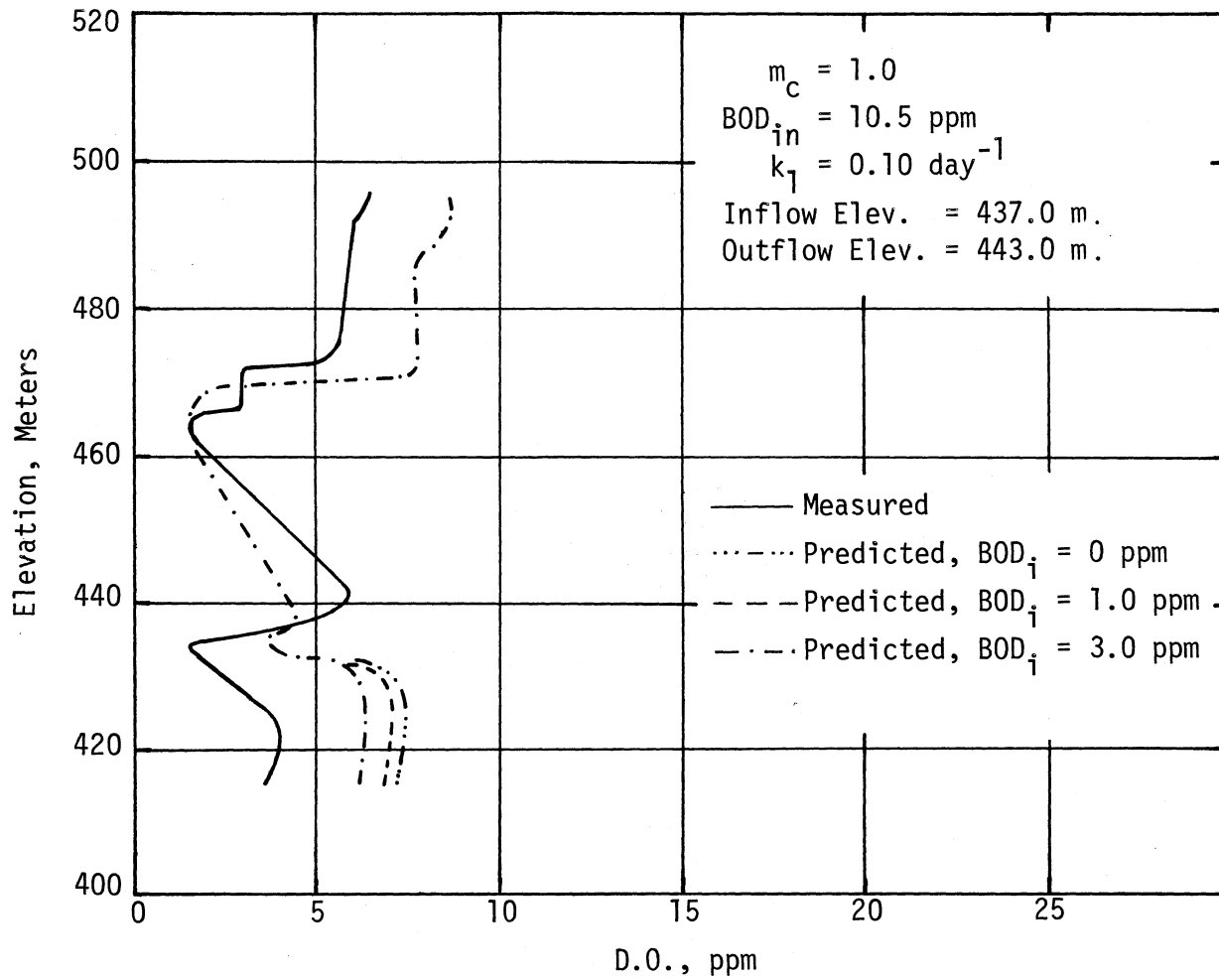


Figure 32. D.O. Profiles for Fontana Reservoir, October 3, 1966



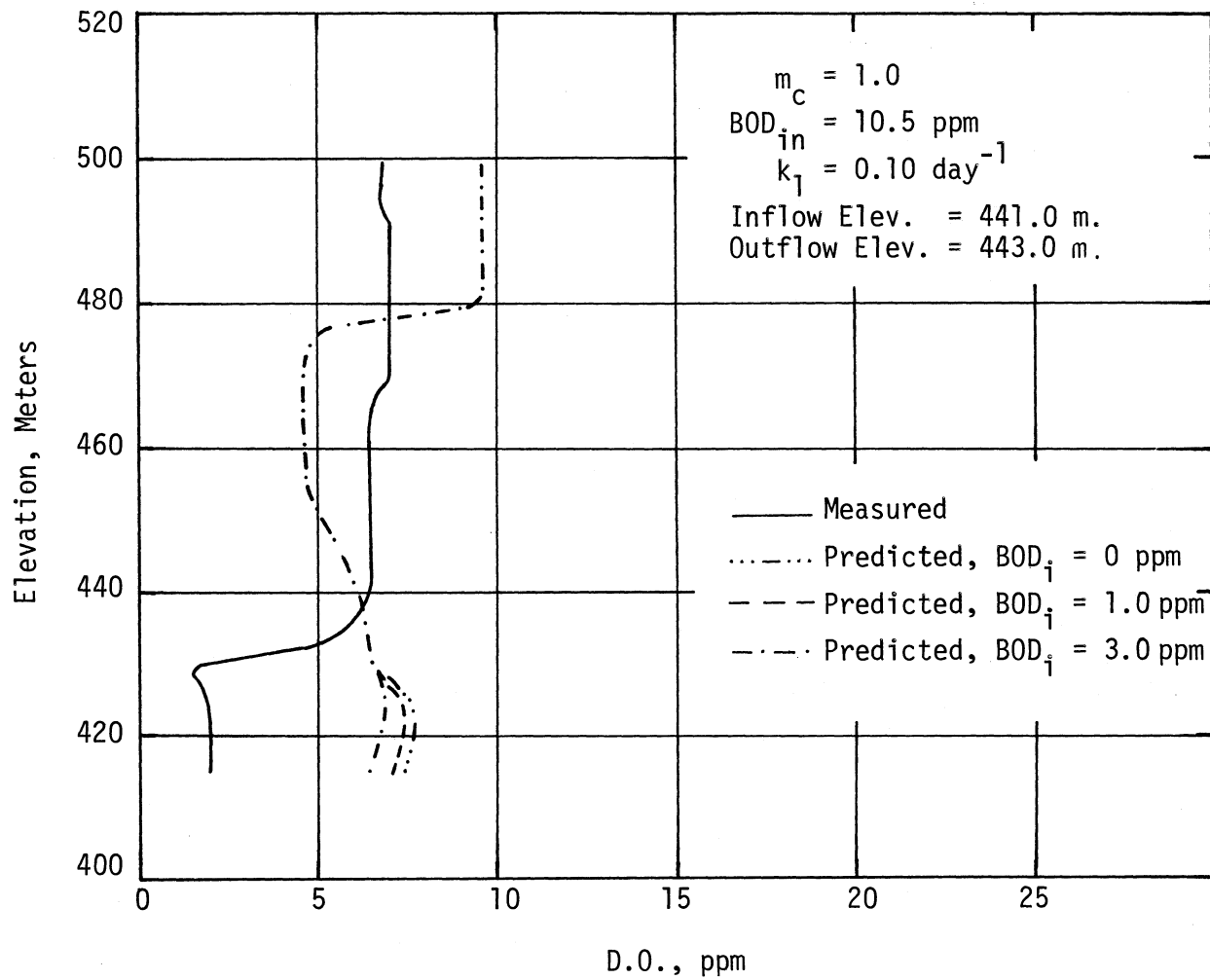


Figure 33. D.O. Profiles for Fontana Reservoir, November 29, 1966

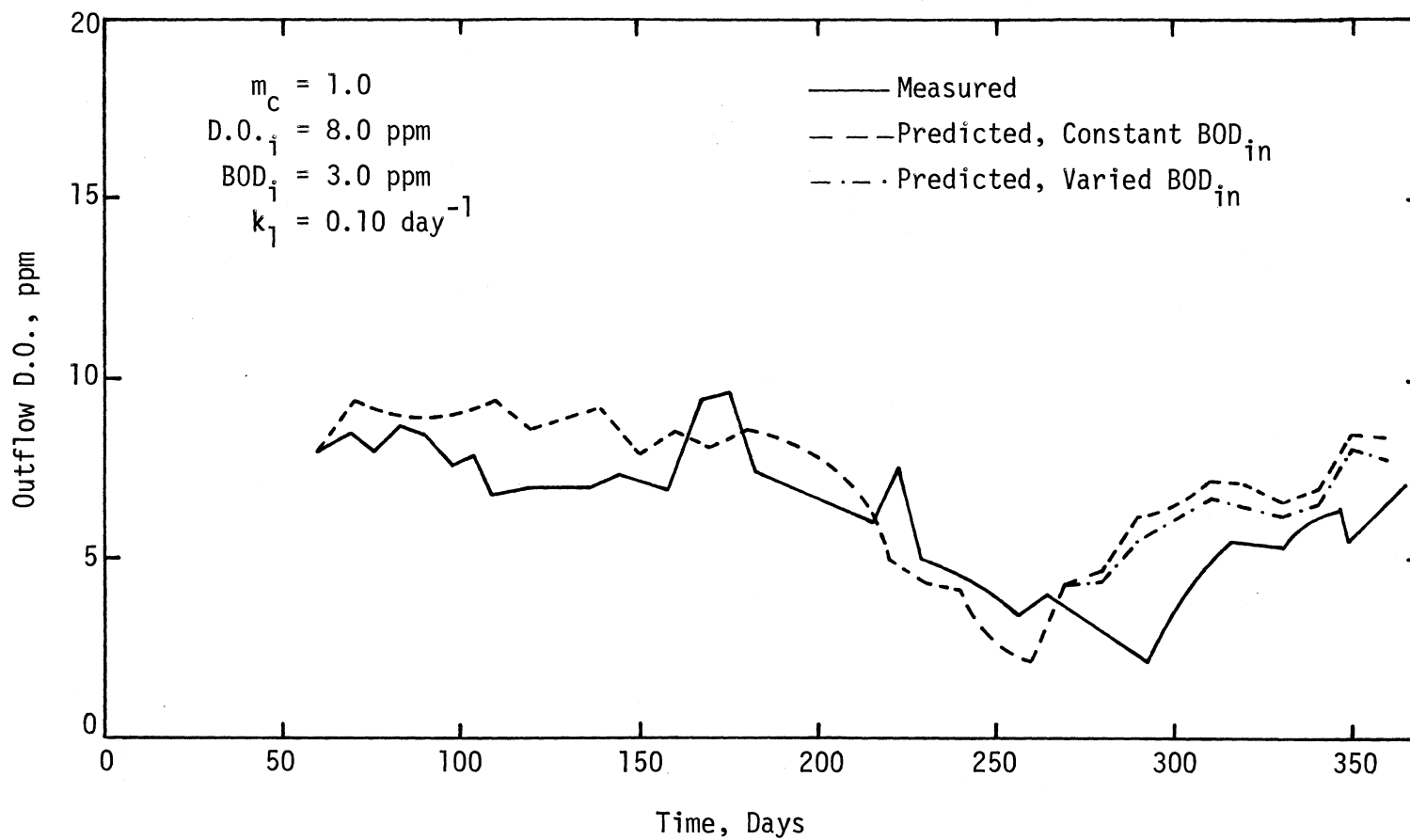


Figure 34. Effect of Inflow BOD on the Outflow D.O. Concentration, Fontana Reservoir, 1966

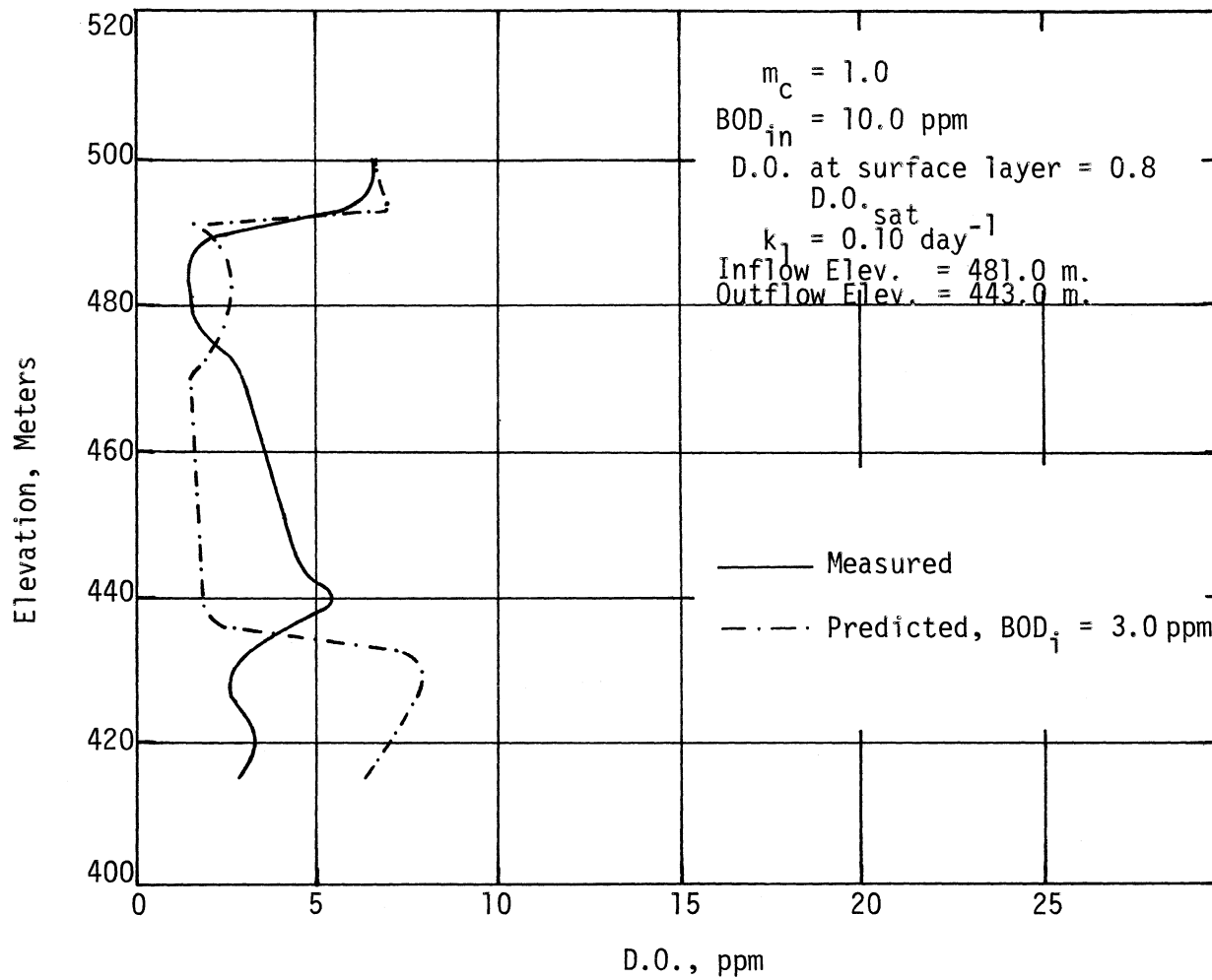


Figure 35. D.O. Profiles for Fontana Reservoir, September 7, 1966

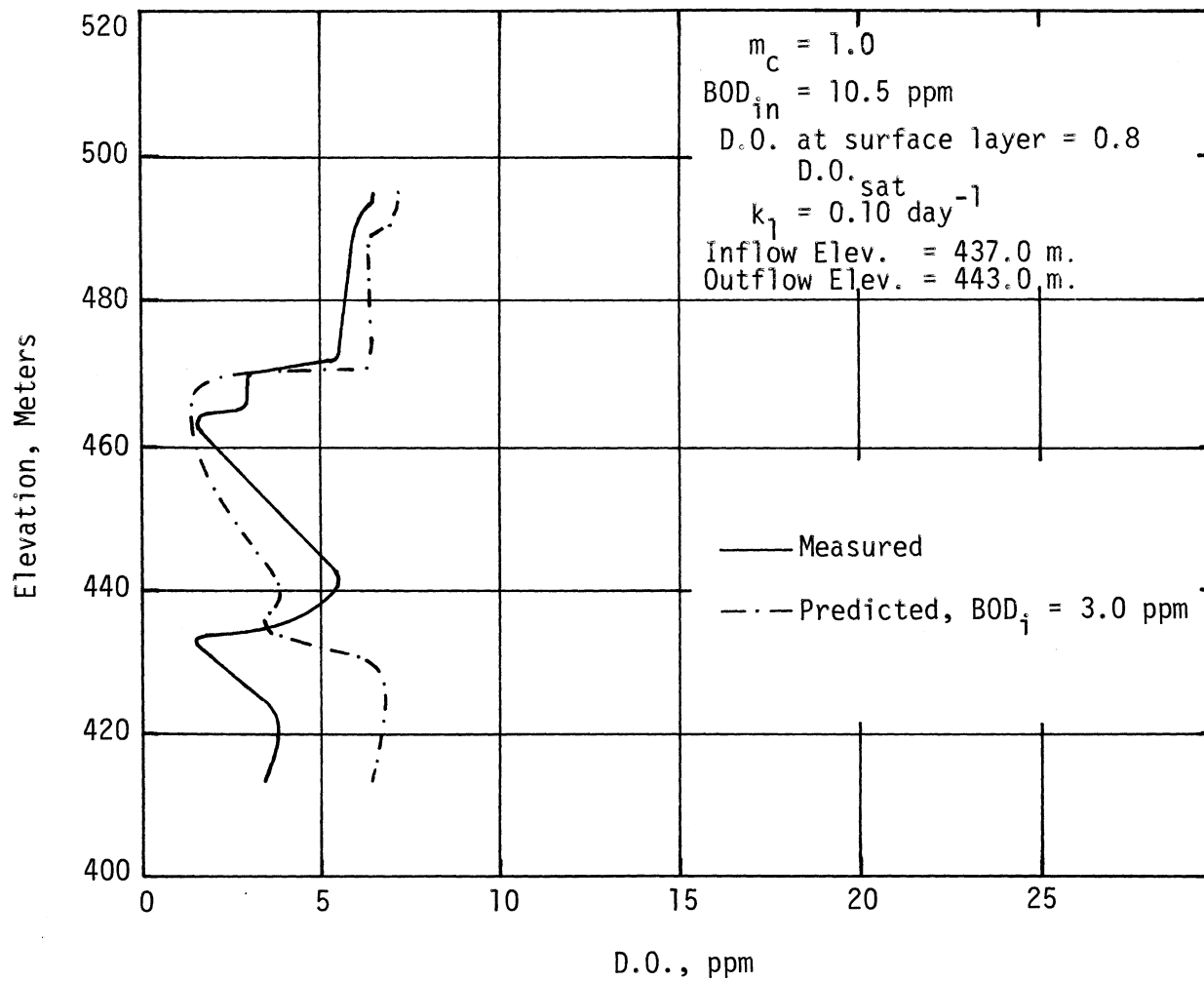


Figure 36. D.O. Profiles for Fontana Reservoir, October 3, 1966

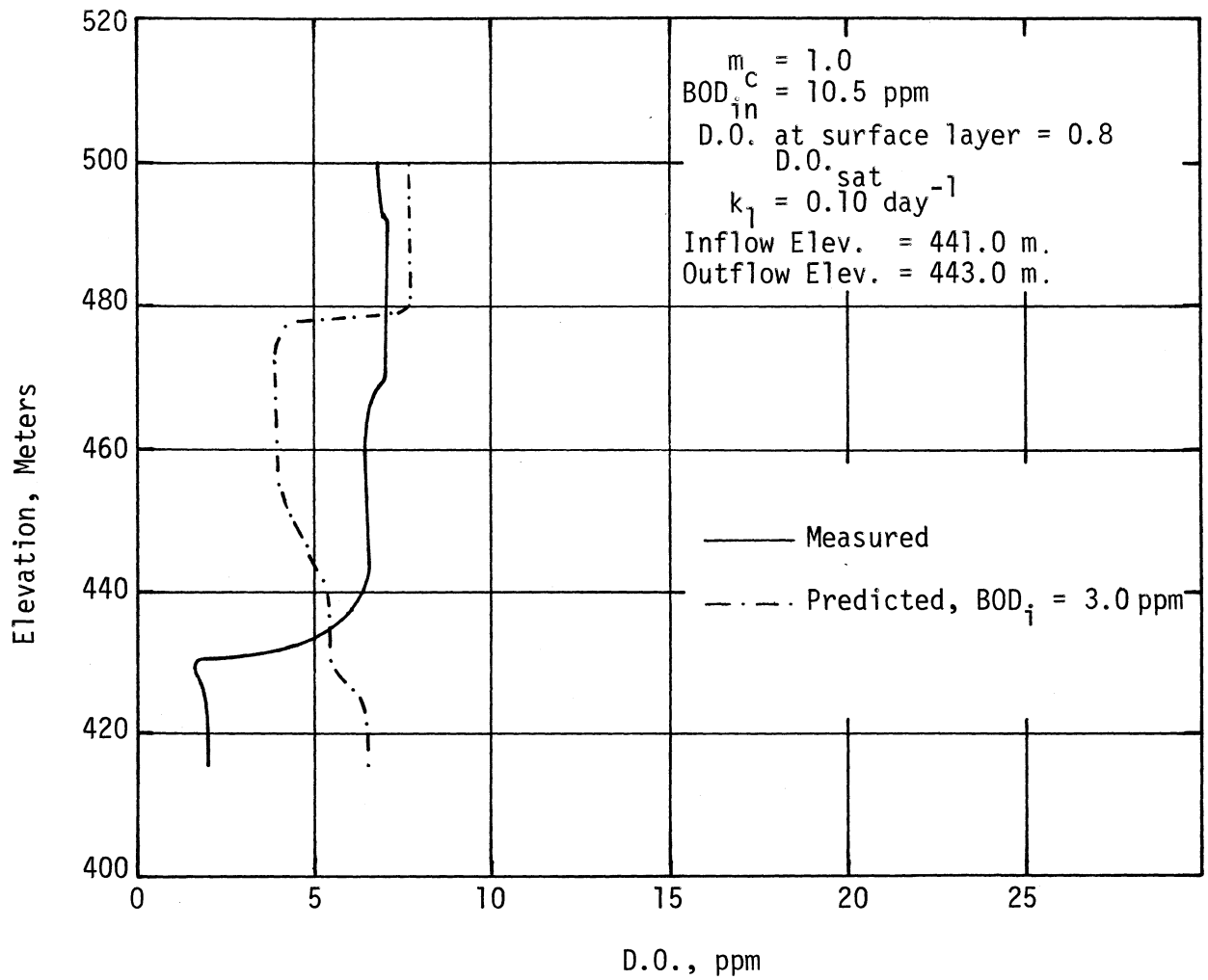


Figure 37. D.O. Profiles for Fontana Reservoir, November 29, 1966

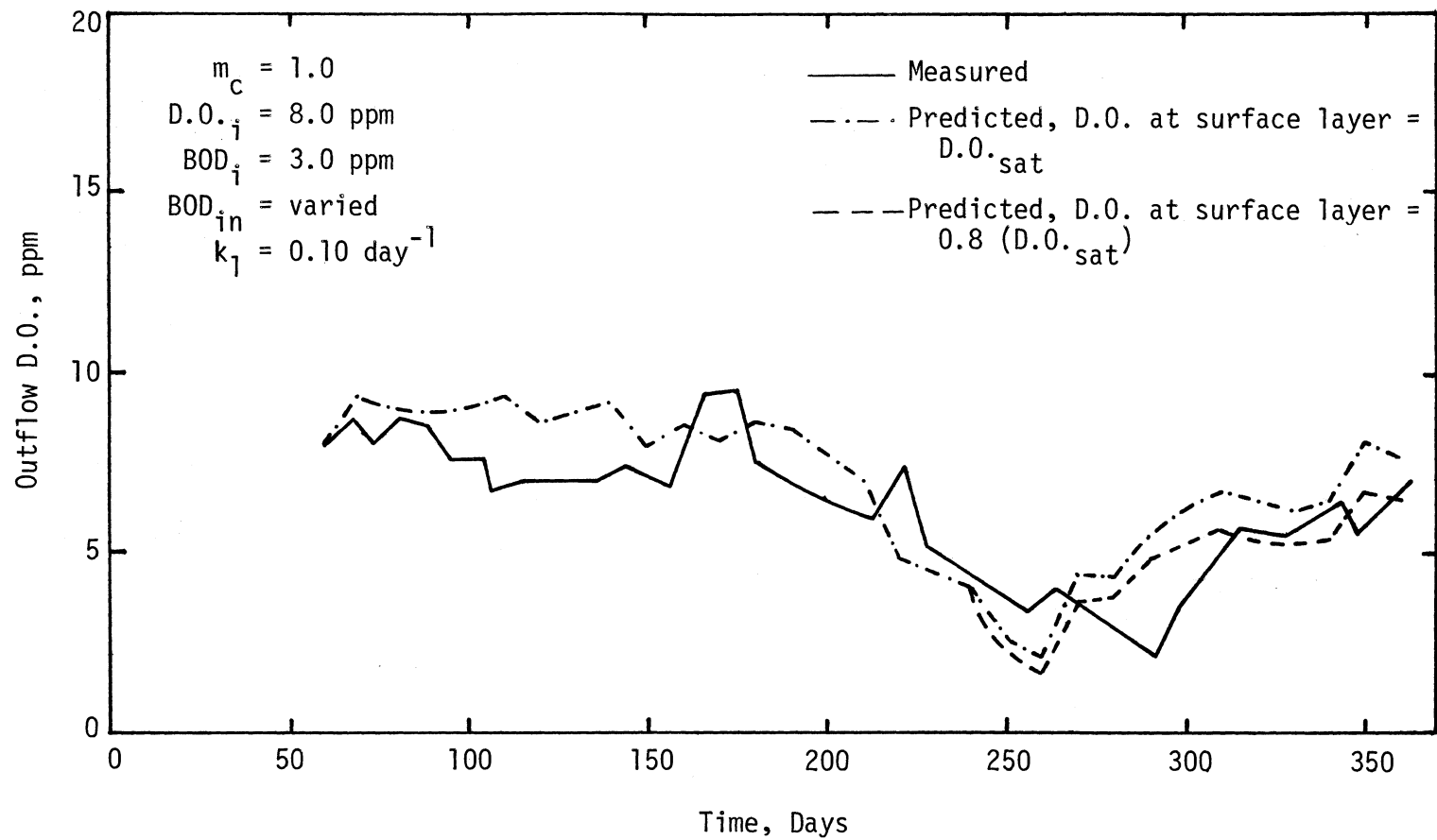


Figure 38. Effect of Surface Boundary Condition for D.O. on Outflow D.O. Concentrations, Fontana Reservoir, 1966

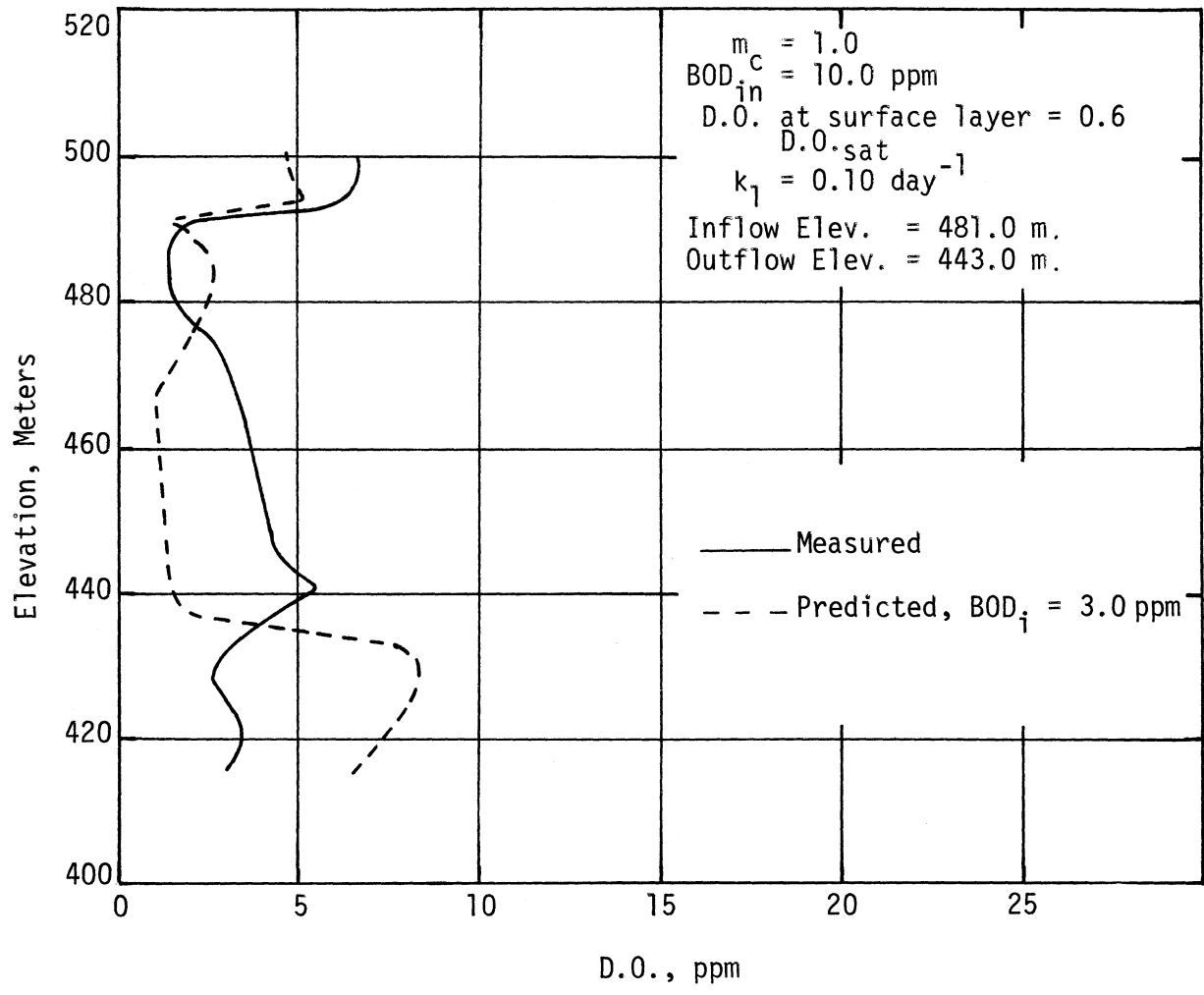


Figure 39. D.O. Profiles for Fontana Reservoir, September 7, 1966

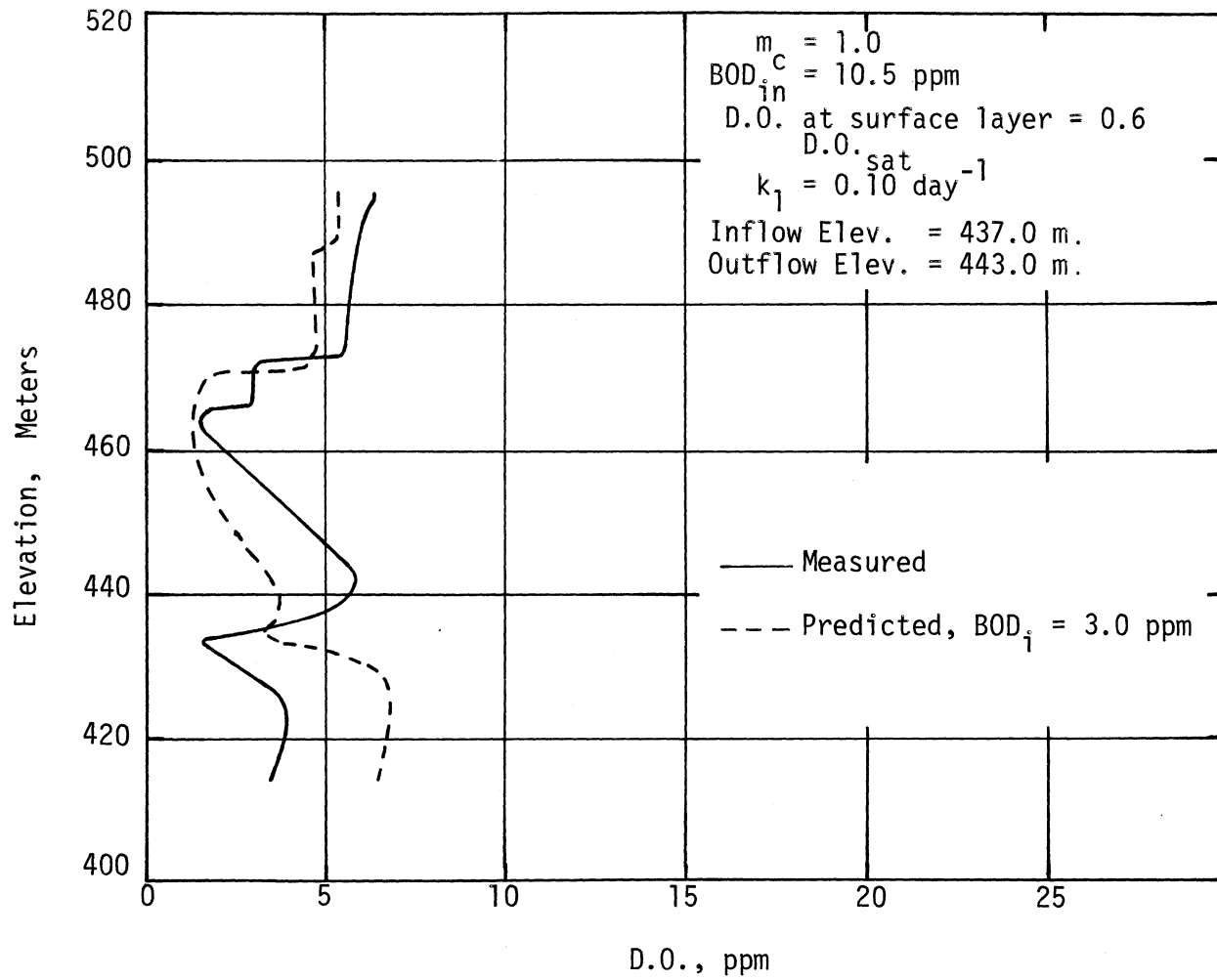


Figure 40. D.O. Profiles for Fontana Reservoir, October 3, 1966



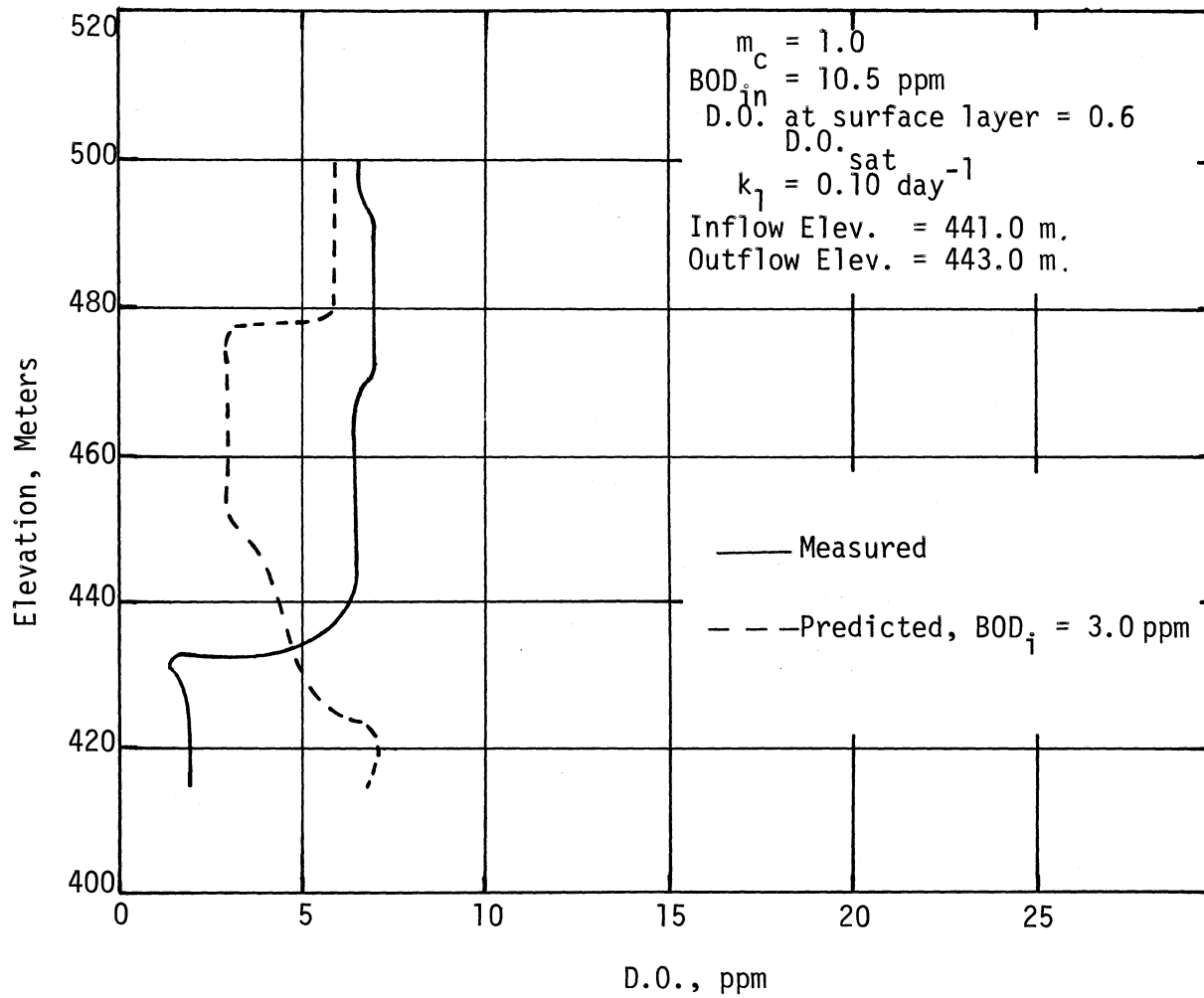


Figure 41. D.O. Profiles for Fontana Reservoir, November 29, 1966

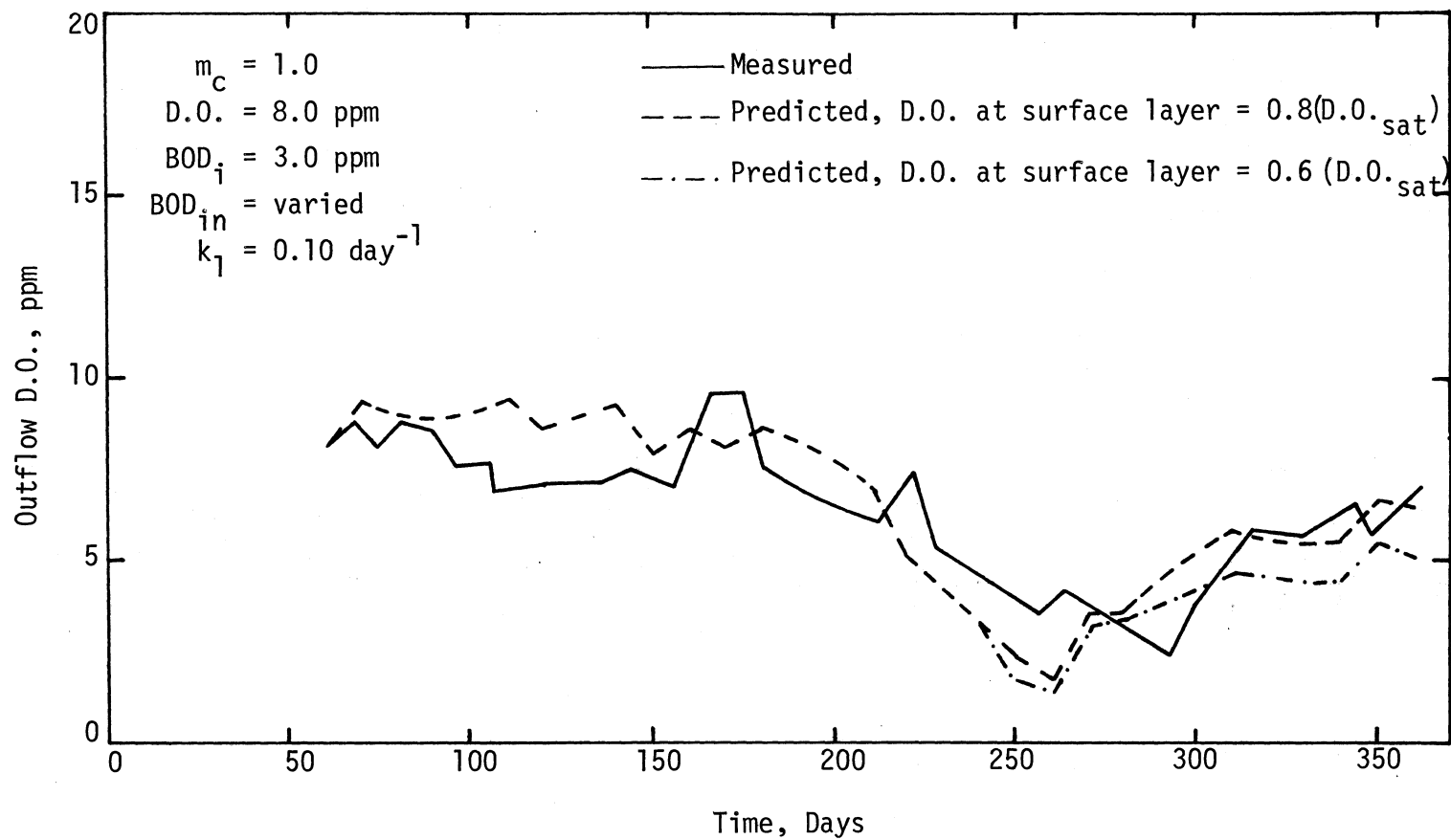


Figure 42. Effect of Surface Boundary Condition for D.O. on Outflow D.O. Concentration, Fontana Reservoir, 1966

model agreed well with those measured.

The comparison of the predicted and measured D.O. profiles for various days of the year for the surface boundary condition having D.O. at the surface saturated, the initial BOD conditions of 0, 1.0, and 3.0 ppm and the constant inflow BOD of 8.0 ppm are presented in Figures 23 to 29, and that of the outflow D.O. concentrations are shown on Figure 30. Figures 23 to 29 indicate that increasing the value of the initial BOD in the reservoir would tend to decrease the predicted D.O. profiles over the yearly cycle of temperature change. However, the initial BOD conditions had affected the predicted D.O. profiles only during the early stages of stratification until about mid-summer, after which the effect of initial BOD conditions were insignificant. The same patterns were found in the predicted outflow D.O. concentrations that the effect of the initial BOD conditions was significant only during the early stages of stratification until about the month of August.

During the summer and during the cooling period there is a tendency of more waste discharge into the rivers and a lot of water is lost due to evaporation during the summer, instead of assuming the constant inflow BOD of 8.0 ppm for the entire year, the inflow BOD would be assumed to be varied after the temperature of the outflow began to rise.

The varied inflow BOD and the figure in which the results can be found are as follows:

Month	Inflow BOD	Figure
April	8.0	23
May	8.0	24
July	8.0	25
August	9.0	--
September	10.0	31
October	10.5	32
November	10.5	33

Figures 31 to 33 indicate that increasing the value of inflow BOD has the effect of decreasing the predicted D.O. profiles, but the changes are very slight and affect only the layers having the same temperature as the inflowing waters and the surrounding layers. Increasing the values of inflow BOD also decrease the predicted outflow D.O. concentrations, as shown in Figure 34. One interesting point concerned with the predicted outflow D.O. concentrations when the inflow BOD was varied is that the increased inflow BOD has the effect on the predicted outflow D.O. concentrations about two months after the inflow BOD started to increase, as shown in Figure 34.

For the case of  $k_1 = 0.05 \text{ day}^{-1}$ , the effect of decreasing the first order decay rate constant  $k_1$  from  $0.10 \text{ day}^{-1}$  to  $0.05 \text{ day}^{-1}$  is to decrease the rate of D.O. consumption within the reservoir. Higher predicted D.O. profiles and outflow D.O. concentrations were found toward the end of the yearly cycle, as shown in Appendix A. However, the changes are not quite as significant.

As shown in Figures 27 to 29 and Figures 31 to 34, during the cool-

ing period the predicted D.O. values near the water surface were higher than those measured. So, instead of using the surface boundary condition of having D.O. saturated at the surface layer for the entire year, D.O. concentration at the surface layer equaled 0.8 of the saturated value was used after the month of August. Better results were obtained, as shown in Figures 35 through 37. The same is true for the predicted outflow D.O. concentrations as shown in Figure 38.

For the sensitivity of the results to the various surface boundary conditions, the surface layer of having D.O. concentration equaled to 0.6 of the saturated value was used after the month of August. The results of the predicted D.O. profiles and outflow D.O. concentrations are found in Figures 39 through 42, which showed that lowering the surface boundary condition for D.O. would result in generally lowering the predicted D.O. concentrations in both the reservoir and in the outflow.

## CHAPTER VI

### DISCUSSION

#### A. The Temperature Model

Comparison of the measured and predicted temperature profiles for various days of the year and the measured and predicted outflow temperatures as functions of time in Chapter V indicated that the entrance mixing had an effect on both the predicted temperature profiles and the predicted outflow temperatures. Increasing the values of mixing coefficient were found to increase the predicted temperatures through the end of the cooling period. During the early stages of the warming period, the effect of increasing the values of mixing coefficients was found to be insignificant. However, after the reservoir was well established in the stratification state and during the cooling period, the effect was quite significant. This was because the entrained water, as mentioned in Chapter III, came from the warm surface water. During the early stages of stratification when the temperatures of the inflowing water are higher or slightly lower than the reservoir water surface temperatures, the inflowing water will enter the reservoir at or just beneath the water surface of the reservoir. Therefore, entrance mixing will affect only the temperatures of the layers near the water surface of the reservoir, and the effect is insignificant because the temperatures of the inflowing water and the warm surface water are only slightly different. However, after the stratification was well established and during

the cooling period, the temperatures of the inflowing water are much lower than the water surface temperatures. The inflowing water, after being entrained by the warm surface water, will sink to its own density level as an interflow or underflow; therefore, the effect is significant because of the greater difference in the temperatures of the inflowing water and the water surface temperatures, and because the effect spreads over the entire depth of the reservoir. Increasing the values of mixing coefficients would tend to increase the temperatures of the inflowing water which, in turn, would tend to increase the predicted temperature profiles in the reservoir.

The same pattern is found in the predicted outflow temperatures-- during the early stages of stratification the entrance mixing does not have any effect on the predicted outflow temperatures since the inflows enter at or near the water surface of the reservoir and the water is withdrawn from a withdrawal layer around the level of the intake. However, after the stratification is well established and during the cooling period, the entrance mixing begins to have a significant effect on the predicted outflow temperatures because the inflows enter the reservoir as the interflows or underflows. Increasing the values of mixing coefficients would tend to increase the predicted outflow temperatures because the temperatures of the inflowing water would tend to be increased by the mixing process at the entrance.

Since the temperature of the water released from a reservoir for downstream uses is likely one of the most meaningful parameters when dealing with the design and management of a reservoir for water quality control, the value of mixing coefficient used was obtained from the sensitivity of the predicted outflow temperatures to the various values

assumed for the mixing coefficient. Figure 22 in Chapter V indicated that the better predicted temperatures were obtained when the value of mixing coefficient  $m_c$  equaled 1.0. Thus, the value of  $m_c = 1.0$  was used in this study.

#### B. The Water Quality Model

Due to the lack of BOD data concerning the BOD of the incoming streams and BOD profiles in the reservoir during the time the D.O. data were measured, the values for the initial BOD on March 1, the BOD of the inflowing water, and the surface boundary conditions for D.O. had to be assumed. The values of 0, 1.0, and 3.0 ppm for the initial BOD conditions in the reservoir on March 1 were assumed for the sensitivity analysis of the results. The resulting sensitivity analysis to the various assumed initial BOD indicates that increasing the value of initial BOD in the reservoir decreases the predicted D.O. profiles in the reservoir over the yearly cycle of temperature change. However, the effect of initial BOD conditions is significant only during the early stages of stratification until about mid-summer, which is corresponding to the time the outflow temperatures start to rise. After this time, the initial BOD conditions in the reservoir change the D.O. profiles very slightly for only a few layers near the bottom of the reservoir. The same trend is found in the predicted outflow D.O. concentrations; the effect of the initial BOD conditions in the reservoir on the outflow D.O. concentrations is significant only during the early stages of stratification until about the month of August. The reason is that during the mid-summer or about the month of August, the temperatures of the outflow are beginning to rise, as shown in Figure 22, Chapter V. This



means that the cold water originally stored in the reservoir was discharged before the month of August except the water near the bottom of the reservoir, and the fact that water released from the reservoir is withdrawn from a withdrawal layer near the level of the intake. Therefore, it is almost impossible for the outflow temperatures to begin to rise if the cold water originally stored in the reservoir was not discharged.

Decreasing the value of the first order decay rate constant,  $k_1$ , from  $0.10$  to  $0.05 \text{ day}^{-1}$  has the effect of increasing the predicted D.O. profiles and outflow D.O. concentrations. However, the changes are not quite as significant because of the low BOD both in the reservoir and in the inflows, and the slow decay rate in the reservoir.

The value of inflow BOD was at first assumed to be a constant of  $8.0 \text{ ppm}$  for the entire year. The predicted D.O. profiles are in good agreement with those measured, except after the mid-summer and during the cooling period when the predicted D.O. profiles near the water surface are higher than those measured as shown in Figures 23 to 30 and Appendix A. Due to the fact that a large amount of water is consumed by evaporation during the summer, and many industries operate only during the summer or store their wastes to discharge after the summer, instead of assuming a constant inflow BOD of  $8.0 \text{ ppm}$  for the entire year the inflow BOD is assumed to be varied and increased up to  $10.5 \text{ ppm}$  after the outflow temperatures start to rise. This has the effect of improving the predicted D.O. profiles near the water surface of the reservoir after the month of August. However, the changes are not very significant because the increased inflow BOD tends to decrease the predicted D.O. values only in the layers having the same temperature as the inflow-

ing water and the surrounding layers, and because of the low decay rate in the reservoir.

Increasing the values of the inflow BOD after the outflow temperatures begin to rise also decreases the predicted outflow D.O. concentrations. However, the increased inflow BOD affects the predicted outflow D.O. concentrations about two months after the inflow BOD starts to increase. This indicates that during the month of August it takes about two months for the water entering the reservoir to be released from the reservoir.

Figures 23 through 29 indicated that the predicted D.O. profiles near the bottom of the reservoir were higher than those measured. After reviewing the inflow temperatures and the inflow D.O. data, one possible explanation for the high predicted D.O. profiles near the bottom of the reservoir might be that during March 6 to 9 the temperatures of the inflowing water were unexpectedly low but the dissolved oxygen levels were almost saturated. The inflows temperatures during that time were lower than that of the water in the reservoir, and the inflows entered the reservoir as underflows. Therefore, high D.O. content water was brought to the bottom of the reservoir during that time and no inflow temperatures lower than that of March 8 until December 5. Thus, the high D.O. content water was at the bottom of the reservoir at least until after December 5 and caused the high predicted D.O. profiles near the bottom of the reservoir. The effect did not show in the measured D.O. profiles because the inflow BOD during that time was higher than the assumed constant value of 8.0 ppm or the oxygen demand of organic material originally present at the bottom of the reservoir.

The surface boundary condition for D.O. was at first assumed to be

saturated with D.O. for the entire year. The predicted D.O. profiles obtained are in good agreement with those measured, except the predicted D.O. profiles near the water surface of the reservoir after the month of August. This is because of the fact that there is a tendency of more waste discharge entering the streams after the summer and the amount of oxygen produced by photosynthesis might be lower due to algae death or less sunlight after the summer. Therefore, instead of assuming the surface boundary condition for D.O. to be saturated with D.O. for the entire year, the surface boundary conditions for D.O. after the month of August were assumed to have D.O. equal to 0.8 and 0.6 of the saturated values for the sensitivity analysis of the results. The resulting sensitivity analysis to the various assumptions of surface boundary conditions for D.O. indicates that decreasing the value of D.O. assumed for the surface boundary conditions decreases the predicted D.O. profiles and outflow D.O. concentrations. Decreasing the value of D.O. assumed for the surface boundary conditions does not only decrease the predicted D.O. at the surface layer, but also the deeper layers as well. This is due to the convective mixing process and because the D.O. at the surface layer is the major source for the diffusion of D.O. to the deeper layer in the reservoir. Since lowering the D.O. at the surface layer affects the predicted D.O. values at lower layers, it also affects the predicted outflow D.O. concentrations, as well. The results obtained as shown on Figures 23 through 26 and 35 through 38 indicated that the better predicted D.O. values are obtained for both the D.O. profiles in the reservoir over the yearly cycle of temperature change and the outflow D.O. concentrations when the surface boundary condition for D.O. was assumed to be saturated with D.O. until the month of August. After that time

the surface boundary condition for D.O. having D.O. concentration equal to 0.8 of the saturated value was assumed.

## CHAPTER VII

### CONCLUSIONS

Based on the results of the temperature and water quality models for deep, horizontally stratified reservoirs, the following conclusions can be drawn:

1. The temperature distribution of water in a stratified reservoir is affected by the horizontal advection of inflows and outflows, the vertical advection and diffusion of heat, the absorption and transmission of solar radiation, and convection due to surface cooling.

2. The entrance mixing has a significant effect on both the temperature profiles in the reservoir and the outflow temperatures after the reservoir was well established in the stratification state and during the cooling period.

3. In stratified reservoirs, the temperature of the inflow affects the detention time of water in the reservoir. The water which enters at or just beneath the reservoir water surface and the bottom of the reservoir will remain in the reservoir for a longer period of time than the water which enters the reservoir as the interflow.

4. The vertical distribution of dissolved oxygen in deep stratified reservoirs is governed by the horizontal advection of inflows and outflows, the vertical advection and diffusion of mass, the rate of BOD removal, the convective mixing associated with cooling at the surface, and the D.O. concentration of the surface layer.

5. The dissolved oxygen concentration of the outflow at any time is dependent on the withdrawal layer thickness, the temperature profile, and the dissolved oxygen profile in the reservoir at that time.

6. The initial BOD conditions in the reservoir on the day the calculations of D.O. and BOD start, has the significant effect on the D.O. profiles in the reservoir and outflow D.O. concentrations only during the early stages of stratification until the outflow temperatures begin to rise. After this time, the effect of initial BOD is insignificant.

7. The effect of BOD is insignificant over the range of pollutant presented.

8. A one-dimensional mathematical representation of heat and mass transport processes provides a satisfactory means of predicting the temperature and dissolved oxygen behavior of deep reservoirs with horizontal isotherms and low densimetric Froude number.

## CHAPTER VIII

### SUGGESTIONS FOR FUTURE STUDY

Several suggestions for future study on the development of the mathematical models for predicting the temperature and the water quality parameter distributions are outlined as follows:

1. Modify the present mathematical model to a two-dimensional model which is capable of predicting the temperatures and dissolved oxygen distributions in reservoirs in which the horizontal variation of temperatures and dissolved oxygen concentrations with time are large, as in weakly-stratified reservoirs.
2. Perform a sensitivity analysis to determine the effect on the predicted temperatures and dissolved oxygen concentrations to the various velocity distribution profiles of the inflows other than normal distribution, such as gamma distribution.
3. Study the effect of dissolved substance concentrations on the level of entrance of the inflow. It is known that in most reservoirs the density distribution is entirely a function of the temperature distribution. However, in some reservoirs the concentration of dissolved substance is high enough to increase the density to such an extent that temperature is not the only governing factor.

## SELECTED BIBLIOGRAPHY

1. Anderson, E. R., "Energy Budget Studies in Water Loss Investigations - Lake Hefner Studies." Technical Report, USGS, Professional Paper 269 (1954).
2. Beard, L. R., Willey, R. G., "An Approach to Reservoir Temperature Analysis." Water Resources Research, 6, 1, 1335-1345 (1970).
3. Bella, D. A., "Dissolved Oxygen Variations in Stratified Lakes." J. San. Engr. Div., ASCE, 96, SA5, 1129-1146 (1970).
4. Bella, D. A. Discussion of "Management and Measurement of DO in Impoundments," by J. M. Symons, W. H. Irwin, R. M. Clark, and G. G. Robeck, J. San. Engr. Div., ASCE, 94, SA5, 1034-1037 (1968).
5. Bella, D. A., Dobbins, W. E., "Difference Modeling of Stream Pollution." J. San. Engr. Div., ASCE, 94, SA5, 995-1016 (1968).
6. Bella, D. A., Grenney, W. J., "Finite - Difference Convection Errors." J. San. Engr. Div., ASCE, 96, SA6, 1361-1375 (1970).
7. Brooks, N. H., Koh, R. C. Y., "Selective Withdrawal From Density Stratified Reservoirs." J. Hydraulics Div., ASCE, 95, HY4, 1369-1400 (1969).
8. Carnahan, B., Luther, H. A., Wilkes, J. O., Applied Numerical Methods. John Wiley & Sons, Inc., New York (1969).
9. Churchill, M. A., "Effects of Density Currents in Reservoirs on Water Quality." Water and Sewage Works, 112, 135-142 (1965).
10. Churchill, M. A., "Effects of Storage Impoundments on Water Quality." J. San. Engr. Div., ASCE, 83, SA1, 1171-1193 (1957).
11. Churchill, M. A., Nicholas, W. R., "Effects of Impoundments on Water Quality." J. San. Engr. Div., ASCE, 93, SA6, 73-90 (1967).
12. Currie, J. W., Halter, A. N., Layton, R. D., "A Model for Stimulating River and Reservoir Temperatures With Applications for Anadromous Fish Management." Water Resources Research Institute, WRI-26, Oregon State University, Corvallis, Oregon (1974).



13. Daily, J. W., Harleman, D. R. F., Fluid Dynamics. Addison Wesley Publishing Company, Inc., Reading, Mass. (1965).
14. Dake, J. M. K., Harleman, D. R. F., "Thermal Stratification in Lakes." Water Resources Research, 5, 2, 484-495 (1969).
15. Debler, W. R., "Stratified Flow Into a Line Sink." J. Engr. Mechanics Div., ASCE, 85, EM3, 51-65 (1959).
16. Delay, W. H., Seaders, J., "Predicting Temperatures in Rivers and Reservoirs." J. San. Engr. Div., ASCE, 92, SA1, 115-133 (1966).
17. Dresnack, R., Dobbins, W. E., "Numerical Analysis of BOD and DO Profiles." J. San. Engr. Div., ASCE, 94, SA5, 789-807 (1968).
18. Dutton, J. A., Bryson, R. A., "Heat Flux in Lake Mendota." Limnology and Oceanography, 7, 1, 80-97 (1962).
19. Edinger, J. E., "Vertical Temperature Structure and Water Surface Heat Exchange." Water Resources Research, 6, 5, 1392-1395 (1970).
20. Elder, R. A., Garrison, J. M., "The Causes and Persistence of Density Currents." Water and Sewage Works, 112, 144-150 (1965).
21. Elder, R. A., Wunderlich, W. O., "Evaluation of Fontana Field Measurements." T. V. A. Engineering Laboratory, Norris, Tenn. (1967).
22. Elder, R. A., Wunderlich, W. O., Discussion of "Predicting Temperatures in Rivers and Reservoirs," by W. H. Delay, F. Seader. J. San. Engr. Div., ASCE, 92, SA6, 120-124 (1966).
23. Goodling, J. S., Arnold, T. G., "Deep Reservoir Thermal Stratification Model." Water Resources Bulletin, AWRA, 8, 4, 745-749 (1972).
24. Handbook of Chemistry and Physics (54th edition). (Ed.) R. C. Weast. The Chemical Rubber Co., Cleveland, Ohio (1973-1974).
25. Harleman, D. R. F., "Stratified Flow." In Handbook of Fluid Dynamics. (Ed.) V. L. Streeter. McGraw-Hill Book Co., New York (1961).
26. Huber, W. C., Harleman, D. R. F., "Laboratory Studies on Thermal Stratification in Reservoirs." Proceedings, Specialty Conference on Current Research into the Effects of Reservoirs on Water Quality, Hydraulics Div., ASCE, Portland, Oregon (1968).
27. Hutchinson, G. E., A Treatise on Limnology, Vol. I. John Wiley and Sons, Inc., New York (1957).

28. Johnson, B. E., Wunderlich, W. O., "Field Measurement Techniques in Large Reservoirs." T. V. A. Engineering Laboratory, Norris, Tenn. (1970).
29. Kittrell, F. W., "Effects of Impoundments on Dissolved Oxygen Resources." Sewage and Industrial Wastes, 31, 9, 1065-1081 (1959).
30. Kittrell, F. W., "Thermal Stratification in Reservoirs." Symposium on Streamflow Regulation for Quality Control, Publication No. 999-WP-30, Public Health Service, Cincinnati, Ohio (1965).
31. Koh, R. C. Y., "Viscous Stratified Flow Towards a Sink." J. of Fluid Mechanics, 24, 3, 555-575 (1966).
32. Kohler, M. A., "Lake and Pan Evaporation." In Water Loss Investigations - Lake Hefner Studies. Technical Report, USGS, Professional Paper 269 (1954).
33. Love, S. K., "Relationship of Impoundment to Water Quality." J. of American Water Works Association, 53, 5, 559-568 (1961).
34. Markofsky, M., Harleman, D. R. F., "Prediction of Water Quality in Stratified Reservoirs." J. of the Hydraulics Div., ASCE, 99, HY5, 729-745 (1973).
35. Mitchell, A. R., Computational Methods in Partial Differential Equations. John Wiley and Sons, Inc., New York (1969).
36. Munk, W. H., Anderson, E. R., "Notes on a Theory of the Thermocline." J. of Marine Research, 7, 276-295 (1948).
37. Murrill, P. W., Smith, C. L., Fortran IV Programming for Engineers and Scientists. International Textbook Co., Scranton, Pa. (1971).
38. O'Connell, R. L., Thomas, N. A., "Effect of Benthic Algae on Stream Dissolved Oxygen." J. San. Engr. Div., ASCE, 91, SA3, 1-16 (1965).
39. Orlob, G. T., "A Mathematical Model of Thermal Stratification in Deep Reservoirs." Proceedings, Conference of the American Fisheries Society, Portland, Oregon (1965).
40. Orlob, G. T., Roesner, L. A., Norton, W. R., "Mathematical Models for the Prediction of Thermal Energy Changes in Impoundments." Final Report to FWPCA by Water Resources Engineers, Inc. (1969).
41. Orlob, G. T., Selna, L. G., "Mathematical Simulation of Stratification in Deep Reservoirs." Proceedings, Specialty Conference on Current Research into the Effects of Reservoirs on Water Quality, Hydraulics Div., ASCE, Portland, Oregon (1968).

42. Orlob, G. T., Selna, L. B., "Temperature Variations in Deep Reservoirs." J. of the Hydraulics Div., ASCE, 96, HY2, 391-410 (1970).
43. Park, G. G., Schmidt, P. S., "Numerical Modeling of Thermal Stratification in a Reservoir with Large Discharge-to-volume Ratio." Water Resources Bulletin, AWRA, 9, 5, 932-941 (1973).
44. Posey, F. H., DeWitt, J. W., "Effects of Reservoir Impoundments on Water Quality." J. of the Power Div., ASCE, 96, P01, 173-185 (1970).
45. Raphael, J. M., "Prediction of Temperature in Rivers and Reservoirs." J. of Power Div., ASCE, 88, P02, 157-181 (1962).
46. Rohwer, C., "Evaporation from Free Water Surfaces." U. S. Dept. of Agriculture Technical Bulletin No. 271 (1931).
47. Ryan, P. J., Harleman, D. R. F., "Temperature Prediction in Stratified Water." EPA, Water Pollution Control Research Series, 16130 DJH (1971).
48. Slotta, L. S., "Reservoir Temperatures," in Reservoir: Problems and Conflicts Seminar conducted by WRII, Oregon State University, Corvallis, Oregon (1969).
49. Smith, S. A., Bella, D. A., "Dissolved Oxygen and Temperature in a Stratified Lake." J. Water Pollution Control Federation, 45, 1, 119-133 (1973).
50. Spangenberg, W. G., Rowland, W. R., "Convective Circulation in Water Induced by Evaporative Cooling." The Physics of Fluids, 4, 6, 743-750 (1961).
51. Streeter, H. W., Phelps, E. B., "A Study of the Pollution and Natural Purification of the Ohio River." U. S. Public Health Service Bulletin, 146 (1925).
52. Stuart, F., Fortran Programming. John Wiley and Sons, Inc., New York (1969).
53. Sylvester, R. O., "Effects of Water Uses and Impoundments on Water Temperature." Proceedings, 12th Pacific Northwest Symposium on Water Pollution Research, Corvallis, Oregon (1963).
54. Symons, J. M., "Water Quality Behavior in Reservoirs." U. S. Public Health Service Bulletin, Cincinnati, Ohio (1969).
55. Symons, J. M., Irwin, W. H., Robeck, G. G., "Impoundment Water Quality Changes Caused by Mixing." J. San. Engr. Div., ASCE, 93, SA2, 1-20 (1967).

56. Symons, J. M., Robeck, G. G., "Impoundment Research." Water and Wastes Engineering, 3, 66-68 (1966).
57. Symons, J. M., Weibel, S. R., Robeck, G. G., "Impoundment Influences on Water Quality." J. of American Water Works Association, 57, 1, 51-75 (1965).
58. Symons, J. M., Weibel, S. R., Robeck, G. G., "Influence of Impoundments on Water Quality - A Review of Literature and Statement of Research Needs." Publication No. 999-WP-18, U. S. Public Health Service, Cincinnati, Ohio (1964).
59. Tennessee Valley Authority, "Fontana Reservoir, 1966 Field Data, Parts I, II and III." Div. of Water Control Planning, Engineering Laboratory, Norris, Tenn. (1969).
60. Tennessee Valley Authority, "The Prediction of Withdrawal Layer Thickness in Density Stratified Reservoirs." Laboratory Report No. 4, Div. of Water Control Planning, Engineering Laboratory, Norris, Tenn. (1969).
61. Tennessee Valley Authority, "Vertical Diffusivity in Density - Stratified Reservoirs." Advance Report No. 8, Div. of Water Control Planning, Engineering Laboratory, Norris, Tenn. (1969).
62. Tennessee Valley Authority, "Heat and Mass Transfer Between a Water Surface and the Atmosphere." Laboratory Report No. 14, Div. of Water Control Planning, Engineering Laboratory, Norris, Tenn. (1972).
63. Velz, C. J., Gannon, J. J., "Forecasting Heat Loss in Ponds and Streams." J. Water Pollution Control Federation, 32, 4, 392-417 (1960).
64. Whitaker, S., Introduction to Fluid Mechanics. Prentice Hall, Inc., Englewood Cliffs, New Jersey (1968).
65. Wunderlich, W. O., "The Dynamic of Density - Stratified Reservoirs." T. V. A., Engineering Laboratory, Norris, Tenn. (1970).
66. Wunderlich, W. O., Elder, R. A., "Effect of Intake Elevation and Operation on Water Temperature." J. of the Hydraulics Div., ASCE, 95, HY6, 2081-2091 (1969).
67. Wunderlich, W. O., Elder, R. A., "Graphical Temperature and Dissolved Oxygen Prediction Methods." T. V. A. Advance Report No. 9, Engineering Laboratory, Norris, Tenn. (1970).
68. Wunderlich, W. O., Elder, R. A., "The Influence of Reservoir Hydrodynamics on Water Quality." Proceedings, 6th Sanitary and Water Resources Engineering Conference, Vanderbilt University, Nashville, Tenn. (1967).

69. Wunderlich, W. O., Elder, R. A., "Mechanics of Flow Through Man-made Lakes." Proceedings, Symposium on Man-made Lakes, Their Problems and Environmental Effects, Knoxville, Tenn. (1971).
70. Wunderlich, W. O., Elder, R. A., "The Mechanics of Stratified Flow in Reservoirs." Proceedings, Symposium of the American Fisheries Society, Athens, Georgia (1967).
71. Wunderlich, W. O., Elder, R. A., "The Modeling of Reservoir Hydrodynamics and Its Influence on Water Quality." T. V. A. Engineering Laboratory, Norris, Tenn. (1968).
72. Yih, C. S., Dynamics of Non-homogeneous Fluids. MacMillan Company, New York (1965).
73. Yih, C. S., "On the Flow of a Stratified Fluid." Proceedings, 3rd U. S. National Congress of Applied Mechanics, ASME, Providence, R. I., 857-871 (1958).
74. Yotsukura, N., Fiering, M. B., "Numerical Solution to a Dispersion Equation." J. of the Hydraulics Div., ASCE, 90, HY5, 83-104 (1964).

APPENDIX A

D.O. PROFILES AND OUTFLOW D.O. CONCENTRATION

FOR  $k_1 = 0.05 \text{ DAY}^{-1}$

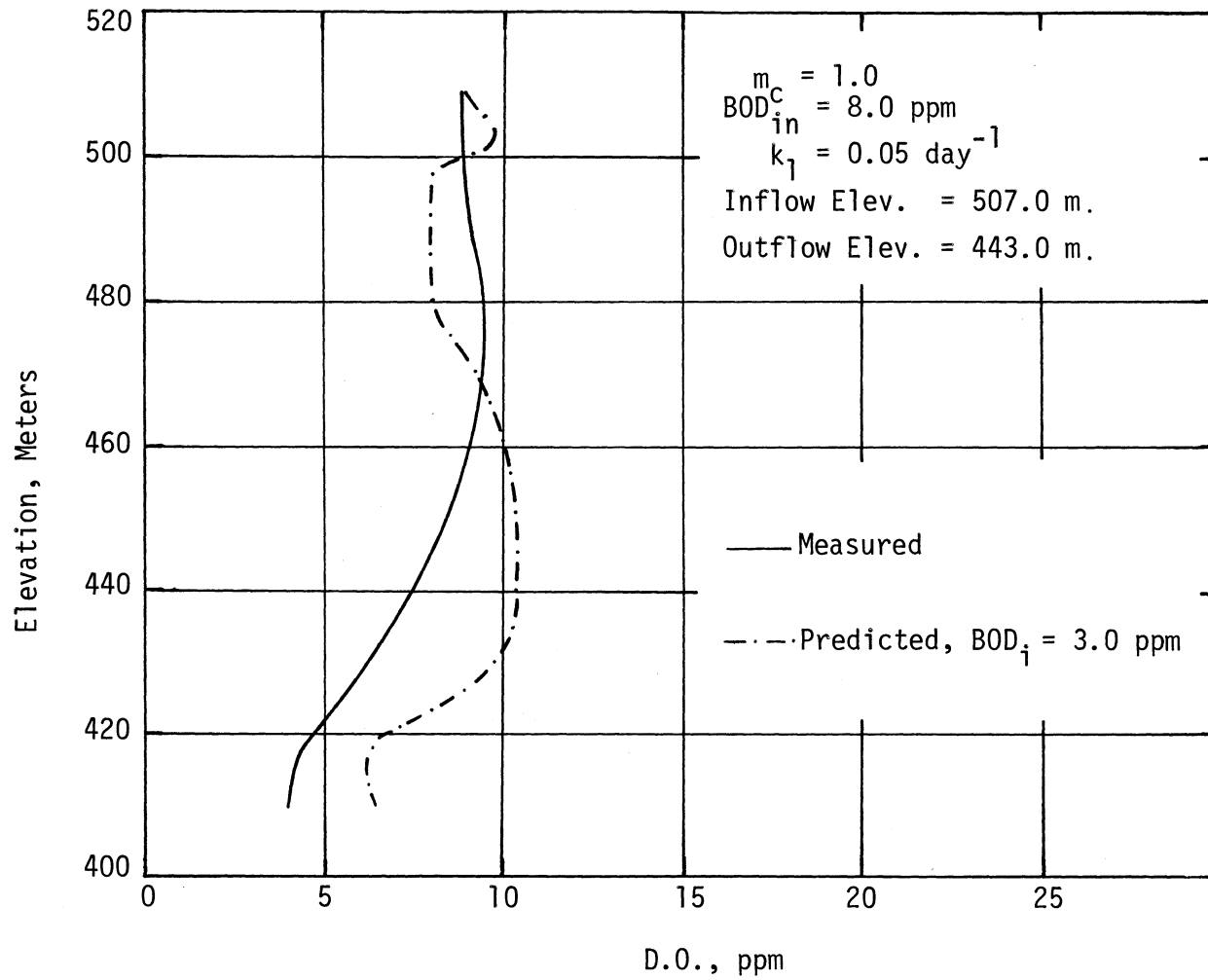


Figure 43. D.O. Profiles for Fontana Reservoir, May 20, 1966

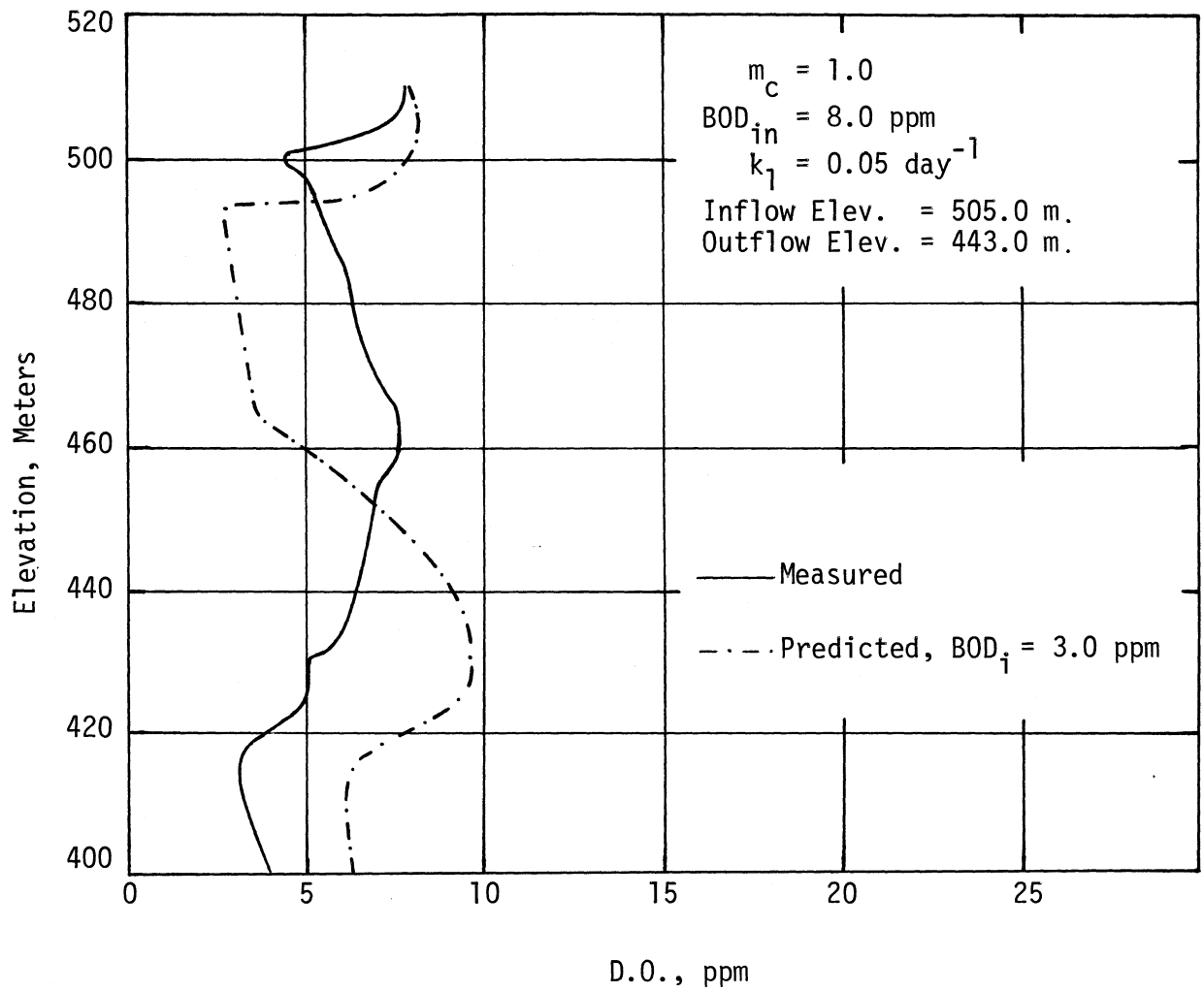


Figure 44. D.O. Profiles for Fontana Reservoir, July 19, 1966



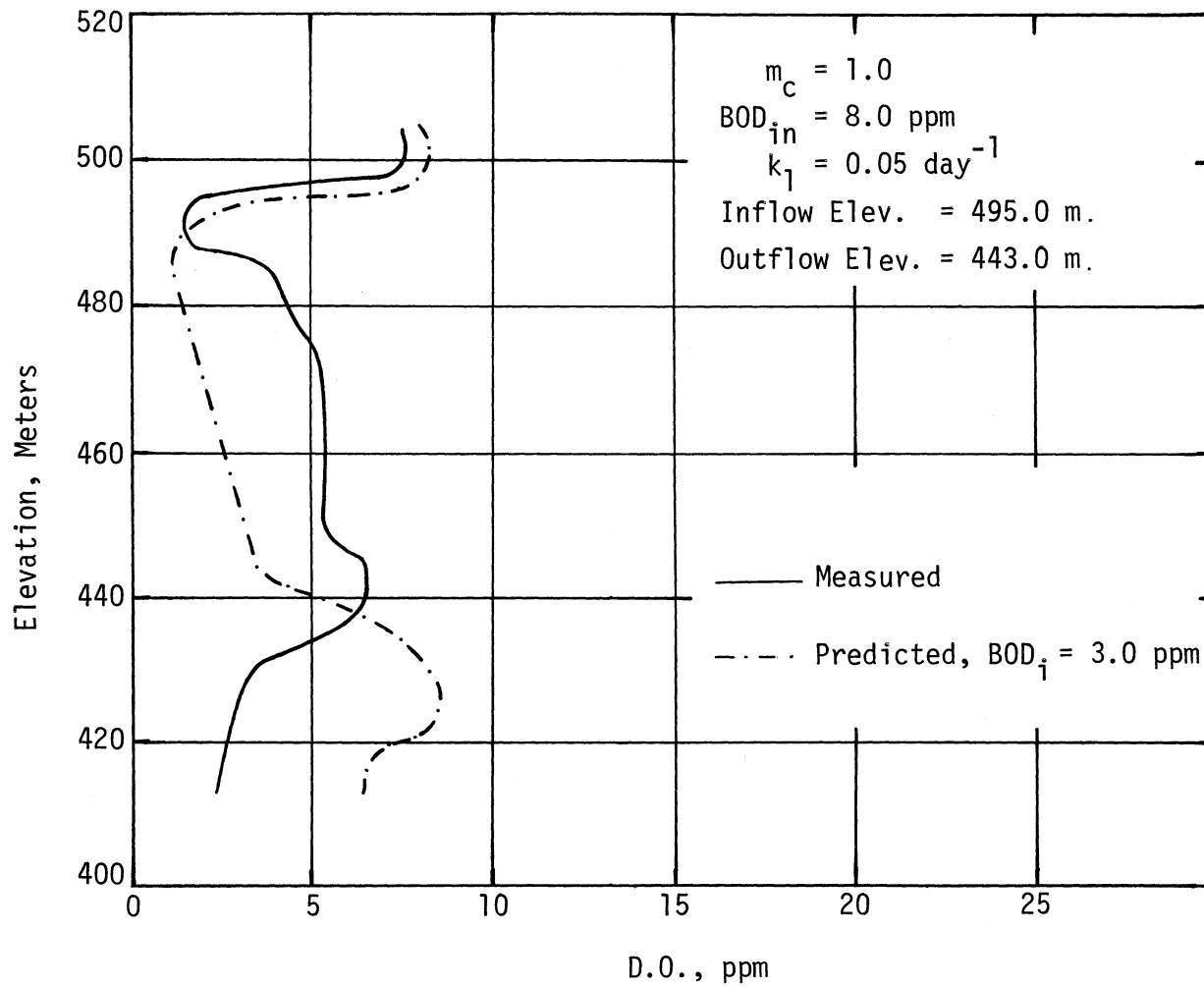


Figure 45. D.O. Profiles for Fontana Reservoir, August 12, 1966

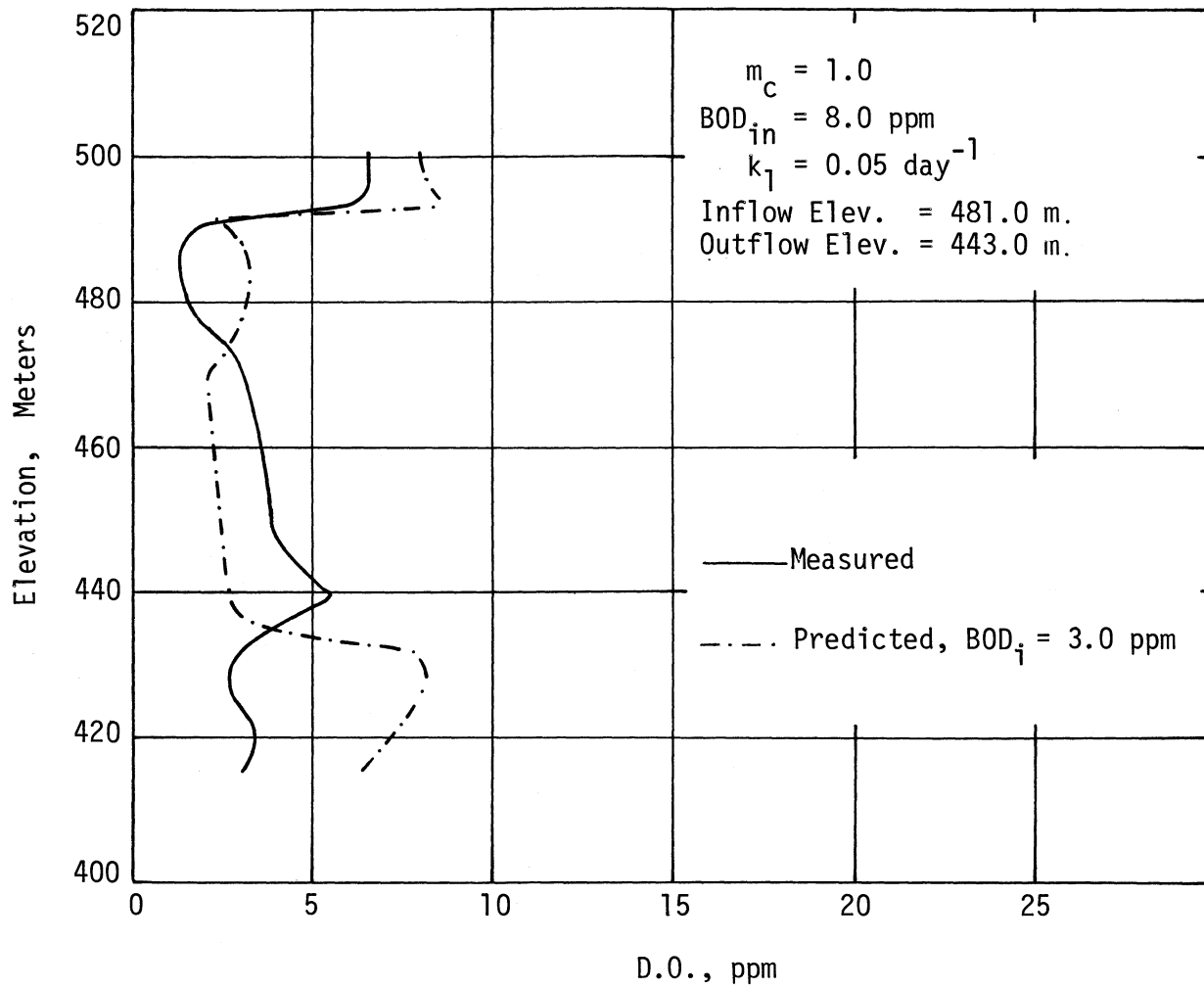


Figure 46. D.O. Profiles for Fontana Reservoir, September 7, 1966

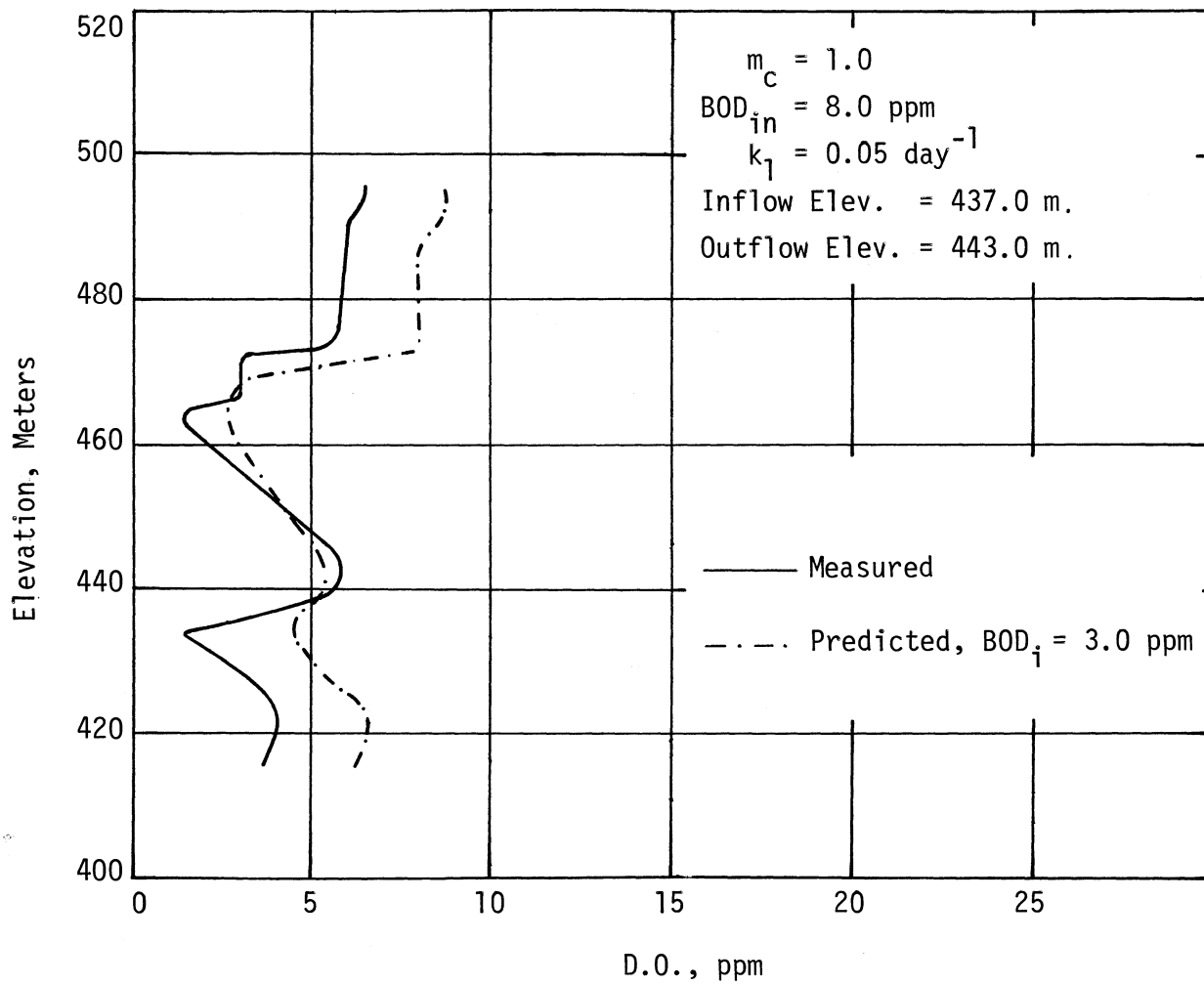


Figure 47. D.O. Profiles for Fontana Reservoir, October 3, 1966

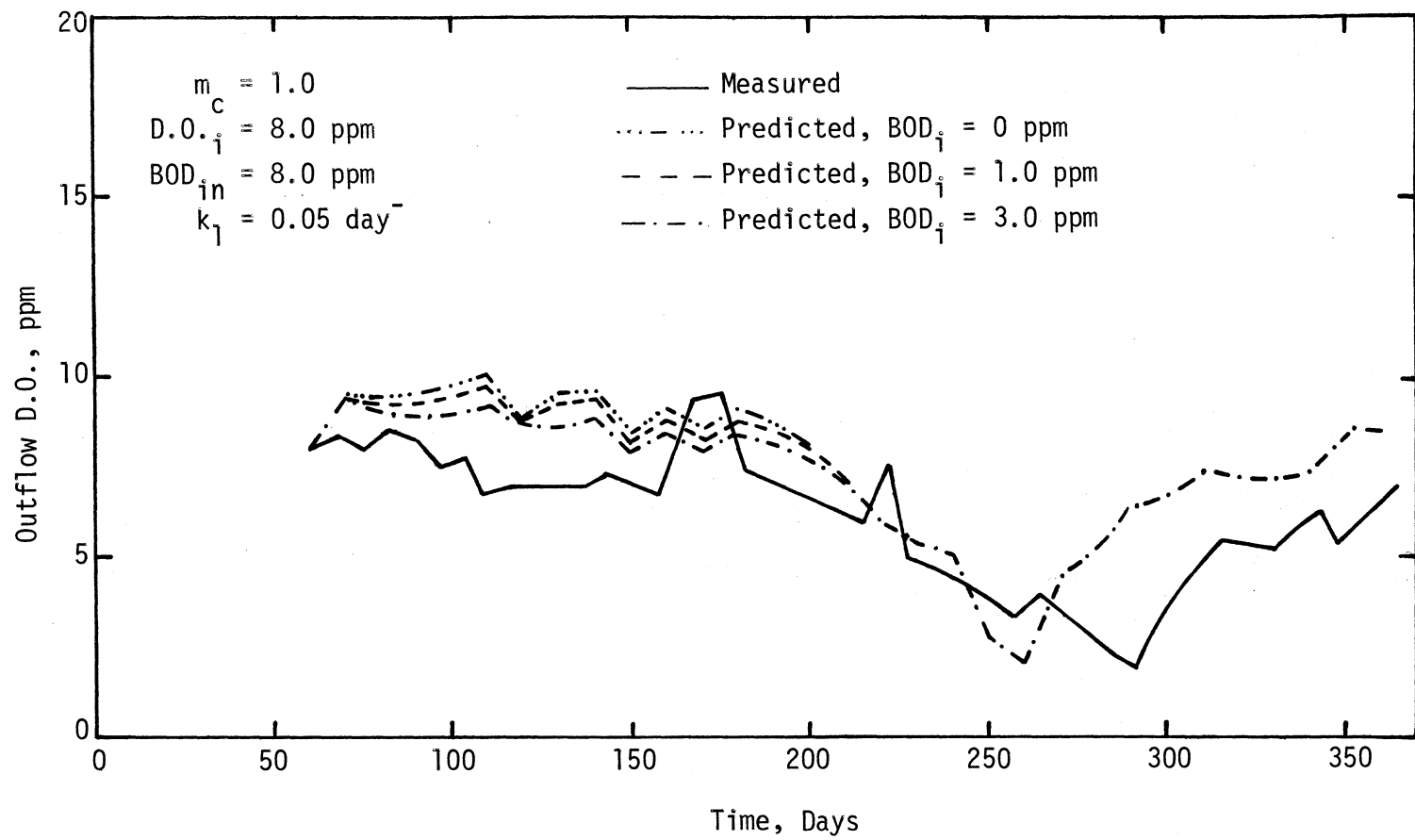


Figure 48. Outflow D.O. Concentrations, Fontana Reservoir, 1966

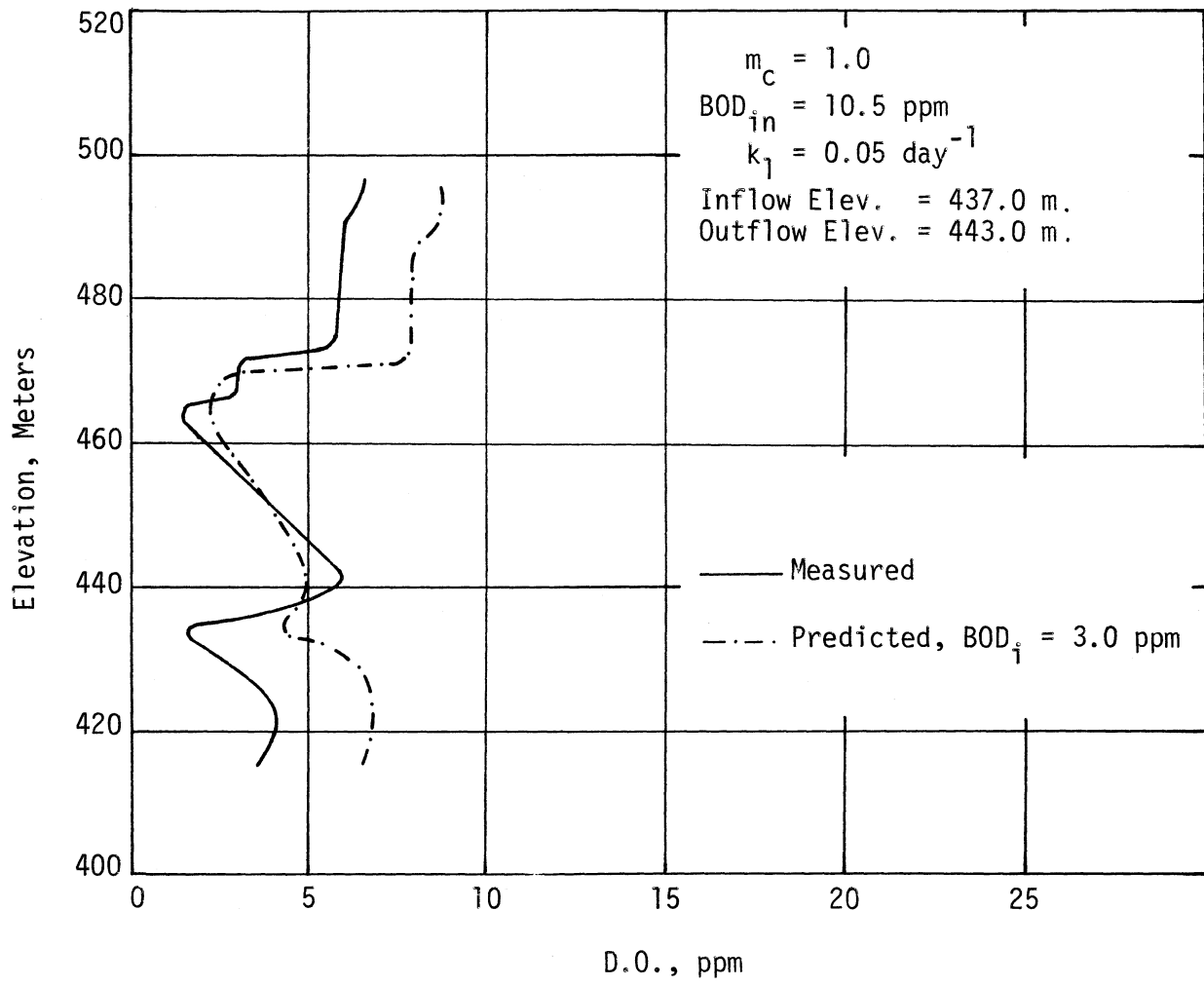


Figure 49. D.O. Profiles for Fontana Reservoir, October 3, 1966

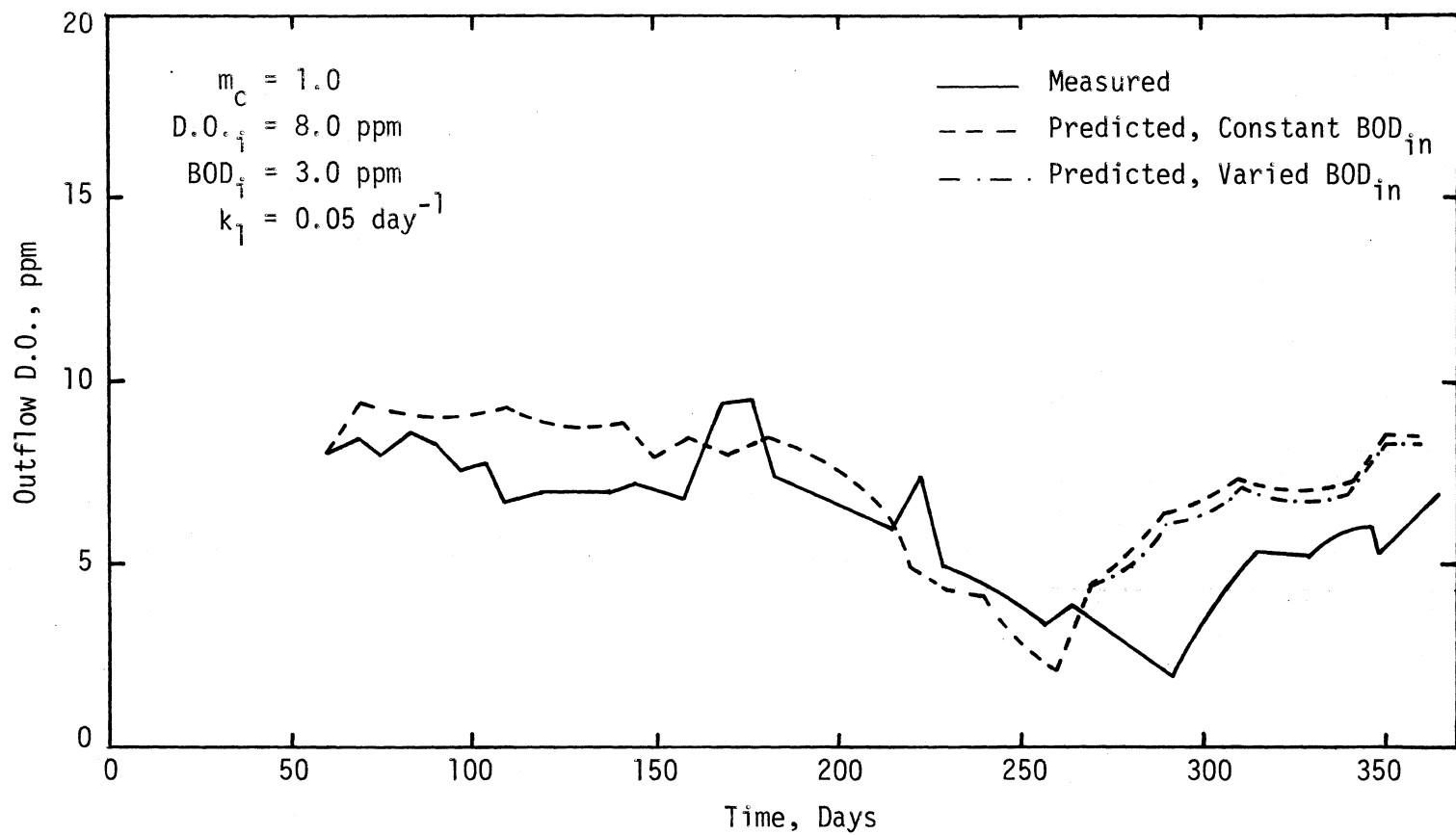


Figure 50. Effect of Inflow BOD on the Outflow D.O. Concentrations, Fontana Reservoir, 1966

APPENDIX B

THE EFFECT OF MIXING COEFFICIENT ON  
OUTFLOW D.O. CONCENTRATIONS

TABLE III  
EFFECTS OF MIXING COEFFICIENTS ON OUTFLOW D.O. CONCENTRATIONS

No. of days since March 1	Outflow D.O. (ppm)*					
	Measured	Predicted				
		$m_c$				
		0	0.5	1.0	1.5	2.0
1	8.0	8.0	8.0	8.0	8.0	8.0
11	8.3	11.1	9.7	9.4	9.3	9.2
21	8.4	10.3	9.2	9.0	8.9	8.8
31	8.4	10.1	9.1	8.9	8.7	8.6
41	7.7	10.0	9.4	9.1	8.9	8.5
51	6.8	10.0	9.9	9.5	9.3	9.1
61	7.0					
71	7.0	10.0	9.4	9.0	8.8	8.6
81	7.1	10.0	9.5	9.2	8.9	8.7
91	7.0	10.0	8.3	8.0	7.9	7.9
101	7.3	9.9	9.1	8.7	8.4	8.2
111	9.4	9.8	8.6	8.1	7.9	7.7
121	7.4	8.6	8.9	8.6	8.4	8.3
131	7.0	8.5	8.7	8.4	8.2	8.1
141	6.6	8.0	8.1	7.9	7.7	7.7
151	6.1	6.7	7.1	7.0	7.0	7.1
161	7.4	4.2	4.8	5.1	5.3	5.5
171	5.0	2.0	3.5	4.3	4.8	5.2
181	4.5	0.9	2.6	3.4	3.8	4.1
191	3.9	0.8	1.8	2.4	2.8	3.1
201	3.6	1.4	1.4	1.8	2.2	2.5
211	3.5	2.5	2.3	3.7	3.6	3.7
221	2.9	1.6	3.2	3.8	4.2	4.4
231	2.1	1.6	3.7	4.8	5.4	5.7
241	3.5	3.2	4.7	5.2	5.4	5.5
251	5.0	3.3	5.2	5.8	5.9	7.3
261	5.2	3.8	5.5	7.6	7.5	7.7
271	5.2	2.2	4.3	5.2	5.6	5.8
281	6.0	2.0	4.5	5.4	6.8	7.3
291	5.4	4.0	5.2	6.7	7.3	7.6
301	6.6	4.3	5.4	6.5	7.2	7.6

\*  $BOD_i = 3$  ppm  
 $BOD_{in} = \text{varied}$   
 $k_1 = 0.1 \text{ day}^{-1}$   
 $D.O. \text{ at surface} = 0.8(D.O._{sat})$



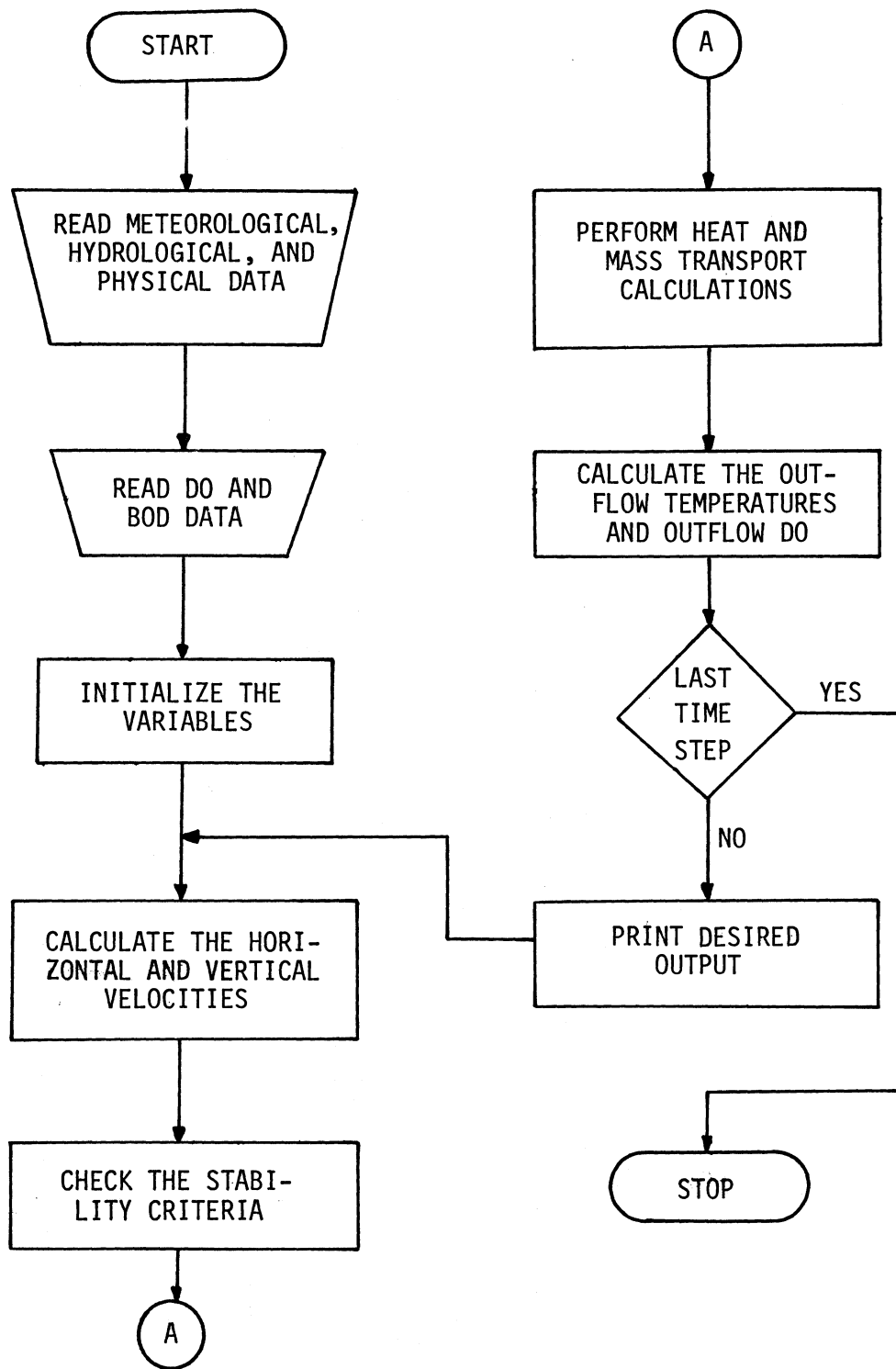
TABLE IV  
EFFECTS OF MIXING COEFFICIENTS ON OUTFLOW D.O. CONCENTRATIONS

No. of days since March 1	Outflow D.O. (ppm)*					
	Measured	Predicted				
		$m_c$				
		0	0.5	1.0	1.5	2.0
1	8.0	8.0	8.0	8.0	8.0	8.0
11	8.3	11.1	9.7	9.4	9.3	9.2
21	8.4	10.3	9.2	9.0	8.9	8.8
31	8.4	10.1	9.1	8.9	8.7	8.6
41	7.7	10.0	9.4	9.1	8.9	8.5
51	6.8	10.0	9.9	9.5	9.3	9.1
61	7.0					
71	7.0	10.0	9.4	9.0	8.8	8.6
81	7.1	10.0	9.5	9.2	8.9	8.7
91	7.0	10.0	8.3	8.0	7.9	7.9
101	7.3	9.9	9.1	8.7	8.4	8.2
111	9.4	9.8	8.6	8.1	7.9	7.7
121	7.4	8.6	8.9	8.6	8.4	8.3
131	7.0	8.5	8.7	8.4	8.2	8.1
141	6.6	7.9	8.1	7.9	7.7	7.7
151	6.1	6.7	7.1	7.0	7.0	7.1
161	7.4	4.2	4.7	5.1	5.3	5.5
171	5.0	2.0	3.5	4.3	4.8	5.2
181	4.5	0.9	3.1	4.1	4.7	5.1
191	3.9	0.8	2.1	2.8	3.3	3.7
201	3.6	1.4	1.6	2.1	2.6	3.0
211	3.5	2.5	3.9	4.4	4.3	4.4
221	2.9	1.6	3.6	4.5	5.0	5.3
231	2.1	1.6	4.3	5.6	6.4	6.9
241	3.5	3.2	5.4	6.1	6.5	6.6
251	5.0	3.4	5.9	6.8	7.0	8.9
261	5.2	3.8	6.8	6.5	6.8	8.5
271	5.2	2.3	4.9	6.1	6.7	7.0
281	6.0	2.3	5.3	6.5	8.3	8.9
291	5.4	4.4	6.0	8.0	8.8	9.4
301	6.6	5.1	6.5	7.8	8.7	9.3

\*  $BOD_i = 3$  ppm  
 $BOD_{in} =$  varied  
 $k_1 = 0.10$  day<sup>-1</sup>  
D.O. at surface = D.O.<sub>sat</sub>

APPENDIX C

FLOW DIAGRAM REPRESENTATION OF MODELS



APPENDIX D  
THE COMPUTER PROGRAMS AND THE  
INPUT DATA

PLEASE NOTE:

Pages 155-167, The Computer Programs and the Input Data on these pages has extremely small print. Will be unreadable on microfilm. Filmed as received.

UNIVERSITY MICROFILMS.

```

C 'QUALITY PARAMETER MODELS FOR STRATIFIED IMPOUNDMENTS'
C THE COMPUTER PROGRAM FOR CALCULATING THE TEMPERATURE DISTRIBUTIONS
C WITHIN AND IN THE DISCHARGE FROM THE RESERVOIRS, ALSO COMPUTING THE
C DO PROFILES AND OUTFLOW DO CONCENTRATIONS FOR DEEP RESERVOIRS.
C THE PROGRAM CONSISTS OF 1 MAIN PROGRAM, 7 SUBROUTINES, AND 9 FUNCTIONS.
C THE MAIN PROGRAM
C -READS IN ALL THE INPUT DATA, SUCH AS HYDRAULICS DATA, HYDROLOGIC DATA,
C AND METEOROLOGICAL DATA, INITIAL DO AND BOD, AND INFLOW DO AND BOD.
C -INITIALIZES VARIABLES.
C -CALLS THE SUBROUTINES FOR THE CALCULATIONS OF INFLOW AND OUTFLOW
C VELOCITIES, VERTICAL VELOCITIES, HEAT INFLOWS AND OUTFLOWS, CONVECTIVE
C MIXING OF HEAT AND MASS, AND THE DISTRIBUTION OF DO AND BOD.
C -PERFORMS THE HEAT TRANSPORT CALCULATIONS FOR EACH TIME STEP.
C -PRINTS OUT THE DESIRED OUTPUT.
C ALL UNITS USED IN THE CALCULATIONS ARE IN METERS, KILOGRAMS, DAYS,
C KILOCALORIES, DEGREE CENTIGRADES AND PPM, UNLESS OTHERWISE SPECIFIED.
C FUNCTION SHUTIN(I)
C CALCULATE THE HEAT INPUT DUE TO NET SOLAR RADIATION.
C SUBROUTINE FLOWPT(N)
C CALCULATE THE HORIZONTAL INFLOW AND OUTFLOW VELOCITIES, VERTICAL
C VELOCITIES, AND WITHDRAWAL LAYER THICKNESS.
C SUBROUTINE EMOATIN(I)
C CALCULATE THE MIXED INFLOW DO AND BOD.
C SUBROUTINE CNMIXH(I)
C CALCULATE THE TEMPERATURES OF TOP LAYERS DUE TO CONVECTIVE MIXING
C BY THE WEIGHTED AVERAGE OF TEMPERATURES AND VOLUMES OF THE LAYERS
C THAT ARE MIXED.
C SUBROUTINE DDMIN(I)
C CALCULATE THE DISTRIBUTION OF DO AND BOD CONCENTRATIONS IN THE
C RESERVOIR.
C SUBROUTINE CNMIX(I)
C CALCULATE THE CONCENTRATIONS OF DO OR BOD OF TOP LAYERS DUE TO
C CONVECTIVE MIXING BY THE WEIGHTED AVERAGE OF DO OR BOD AND VOLUME OF
C THE LAYERS THAT ARE MIXED.
C FUNCTION SHOUT(I)
C CALCULATE THE HEAT LOSSES DUE TO WATER SURFACE RADIATION, EVAPORATION,
C AND CONDUCTION.
C SUBROUTINE TOUT
C CALCULATE THE OUTFLOW TEMPERATURES.
C SUBROUTINE DTFCOM(I)
C CALCULATE THE OUTFLOW DO CONCENTRATIONS.
C FUNCTIONS QOIN(I), TTIN(I), DOOIN(I), BODO(I), DIJ(N), DIFMASIJ, NI, AND
C QOUT(I), TJ ARE FOR THE CALCULATIONS OF INFLOW RATES, TEMPERATURES, DO
C AND BOD CONCENTRATIONS, THE DIFFUSIVITY OF HEAT AND MASS, AND THE
C OUTFLOW RATES FROM READ IN VALUES, RESPECTIVELY.
C LIST OF VARIABLES
C A =CALCULATED HORIZONTAL AREA OF THE RESERVOIR.
C AA =HORIZONTAL AREA OF THE RESERVOIR AVAILABLE.
C AAB =THE LOWEST ELEVATION OF THE AVAILABLE HORIZONTAL AREA OF THE
C RESERVOIR.
C AR =CALCULATED ATMOSPHERIC RADIATION.
C ATRAD =VALUES OF THE ATMOSPHERIC RADIATION READ IN.
C AYSUR =HORIZONTAL AREA AT THE WATER SURFACE OF THE RESERVOIR.
C W =WIDTH OF THE RESERVOIR.
C BETA =RATIO OF RADIATION ABSORBED AT THE WATER SURFACE TO NET INCOMING
C RADIATION.
C BOD =VALUES OF INFLOW BOD.
C BODI =INITIAL BOD IN THE RESERVOIR.
C CC =CONCENTRATIONS OF DO OR BOD IN THE RESERVOIR.
C CCC =MIXED INFLOWS OF DO OR BOD.
C CONDOC =HEAT LOSSES DUE TO CONDUCTION.
C CONST =CONSTANT FOR THE CALCULATION OF WITHDRAWAL LAYER THICKNESS.
C COUT =OUTFLOW DO CONCENTRATIONS.
C DAA =DISTANCE BETWEEN THE AVAILABLE HORIZONTAL AREAS.
C DATRAD =TIME INTERVAL BETWEEN INPUT VALUES OF ATMOSPHERIC RADIATION.
C DD =DIFFUSIVITY OF HEAT.
C DIM =DIFFUSIVITY OF MASS.
C DO =VALUES OF INFLOW DO.
C DOI =INITIAL DO IN THE RESERVOIR.
C DOSA =SATURATED VALUE OF DO.
C DSURF =TIME INTERVAL BETWEEN INPUT VALUES OF WATER SURFACE ELEVATIONS.
C DT =TIME INCREMENT.
C DTBOD =RATE OF CHANGE OF TEMPERATURE WITH DEPTH.
C DTBOD =TIME INTERVAL BETWEEN INPUT VALUES OF BOD.
C DTDO =TIME INTERVAL BETWEEN INPUT VALUES OF DO.
C DTDO =TIME INTERVAL BETWEEN INPUT VALUES OF DIFFUSIVITY OF HEAT.
C DTDO =TIME INTERVAL BETWEEN INPUT VALUES OF DIFFUSIVITY OF MASS.
C DTDO =TIME INTERVAL BETWEEN INPUT VALUES OF DO.
C DTSEE =TIME INTERVAL BETWEEN INPUT VALUES OF SOLAR RADIATION.
C DTOT =TIME INTERVAL BETWEEN INPUT VALUES OF INFLOWS.
C DTOT =TIME INTERVAL BETWEEN INPUT VALUES OF OUTFLOWS.
C DTSTGH =TIME INTERVAL BETWEEN INPUT VALUES OF RELATIVE HUMIDITIES.
C DTTA =TIME INTERVAL BETWEEN INPUT VALUES OF AIR TEMPERATURES.
C DTTI =TIME INTERVAL BETWEEN INPUT VALUES OF INFLOWS TEMPERATURES.
C DTWIND =TIME INTERVAL BETWEEN INPUT VALUES OF WIND SPEED.
C DXXL =DISTANCE BETWEEN THE AVAILABLE LENGTHS OF THE RESERVOIR.
C DY =DISTANCE INCREMENT.
C DYSUR =THICKNESS OF SURFACE ELEMENT.
C EA =VAPOR PRESSURE OF AIR.
C EL =ELEVATION.
C ELOUT =ELEVATION OF THE OUTLET.
C EPSIL =DENSITY GRADIENT AROUND THE INTAKE.
C ES =SATURATED VAPOR PRESSURE AT WATER SURFACE TEMPERATURE.
C ET =TIME SINCE THE START OF THE CALCULATION.
C EVAP =HEAT LOSSES DUE TO EVAPORATION.
C FEE =INCOMING SOLAR RADIATION.
C FLOWOT =TOTAL OUTFLOW RATE.
C GRAY =ACCELERATION DUE TO GRAVITY.
C HAFDEL =HALF OF THE WITHDRAWAL LAYER THICKNESS.
C HCAP =SPECIFIC HEAT OF WATER.
C HEATOT =TOTAL OUTFLOW HEAT.
C JEUP =NO. OF ELEMENT CORRESPONDING TO THE BOTTOM OF EUPHOTIC ZONE.
C JM =NO. OF ELEMENT OF SURFACE LAYER.
C JMP =MAXIMUM POSSIBLE NO. OF ELEMENT OF SURFACE LAYER.
C JOUT =NO. OF ELEMENT CORRESPONDING TO THE OUTLET ELEVATION.
C KDMIX =NO. OF LAYERS INVOLVED IN MIXING AT THE ENTRANCE.
C KMIX =MIXING AT THE ENTRANCE.
C LOUT =NO. OF THE ELEMENT AT THE OUTLET.
C N =NO. OF TIME STEP.
C NAA =NO. OF HORIZONTAL AREA AVAILABLE.
C NATRAD =NO. OF ATMOSPHERIC RADIATION AVAILABLE.
C NBOD =NO. OF INFLOW BOD CONCENTRATIONS AVAILABLE.
C NDOCOM =NO. OF INFLOW DO CONCENTRATIONS AVAILABLE.
C NDD =NO. OF INPUTS OF DIFFUSIVITY OF HEAT.
C NDM =NO. OF INPUTS OF DIFFUSIVITY OF MASS.
C NFEE =NO. OF INPUTS SOLAR RADIATION AVAILABLE.
C NOUT =NO. OF OUTFLOWS.
C NOI =NO. OF INFLOW RATES AVAILABLE.
C NOO =NO. OF OUTFLOW RATES AVAILABLE.
C NSTGH =NO. OF RELATIVE HUMIDITIES AVAILABLE.
C NSURF =NO. OF SURFACE ELEVATION AVAILABLE.
C NTA =NO. OF AIR TEMPERATURES AVAILABLE.
C NTI =NO. OF INFLOW WATER TEMPERATURES AVAILABLE.
C NTSPRI =NO. OF TIME STEP BETWEEN PRINT OUT OF OUTPUT.
C NWIND =NO. OF WIND SPEEDS AVAILABLE.
C NXXL =NO. OF LENGTHS OF RESERVOIR AVAILABLE.
C PST =VALUES OF THE CALCULATED RELATIVE HUMIDITIES.
C QT =INFLOW RATES.
C QIN =QOIN=CALCULATED INFLOW RATES.
C QO =OUTFLOW RATES.
C QOUT =CALCULATED OUTFLOW RATES.

```

```

C QMIX =RATE OF RESERVOIR WATER MIXED WITH THE INFLOWS.
C RAD =DIFFERENCE BETWEEN WATER SURFACE RADIATION AND ATMOSPHERIC
C RADIATION
C RHO =WATER DENSITY.
C SAPEA =AVERAGE HORIZONTAL AREA OF SURFACE ELEMENT.
C SIGM =RELATIVE HUMIDITIES.
C SIGMAI=INFLOW STANDARD DEVIATION.
C SIGMAO=OUTFLOW STANDARD DEVIATION.
C SLOPE =SLOPE OF THE RESERVOIR.
C STDDEV=VALUE FROM NORMAL CURVE TABLE FOR 95% CONFIDENCE INTERVAL.
C SURF =SURFACE ELEVATIONS.
C T =TEMPERATURES IN THE RESERVOIR.
C TA =AIR TEMPERATURES.
C TI =INFLOW TEMPERATURES.
C TIN =TIN=CALCULATED INFLOW TEMPERATURES.
C TOUTC =OUTFLOW TEMPERATURES.
C TP =TEMPERATURE OF RESERVOIR WATER MIXED WITH INFLOW WATER.
C TS =MIXED INFLOW TEMPERATURES.
C TSTOP =TIME TO STOP THE CALCULATION.
C TZERO =INITIAL TEMPERATURE IN THE RESERVOIR.
C UI =INFLOW VELOCITIES.
C UIMAX =MAXIMUM INFLOW VELOCITIES.
C UO =OUTFLOW VELOCITIES.
C UOMAX =MAXIMUM OUTFLOW VELOCITIES.
C UOT =OUTFLOW VELOCITIES OF EACH ELEMENT FOR EACH OUTLET.
C V =VERTICAL VELOCITIES.
C WIND =WIND SPEEDS.
C XK1 =FIRST ORDER DECAY RATE CONSTANT.
C XK2 =REGENERATION RATE CONSTANT.
C XL =CALCULATED LENGTH OF THE RESERVOIR.
C XMIXC =MIXING COEFFICIENT.
C XNUE =BULK EXTINCTION COEFFICIENT.
C XXL =LENGTH OF THE RESERVOIR AVAILABLE.
C XXLB =LOWEST ELEVATION OF THE AVAILABLE LENGTH.
C YBOT =ELEVATION OF THE BOTTOM OF THE RESERVOIR.
C YSUR =ELEVATION OF WATER SURFACE.
COMMON T(102,2),EL(102),XL(102),AT(102),TI(366),TA(366),SIGM(366)
COMMON FEE(366),WIND(366),DD(366),OI(366),OI(366),SI(366),NPR
COMMON UOMAX(5),UIMAX(1),DTI,DTTA,DTSIG,DTFEE,DTWIND,DTDD,DTOI
COMMON DTQQ,JM,JOUT,JIN,YSUR,YOUT,DT,DY
COMMON TSTOP,EVPCON,STDDEV,SIGMAI,SIGMAO
COMMON EVAP,AD,TAIR,PSI,DTDD,HAFDEL,EPSTL,GJ
COMMON V(102,1),UI(102,1),DT,YBOT,NN,BETA,CONST
COMMON XMIXC,RHO,HCAP,KMIX,JMIXB,KDMIX,QMIX,ATRAD,ATRAD(366)
COMMON AP,WINOY,B(102),S(102),EM(102),EX(102),UOT(102,1)
COMMON QIN(400),TIN(400),QMIX(102),JMIX,KMIX,EX(102),DX(102),NM
COMMON DIM(366),CC(20,102,2),CC(20,366),COUT(20,366)
COMMON NOUT,LOUT(5),ELOUT(5),TOUT(5),UOT(102,5)
COMMON SAPEA,SURF(366),EO,E1,F2,E3,ET
COMMON DTDD,DTDDO,DD(366),BDD(366),DYSUR,AYSUP
COMMON XK1,XK2,NUE,EL(366),JCUR,IT,NW
DIMENSION AA(102),XXL(102)
READ (5,901) JM,NTSPRI,KMIX,KDMIX
READ (5,901) NT(NTA,NSIGH,NFEE,NSURF,NDD,NQI,NQO,NOUT,NDIM)
READ (5,901) (LOUT(I),I=1,NOUT)
READ (5,901) NAA,NXXL,WIND,NATRAD,JMP
READ (5,901) NDOCON,NBOD
READ (5,902) YSUR,DY,DT,TSTOP,TZERO,EVPCON
READ (5,902) STDDEV,SIGMAI,XNUE,BETA,RHO,HCAP,CONST,KMIXC
READ (5,902) DTI,DTTA,DTSIG,DTFEE,DSURF,DTDD,DTOI,DTQQ
READ (5,902) DTDIM
READ (5,902) DAA,DXL,DTWIND,DATRAD,AA8,XXLB
READ (5,902) DTDD,DTDDO
READ (5,902) (FEE(I),I=1,NFEE)
READ (5,902) (ATRAD(I),I=1,NATRAD)
READ (5,902) (WIND(I),I=1,NWIND)
READ (5,902) (SIGM(I),I=1,NSIGH)
READ (5,902) (AA(I),I=1,NAA)
READ (5,902) (XXL(I),I=1,NXXL)
READ (5,902) (SURF(I),I=1,NSURF)
READ (5,902) (ELOUT(I),I=1,NOUT)
READ (5,902) (DD(I),I=1,NDD)
READ (5,902) (DTM(I),I=1,NDIM)
READ (5,902) (TA(I),I=1,NTA)
READ (5,902) (TI(I),I=1,NTI)
READ (5,902) (QI(I),I=1,NQI)
DO 300 I=1,NOUT
300 READ (5,902) (QOIN(I),N=1,NQO)
READ (5,902) (OI,BDD)
READ (5,902) XK1,XK2
READ (5,902) (DD(I),I=1,NDOCON)
READ (5,902) (BDD(I),I=1,NBDD)
YBOT=ELOUT(I)-DY*FLOAT(LOUT(I)-I)
DO 3 I=1,JMP
EL(I) = YBOT+DY*FLOAT(I-1)
RA = (EL(I)-NAR)/DAA
L = PA
A(I) = AA(L+1)+(RA-FLOAT(L))*(AA(L+2)-AA(L+1))
RA = (EL(I)-XXLB)/DXL
L = RA
XL(I)=XXL(L+1)+(RA-FLOAT(L))*(XXL(L+2)-XXL(L+1))
3 B(I)=A(I)/XL(I)
WRITE (6,904) JM,YSUR,RHO
WRITE (6,905) (LOUT(I),ELOUT(I),I=1,NOUT)
WRITE (6,906) DT,YBOT,XNUE
WRITE (6,907) DT,TZERO,BETA
WRITE (6,908) SIGMAI,HCAP
WRITE (6,909) TSTOP,STDDEV
WRITE (6,910) EVPCON,CONST,KMIXC
WRITE (6,923) KMIXB,KMIXC
DO 850 N=1,360
DTIN(N)=0.0
TIN(N)=0.0
850 CONTINUE
DO 851 I=1,JMP
TI(I,1) = TZERO
851 QMIX(I)=0.0
DO 852 J=1,JMP
CC(1,J,1)=DDI
CC(1,J,2)=DDO
CC(2,J,2)=RDDI
852 CC(2,J,1)=BDDI
NW=0
DT=DT
NPR=0
JM=JM
N=0
JMIXB=JM-KMIXC
QMIX=0.0
ET=0.0
RAD=0.0
EVAP=0.0
TAIR=0.0
EPSTL=0.0
HAFDEL=0.0
JIN=JM
CUMQIN=0.0
CUMQOI=0.0
NDDI=NTSPRI-1
DYSUR=YSUR-EL(JM)+DY/2.0
IF (YSUR-EL(JM)) 858,858,859
858 AYSUR=A(JM)-DY/2.0-DYSUR*(A(JM)-A(JM-1))/DY

```

```

GO TO 860
859 AYSUR=AJM)+(DYSUR-DY/2.0)*(AJM+1-AJM)/DY
860 SAREA=(AYSUR+(AJM+AJM-1))/2.0/2.0
SAREAL=SAREA
DYSUR1=DYSUR
JML=JM
F2=0.0
E1=0.0
F0=A(1)/2.0+SARFA*DYSUR/DY
JMM=JM-1
DO 13 I=2,JMM
13 EO=EO+A(I)
EO=EO*DY*TZEP(1+RH)*HCAP
IF(JM-60) 15,15,16
15 JP=JM
GO TO 17
16 JP=60
17 GO TO 20
20 NN=1
ET=ET+DT
NOO1=NOO1+1
GO TO (24,22),KMTX
22 TP=0.0
DO 23 J=JMXB,JM
23 TP=TP+(J,1)
TP=TP/FLOAT(KDMIX+1)
TS=(TTIN(N)+TP*XMXC)/(1.0+XMXC)
GO TO 25
24 TS=TTIN(N)
25 CONTINUE
DO 27 I=1,JM
J=J+1-1
IF(TS-T(J,1)) 27,30,30
27 CONTINUE
30 JIN=J+1
IF(JIN-JM) 32,32,33
33 JIN=JM
32 CONTINUE
NN=NN+1
JUP=JM-4.6/XNUE/DY
WRITE (6,911) JEUP
IF(JIN-DEIP) 192,193,193
193 NLEVE(N)=1
GO TO 190
192 NLEVE(N)=2
190 CONTINUE
QIN(N)=QOIN(N)
TIN(N)=TTIN(N)
JJP=JM
CUMQIN=CUMQIN+QIN(N)*DT
DO 332 I=1,NDUT
332 CUMQCT=CUMQCT+QOUT(N,I)*DT
QIO=CUMQIN-CUMQCT
IF(QIO) 34,34,35
35 SUM=SAREAL*DYSUR1
DO 36 M=1,JM
SUM=SUM+AJM*(M-1)*DY
IF(QIO-SUM) 37,37,36
36 CONTINUE
34 SUM=DYSUR*SARFA1
DO 38 M=1,JM
IF(ABS(QIO)-SUM) 39,39,38
38 SUM=SUM+AJM*(M-1)*DY
37 YSUR=EL(JM)+(M-0.5)*DY+(QIO-SUM)/AJM*(M-1)
GO TO 40
39 YSUR=EL(JM)-(M-0.5)*DY+(QIO+SUM)/AJM*(M-1)
40 DYS=YSUR-EL(JM)+DY/2.0
IF(DYS) 41,42,42
42 M=FIX(DYS/DY)
GO TO 43
41 M=FIX(DYS/DY)-1
43 JM=JM+M
DYSUR=YSUR-EL(JM)+DY/2.0
R=ET/DSUPF
L=R
RR=R-FLOAT(L)
SURRES=SURF(L)+R*(SURF(L+1)-SURF(L))
IF(SUR-EL(JM)) 58,58,59
58 AYSUP=(AJM)-(DY/2.0-DYSUR)*(AJM-AJM-1)/DY
GO TO 61
59 AYSUR=AJM+(DYSUR-DY/2.0)*(AJM+1-AJM)/DY
61 SAREA=(AYSUR+(AJM+AJM-1))/2.0/2.0
SUMV=0.0
JMM=JM-1
IF(JM-JM1) 510,511,512
512 DO 513 J=JM1,JMM
513 SUMV=SUMV+AJM*DY
511 SUMV=SUMV+SAREA*DYSUR-SAREAL*DYSUR1
GO TO 515
510 JMM1=JM1-1
DO 514 J=JM,JMM1
514 SUMV=SUMV+AJM*DY
SUMV=(SUMV+SARFA1*DYSUR1-SAREAL*DYSUR)
515 FRRQR=SUMV-QIO
DYCER=FRRQR/SAREA
DYSUP=DYSUP-DYCCP
IF(DYSUR-0.5) 506,506,507
506 DYSUR=DYSUP+DY
JM=JM-1
507 MP=JM-JM
IF(MP) 44,44,50
DO 51 I=1,MP
J=JM+1-1
51 T(J,1)=T(JM,1)
44 T(JM,1)=T(JM,1)
JMXB=JM-KDMIX
IF(JM-60) 53,53,54
53 JP=JM
GO TO 45
54 JP=60
45 CONTINUE
MM=2
DO 891 M=1,MM
IF(JM-JXM) 890,891,892
890 CC(M,JM,1)=2.0*CC(M,JM,1)+CC(M,JXM,1)*AJXM/A(JM)
GO TO 891
892 CC(M,JXM,1)=0.5*CC(M,JXM,1)+AJXM/(AJXM+0.5*A(JM))
CC(M,JM,1)=CC(M,JXM,1)
891 CONTINUE
CALL FLOWRT(N)
VVV=ABS(VI2,1)
DO 501 J=3,JM
IF(VVV-ABS(VI,J,1)) 502,501,501
502 VVV=ABS(VI,J,1)
501 CONTINUE
VM=DY/DTT
IF(VVV-VM) 503,504,504
504 DT=DY/VVV
IDT=DT/DT+1
DT=DT/IDT
GO TO 505
503 IDT=1

```



```

505 DO 79 M=1,101
      CALL EMDMIN(N)
      CALL DDFMIN(N)
      JMM=JM-1
      DO 114 J=2,JMM
        ARJ1=(A(J)+A(J+1))/2.0
        ARJ2=(A(J)+A(J+1))/2.0
        DELTA=(1.0-BETA)*SHTIN(N)*(EXP(-XNUE*(YSUR-EL(J)-DY/2.0))*ARJ1-
        IFXP1-XNUE*(YSUR-EL(J)+DY/2.0))*ARJ2)/A(J)/DY/HCAP/RHO
        IF(V(J,1)) 1160,1160,1161
1160 IF(V(J+1,1)) 1170,1170,1171
1170 DELTB=(V(J,1)+V(J+1,1))*A(J)+A(J-1))/2.0-V(J+1,1)*T(J,1)*A(J+1)+
      A(J))/2.0)/A(J)/DY
      GO TO 1162
1171 DELTB=(V(J,1)+T(J,1))*A(J)+A(J-1))/2.0-V(J+1,1)*T(J,1)*A(J+1)+
      A(J))/2.0)/A(J)/DY
      GO TO 1162
1161 IF(V(J+1,1)) 1172,1172,1173
1173 DELTB=(V(J,1)+T(J-1,1))*A(J)+A(J-1))/2.0-V(J+1,1)*T(J,1)*A(J+1)+
      A(J))/2.0)/A(J)/DY
      GO TO 1162
1172 DELTB=(V(J,1)+T(J-1,1))*A(J)+A(J-1))/2.0-V(J+1,1)*T(J,1)*A(J+1)+
      A(J))/2.0)/A(J)/DY
1162 DELTC=(U(J,1)+TS-U(J,1)*T(J,1)+B(LJ)*DY)/A(J)/DY
      DELTD=DD(1)*T(J,1)-T(J,1))/DY*ARJ1-(T(J,1)-T(J-1,1))/DY*ARJ2)/
      A(J)/DY
      DELT=(DELT+DELTB+DELTC+DELTD)*DT
1114 T(J,2)=T(J,1)+DELT
      IF (V(JM,1)) 1163,1163,1164
1164 DELTJM=DT*(1.0-BETA)*SHTIN(N)*(AYSUR-EXP(-XNUE*DYSUR)*
      1*(A(JM)+A(JM-1))/2.0)/SAREA/DYSUR/HCAP/RHO+
      1*(A(JM)+A(JM-1,1))-T(JM,1))*A(JM)+A(JM-1))/2.0)/SAREA/DYSUR
      1+UI(JM,1)*(TS-T(JM,1))*B(LJ)/SAREA
      1-DD(1)*T(JM,1)-T(JM-1,1))/DY*(A(JM)+A(JM-1))/2.0)/SAREA/DYSUR
      1+(BETA*SHTIN(N)-SHLQUT(N))*AYSUR/RHO/HCAP/DYSUR/SAREA)
      GO TO 1165
1163 DELTJM=DT*(1.0-BETA)*SHTIN(N)*(AYSUR-EXP(-XNUE*DYSUR)*
      1*(A(JM)+A(JM-1))/2.0)/SAREA/DYSUR/HCAP/RHO+
      1*(U(JM,1)+TS-T(JM,1))*B(LJ)/SAREA
      1-DD(1)*T(JM,1)-T(JM-1,1))/DY*(A(JM)+A(JM-1))/2.0)/SAREA/DYSUR
      1+(BETA*SHTIN(N)-SHLQUT(N))*AYSUR/RHO/HCAP/DYSUR/SAREA)
1165 T(JM,2)=T(JM,1)+DELTJM
      FLUXOT=SHLQUT(N)
      IF(V(2,1)) 1160,1167,1167
1167 DELT1=DT*(1.0-BETA)*SHTIN(N)*EXP(-XNUE*(YSUR-EL(1)-DY/2.0))*
      1*(A(2)+A(1))/2.0)/RHO/HCAP
      2*(U(1,1)+B(LJ)*DY/2.0)*TS-T(1,1))
      3*DD(1)*T(2,1)-T(1,1))*A(2)+A(1))/2.0)/DY)/A(1)/DY*2.0
      GO TO 1168
1166 DELT1=DT*(1.0-BETA)*SHTIN(N)*EXP(-XNUE*(YSUR-EL(1)-DY/2.0))*
      1*(A(2)+A(1))/2.0)/RHO/HCAP
      2*(U(1,1)+B(LJ)*DY/2.0)*TS-T(1,1))-V(2,1)*A(2)+A(1))/2.0
      2*(T(2,1)-T(1,1))
      3*DD(1)*T(2,1)-T(1,1))*A(2)+A(1))/2.0)/DY)/A(1)/DY*2.0
1168 T(1,2)=T(1,1)+DELT1
      DO 1118 J=1,JM
1118 T(J,1)=T(J,2)
      IF (ARST(JM,2))-100.0) 60,57,57
      57 TSTOP=ET
      GO TO 80
      60 IF (T(JM,2)+0.01-T(JM-1,2)) 63,779,779
      63 CONTINUE
      CALL CNMIX(N)
      CALL CNMIX(N)
      779 CONTINUE
      CALL DTFCUN(N)
      79 CONTINUE
      DT=DTT
      DO 78 I=1,NOUT
        I1=I
        CALL TOUT(HEATOT,FLUXOT)
        TOUTC(I)=HEATOT/FLUXOT
      78 CONTINUE
      E1=A(1)*DY/2.0*T(1,1)
      JMM=JM-1
      DO 111 J=2,JMM
        E1=E1+A(J)*DY*T(J,1)
        E1=E1+PHO*HCAP
        E2=F2*SHTIN(N)*AYSUR*DT*QIN(N)*DT*TIN(N)*RHO*HCAP
        E3=E3+FLUXOT*AYSUR*DT
      DO 112 I=1,NOUT
        F3=E3+QOUTEN(I)*DT*TOUTC(I)*RHO*HCAP
        ENRAT=(E1-F0)/(E2-E3)
        TENRAT=(F1+E3)/(E2+E3)
        TF(N-NPR) 100,100,80
      80 NPR = NPR+NTSPRI
        WRITE (6,912) ET,SURMES,TIN(N)
        WRITE (6,913) N,YSUR,TAP
        WRITE (6,914) JM,EL(J),PST
        FN=SHTIN(N)
        WRITE (6,915) JIN,EVAP,FN
        WRITE (6,925) DMIX,AR,WINDY
        WRITE (6,916) FLUXOT,RAD,QIN(N)
        F=2.0*HAFDEL
        WRITE (6,918) EPSIL,F,SIGMAO
        DO 88 I=1,NOUT
          FN=COUT(N,I)
      88 WRITE (6,917) ELOUT(I),FN,TOUTC(I)
        WRITE (6,926) ENRAT,E1,E2,E3
        GO TO (89,96), KNIX
      86 WRITE (6,924) TP,TS,TENRAT
      89 WRITE (6,920)
        DO 90 I=1,10
          90 WRITE (6,921) (J,EL(J),T(J,1),J=I,JM,10)
          IF(JM=60) 100,100,91
          91 WRITE (6,920)
          IF(JM=70) 92,93,93
          92 LL=JM
          GO TO 94
          93 LL=70
          94 DO 95 I=61,LL
            95 WRITE (6,921) (J,EL(J),T(J,1),J=I,JM,10)
          100 IF(NTSPRI-NIX1) 1709,1710,1709
          1710 WRITE (6,927) ET
          WRITE (6,928)
          DO 3000 I=1,10
            3000 WRITE (6,921) (J,EL(J),CC(1,J,2), J=I,JP,10)
            TF(JM=60) 222,222,223
            223 IF(JM=60) 3001,3002,3002
          3001 LL=JM
          GO TO 3005
          3002 LL=70
          3005 WRITE (6,928)
          DO 3006 I=61,LL
            3006 WRITE (6,921) (J,EL(J),CC(1,J,2), J=I,JP,10)
            222 WRITE (6,929) COUT(I,N)
          NDOI=0
          1709 IF (ET-TSTOP) 20,1,1
          1 CONTINUE
          901 FOPMAT (1615)
          902 FOPMAT (*F10.5)

```

```

903 FORMAT (3F12.2)
904 FORMAT (1 NUMBER OF SURFACE ELEMENTS*,I3,I3X,SURFACE ELEVATION*,
1F7.2,I3X,DENSITY*,E12.5)
905 FORMAT (1 OUTLET LEVEL*,I3, 26X,OUTLET ELEVATION*,F6.2)
906 FORMAT (1 NY*,F6.2,33X,BOTTOM ELEVATION*,F6.2,I3X,KMUE*,F6.3)
907 FORMAT (1 NY*,F6.2,33X,INITIAL TEMPERATURE*,F6.2,I3X,BETA*,
1F5.2)
908 FORMAT(4X,'INFLOW STD. DEV.=',F6.2,20X,'HEAT CAPACITY=',F6.5)
909 FORMAT (1 STOP AT TIME*,F7.2,22X,OUTFLOW SPREAD CONST.**,F5.2)
910 FORMAT (1 EVAPORATION CONSTANT*,E11.4,10X,CONST IN EQN FOR OUTF
LOW WIDTH*,F10.5,2X,KMIX*,I2)
911 FORMAT (1 JEUP *,I5)
912 FORMAT (1 ELAPSED TIME*,F7.2,22X,ACTUAL SURFACE ELEVATION*,
1F7.2,I3X,'INFLOW TEMPERATURE=',F6.2)
913 FORMAT (1 NO. OF TIME STEPS*,I4,20X,'SURFACE ELEVATION USED*,
1F9.2,I3X,'AIR TEMPERATURE=',F6.2)
914 FORMAT (1 NO. OF SURFACE ELEMENTS*,I3,I3X,'ELEVATION OF INFLOW*',
1F7.2,I3X,'RELATIVE HUMIDITY*',F5.2)
915 FORMAT (1 LEVEL OF INFLOW*,I3,23X,'EVAPORATION FLUX*',E12.5,I4X,
1'INSULATION FLUX*',E12.5)
916 FORMAT (1 HEAT LOSS FLUX*,E12.5,15X,'RADIATION FLUX*',E12.5,
1I6X,'INFLOW RATE*',F11.1)
917 FORMAT (1 OUTLET ELEVATION*,F10.5,I4X,' OUTFLOW RATE*',F10.1,I9X,
1' OUTFLOW TEMPERATURE*',F6.2,'C')
918 FORMAT (1 PSYLOM*,E11.4,23X,'WITHDRAWAL THICKNESS*,F7.2,15X,
1'OUTFLOW STD. DEV.**,F6.2)
920 FORMAT (/71' J ELEV TEMP(C) ')
921 FORMAT (7I13,F6.1,F6.2,3X1)
923 FORMAT (1 NO. OF ELEMENTS IN MIXED LAYER*,I3,8X,'MIXING COEFFICIE
NT**',F5.2)
924 FORMAT (1 TEMP OF MIXING LAYER*,F6.2,15X,'MIXED INFLOW TEMP*',
1F6.2,I9X,'TOTAL ENERGY RATIO**',F9.5)
925 FORMAT (1 MIXING DEPTH**,F5.2,24X,'ATMOSPHERIC RADIATION*',E12.5,
1'9X,'WIND SPEED**',F5.2)
926 FORMAT (1 ENERGY RATIO**,F7.3, 5X,'ENERGY STORED**',E12.5, 5X,'ENERG
Y INFLOW**',E12.5, 3X,'ENERGY OUTFLOW**',E12.5)
927 FORMAT(1 ELAPSED TIME *,F10.5)
928 FORMAT (/71' J ELEV DOPPM) *)
929 FORMAT (/71' DO IN OUTFLOW *,F10.5)
STOP
END
FUNCTION SHTININ)
COMMON T(102,2),EL(102),XL(102),A(102),TI(366),TA(366),SIGH(366)
COMMON FEE(366),WIND(366),DDI(366),QI(366),QOI(366,5),NPR
COMMON UOMAX(5),UIMAX(1),DTTI,DTTA,DTSIGN,DTFEE,DTWIND,DTDD,DTQI
COMMON DTQD,JM,JOUT,JIN,YSUR,YOUT,DT,DY
COMMON TSTOP,EVPCON,STDDV,SIGMA1,SIGMA2
COMMON EVAP,RAO,TAIR,PSI,DTBDY,HAFDEL,EPSIL,GJ
COMMON V(102,1),VI(102,1),DTT,YBOT,NN,BETA,CONST
COMMON XMIX,C,PHO,HCAP,KMIX,JMIX,KDMIX,QMIX,DATRAD,ATRAD(366)
COMMON AR,WINDY,B(102),S(102),EX(102),EXO(102),UO(102,1)
COMMON QIN(401),TINI(401),QMIX(102),MIR,KDMIX,EXI(102),OXI(102),MM
COMMON DIM(366),CC(20,102,2),CCC(20,366),COUT(20,366)
COMMON NOUT,LOUT(5),ELOUT(5),TOUT(5),UOT(102,5)
COMMON SARFA,SURF(366),EO,E1,E2,E3,ET
COMMON DTDD,DTBDY,DT(366),BDD(366),DYSUR,AYSUR
COMMON XN1,XN2,NLEVE(366),JEUP,ITI,NW
DT=DTT*FLOAT(N)
R=ET/DTFEE
L=R
SHTIN=FEE(L)
RETURN
END
SUBROUTINE FLOWPT(N)
COMMON T(102,2),EL(102),XL(102),A(102),TI(366),TA(366),SIGH(366)
COMMON FEE(366),WIND(366),DDI(366),QI(366),QOI(366,5),NPR
COMMON UOMAX(5),UIMAX(1),DTTI,DTTA,DTSIGN,DTFEE,DTWIND,DTDD,DTQI
COMMON DTQD,JM,JOUT,JIN,YSUR,YOUT,DT,DY
COMMON TSTOP,EVPCON,STDDV,SIGMA1,SIGMA2
COMMON EVAP,RAO,TAIR,PSI,DTBDY,HAFDEL,EPSIL,GJ
COMMON V(102,1),VI(102,1),DTT,YBOT,NN,BETA,CONST
COMMON XMIX,C,PHO,HCAP,KMIX,JMIX,KDMIX,QMIX,DATRAD,ATRAD(366)
COMMON AR,WINDY,B(102),S(102),EX(102),EXO(102),UO(102,1)
COMMON QIN(401),TINI(401),QMIX(102),MIR,KDMIX,EXI(102),OXI(102),MM
COMMON DIM(366),CC(20,102,2),CCC(20,366),COUT(20,366)
COMMON NOUT,LOUT(5),ELOUT(5),TOUT(5),UOT(102,5)
COMMON SARFA,SURF(366),EO,E1,E2,E3,ET
COMMON DTDD,DTBDY,DT(366),BDD(366),DYSUR,AYSUR
COMMON XN1,XN2,NLEVE(366),JEUP,ITI,NW
DI 1 I=1,JM
S(1)=(DY*FLOAT(I-1))*2
ARGI=S(1)/2.0/SIGMA1/SIGMA1
IF(ARGI=20.014,4,5
4 EX(I)=EXP(-ARGI)
GO TO 1
5 EX(I)=0.0
1 CONTINUE
DO 2 J=1,JM
IT=ABS(J-JIN)+1
2 EXI(J)=EX(11)
VOLIN=EXI(1)*B(1)*DY/2.0*EXI(JM)*B(JM)*DYSUR
JMH=JM-1
DO 3 J=2,JMH
3 VOLIN=VOLIN+EXI(J)*B(J)*DY
UIMAX(1)=QIN(1)/VOLIN
GO TO (8,7),KMIX
7 UIMAX(1)=UIMAX(1)*(1.0*XMIXC)
8 DO 6 J=1,JM
6 UT(J,1)=UIMAX(1)*EXI(J)
DO 10 LI=1,NOUT
JOUT=LOUT(LI)
DTBDY = (T(JOUT+1,1)-T(JOUT-1,1))/2.0/DY
IF(DTBDY=0.010) 11,11,15
11 JOUT1=JOUT+2
DO 12 J=JOUT1,JMH
IF((T(J+1,1)-T(J,1))/DY-.05) 12,13,13
12 CONTINUE
SIGMA2=100.0*DY
GJ TO 19
13 HAFDEL=FLOAT(J-JOUT)*DY
SIGMA2=HAFDEL/STDDV
19 JOUT2=JOUT-2
DO 21 I=1,JOUT2
J=JOUT2+2-I
IF((T(I,1)-T(I-1,1))/DY-.05) 21,21,22
21 CONTINUE
GO TO 14
22 HAFDL=FLOAT(J-JOUT)*DY
SIGMA1=HAFDL/STDDV
IF(SIGMA1.LT.SIGMA2) SIGMA2=SIGMA1
GO TO 14
15 EPSIL = 2.0*(T(JOUT,1)-4.0)/(151000.0-(T(JOUT,1)-4.0)**2)*DTBDY
QPOW=QOUI(N,LI)/B(JOUT)
HAFDEL = CONST*SQRT(QPOW)/EPSIL**0.25
SIGMA2 = HAFDEL/STDDV
IF(SIGMA2) 20,20,14
20 SIGMA2=1.0
14 CONTINUE
DO 100 I=1,JM
S(1)=(DY*FLOAT(I-1))*2
ARGO=S(1)/2.0/SIGMA2/SIGMA2
IF(ARGO=20.0) 104,105,105

```

```

104 UX(1)=EXP(-ARGO)
GO TO 100
105 UX(1)=C-2
100 CONTINUE
DO 110 J=1,JM
IQ=ABS(J-JOUT)+1
110 EXO(J)=O*(10)
VOLOUT=EXO(1)*B(1)*DY/2.0+EXO(JM)*B(JM)*DYSUR
JMM=JM-1
DO 120 J=2,JMM
VOLOUT=VOLOUT+EXO(J)*B(J)*DY
UQMAX(LT)=QOUT(LT)/VOLOUT
DO 130 J=1,JM
130 UO(J,LT)=UQMAX(LT)*EXO(J)
10 CONTINUE
DO 30 J=1,JM
GO TO (31,32),KMX
32 IF(J-JMIXB) 31,33,33
33 QMIX(J)=QIN(N)*QMIXC/(KDMIX+1)
UO(J,1)=QMIX(J)/B(J)/DY
IF(J,EO,JM) UO(JM,1)=UO(J,1)*DY/DYSUR
GO TO 36
31 UO(J,1)=0.0
DO 35 LT=1,NOUT
35 UO(J,1)=UO(J,1)+UO(J,LT)
36 CONTINUE
V(1,1)=0.0
V(2,1)=UO(1,1)-UO(1,1)*B(1)*DY/(A(1)+A(2))
JMK=JM+1
DO 500 J=3,JMK
V(J,1)=(V(J-1,1)*A(J-2)+A(J-1))/2.0+(UO(J-1,1)-UO(J-1,1))*B(J-1)
1*DY/(A(J)+A(J-1))*2.0
500 CONTINUE
RETURN
END
SUBROUTINE EMOHIN(N)
COMMON T(102,2),EL(102),XL(102),A(102),TI(366),TA(366),SIGH(366)
COMMON FEE(366),INDI(366),DDI(366),QI(366),QOI(366),SI,NPR
COMMON UQMAX(5),UIMAX(1),DTTI,DTTA,DT SIGH,DTFEE,DTWIND,DTDD,DTQI
COMMON DTQD,JM,JOUT,JIN,YSUR,YOUT,DT,DY
COMMON TSTOP,EVPCDN,STDDV,SIGMAI,SIGMAD
COMMON EVAP,RAD,TAIR,PSI,DTBDY,HAFDEL,EPSTL,GJ
COMMON V(102,1),UI(102,1),DTT,YBOT,NN,BETA,CONST
COMMON XMIXC,RHO,HGAP,KMIX,JMIXB,KDMI,X,QMIX,DATRAD,ATRAD(366)
COMMON AP,WINDY,B(102),SI(102),EX(102),EXO(102),UO(102,1)
COMMON QIN(460),TIN(460),QMIK(102),MIXH,DMIX,EXI(102),OX(102),MM
COMMON DIM(366),CC(20,102,2),CC(20,366),COUT(20,366)
COMMON NOUT,LOUT(5),ELOUT(5),TOUTC(5),UOT(102,5)
COMMON SAFP,A,SURF(366),EO,E1,E2,E3,ET
COMMON DTDD,DTBD,DDI(366),BDD(366),DYSUR,AYSUR
COMMON XK1,XK2,NLFEV(366),JEUP,TII,NM
XO=QIN(N)*(1.0+XMIXC)
IF(XO,EO,0.0) GO TO 18002
JMXB=JM-KDMI
JMM=JM-1
NM=2
YQ=QMIX(JM)*CC(1,JM,1)
YQO=QMIX(JM)*CC(2,JM,1)
DO 17000 J=JMXB,JMM
YQ=YQ+QMIX(J)*CC(1,J,1)
17000 YQO=YQO+CC(2,J,1)*QMIX(J)
CC(1,N)=YQ/XO
CC(2,N)=YQO/XO
CC(1,N)=CC(1,N)+QOIN(N)*DDO(N)/XO
CC(2,N)=CC(2,N)+QOIN(N)*DDO(N)/XO
18002 RETURN
END
SUBROUTINE CNMIXH(N)
COMMON T(102,2),EL(102),XL(102),A(102),TI(366),TA(366),SIGH(366)
COMMON FEE(366),INDI(366),DDI(366),QI(366),QOI(366),SI,NPR
COMMON UQMAX(5),UIMAX(1),DTTI,DTTA,DT SIGH,DTFEE,DTWIND,DTDD,DTQI
COMMON DTQD,JM,JOUT,JIN,YSUR,YOUT,DT,DY
COMMON TSTOP,EVPCDN,STDDV,SIGMAI,SIGMAD
COMMON EVAP,RAD,TAIR,PSI,DTBDY,HAFDEL,EPSTL,GJ
COMMON V(102,1),UI(102,1),DTT,YBOT,NN,BETA,CONST
COMMON XMIXC,RHO,HGAP,KMIX,JMIXB,KDMI,X,QMIX,DATRAD,ATRAD(366)
COMMON AP,WINDY,B(102),SI(102),EX(102),EXO(102),UO(102,1)
COMMON QIN(460),TIN(460),QMIK(102),MIXH,DMIX,EXI(102),OX(102),MM
COMMON DIM(366),CC(20,102,2),CC(20,366),COUT(20,366)
COMMON NOUT,LOUT(5),ELOUT(5),TOUTC(5),UOT(102,5)
COMMON SAFP,A,SURF(366),EO,E1,E2,E3,ET
COMMON DTDD,DTBD,DDI(366),BDD(366),DYSUR,AYSUR
COMMON XK1,XK2,NLFEV(366),JEUP,TII,NM
AV1=0.0
AV2=0.0
JMM=JM-1
DO 9 I=1,JMM
JJ=J-1
JJ=J-1
IF(T(J,1)-T(JJ,1)) 6,7,7
6 CONTINUE
IF(I=2) 8,9
8 T(2,1)=(T(2,1)+A(2)+T(1,1)*A(1))/2.0+(A(2)+A(1))/2.0
T(1,1)=T(2,1)
GO TO 7
9 DO 10 K=1,JJ
KJ=J+1-K
KJJ=KJ-1
IF(JM-KJ) 2,2,3
2 AREA=(AYSUR+(A(JM)+A(JM-1))/2.0)/2.0*DYSUR/DY
GO TO 4
3 AREA=A(KJ)
4 AV1=AV1+T(KJ,1)*AREA
AV2=AV2+APFA
TAV=AV1/AV2
IF(TAV-(KJJ,1)) 10,20,20
10 CONTINUE
20 IF(J,EO,JM) MIXH=K
DMIXH(MIXH-1)*DY/DY/2.0
DO 30 L=K,J
30 T(L,1)=TAV
7 AV1=0.0
AV2=0.0
5 CONTINUE
RETURN
END
SUBROUTINE DOFMIN(N)
COMMON T(102,2),EL(102),XL(102),A(102),TI(366),TA(366),SIGH(366)
COMMON FEE(366),INDI(366),DDI(366),QI(366),QOI(366),SI,NPR
COMMON UQMAX(5),UIMAX(1),DTTI,DTTA,DT SIGH,DTFEE,DTWIND,DTDD,DTQI
COMMON DTQD,JM,JOUT,JIN,YSUR,YOUT,DT,DY
COMMON TSTOP,EVPCDN,STDDV,SIGMAI,SIGMAD
COMMON EVAP,RAD,TAIR,PSI,DTBDY,HAFDEL,EPSTL,GJ
COMMON V(102,1),UI(102,1),DTT,YBOT,NN,BETA,CONST
COMMON XMIXC,RHO,HGAP,KMIX,JMIXB,KDMI,X,QMIX,DATRAD,ATRAD(366)
COMMON AP,WINDY,B(102),SI(102),EX(102),EXO(102),UO(102,1)
COMMON QIN(460),TIN(460),QMIK(102),MIXH,DMIX,EXI(102),OX(102),MM
COMMON DIM(366),CC(20,102,2),CC(20,366),COUT(20,366)
COMMON NOUT,LOUT(5),ELOUT(5),TOUTC(5),UOT(102,5)
COMMON SAFP,A,SURF(366),EO,E1,E2,E3,ET
COMMON DTDD,DTBD,DDI(366),BDD(366),DYSUR,AYSUR
COMMON XK1,XK2,NLFEV(366),JEUP,TII,NM

```

```

J4M=JM-1
MM=2
DO 53 M=1,MM
DO 51 I=2,35
IF(I=JUMP) 7211,7211,7212
7212 CONST1=0.0
CONST2=0.0
GO TO 7213
7211 IF(M=1) 736,736,737
736 CONST1=KK1
CONST2=KK2
GO TO 735
737 CONST1=KK1
CONST2=0.0
735 CONTINUE
7213 CONTINUE
AR1=(A(I)+A(I+1))/2.0
AR2=(A(I)+A(I-1))/2.0
IF(V(I,1)) 6,6,7
6 IF(V(I+1,1)) 20,20,21
20 CC(M,1,2)=(CC(M,1,1)*A(I)+DY*(V(I,1)*CC(M,1,1)*AR12-V(I+1,1)*CC(M,
1,1)+1)*AR1+(U(I,1)*CC(M,N)-U(I,1)*CC(M,1,1))*B(I)*DY)/DT/A(I)
2/DY
3-CONST1*CC(2,1,1)*DT
1+(DIM(1)*(CC(M,1+1,1)-CC(M,1,1))/DY*AR1-(CC(M,1,1)-CC(M,1-1,1))/
DY*AR2)/DT/A(I)/DY
GO TO 5
21 CC(M,1,2)=(CC(M,1,1)*A(I)+DY*(V(I,1)*CC(M,1,1)*AR12-V(I+1,1)*CC(M,
1,1)+1)*AR1+(U(I,1)*CC(M,N)-U(I,1)*CC(M,1,1))*B(I)*DY)/DT/A(I)
2/DY
3-CONST1*CC(2,1,1)*DT
1+(DIM(1)*(CC(M,1+1,1)-CC(M,1,1))/DY*AR1-(CC(M,1,1)-CC(M,1-1,1))/
DY*AR2)/DT/A(I)/DY
GO TO 5
7 IF(V(I+1,1)) 22,22,23
23 CC(M,1,2)=(CC(M,1,1)*A(I)+DY*(V(I,1)*CC(M,1,1)*AR12-V(I+1,1)*CC(
M,1,1)+1)*AR1+(U(I,1)*CC(M,N)-U(I,1)*CC(M,1,1))*B(I)*DY)/DT/A(I)
2/DY
3-CONST1*CC(2,1,1)*DT
1+(DIM(1)*(CC(M,1+1,1)-CC(M,1,1))/DY*AR1-(CC(M,1,1)-CC(M,1-1,1))/
DY*AR2)/DT/A(I)/DY
GO TO 5
22 CC(M,1,2)=(CC(M,1,1)*A(I)+DY*(V(I,1)*CC(M,1,1)*AR12-V(I+1,1)*CC(
M,1,1)+1)*AR1+(U(I,1)*CC(M,N)-U(I,1)*CC(M,1,1))*B(I)*DY)/DT/A(
21)/DY
3-CONST1*CC(2,1,1)*DT
1+(DIM(1)*(CC(M,1+1,1)-CC(M,1,1))/DY*AR1-(CC(M,1,1)-CC(M,1-1,1))/
DY*AR2)/DT/A(I)/DY
5 IF(CC(M,1,2)=0.1E-30) 50,50,51
50 CC(M,1,2)=0.0
51 CONTINUE
DO 100 I=36,JMM
IF(I=JUMP) 110,110,120
120 CONST1=0.0
CONST2=0.0
GO TO 130
110 IF(M=1) 140,140,150
140 CONST1=KK1
CONST2=KK2
GO TO 160
150 CONST1=KK1
CONST2=0.0
160 CONTINUE
130 CONTINUE
AR1=(A(I)+A(I+1))/2.0
AR2=(A(I)+A(I-1))/2.0
IF(V(I,1)) 200,200,210
200 IF(V(I+1,1)) 300,300,310
300 CC(M,1,2)=(CC(M,1,1)*A(I)+DY*(V(I,1)*CC(M,1,1)*AR12-V(I+1,1)*CC(M,
1,1)+1)*AR1+(U(I,1)*CC(M,N)-U(I,1)*CC(M,1,1))*B(I)*DY)/DT/A(I)
2/DY
3-CONST1*CC(2,1,1)*DT
1+(DIM(1)*(CC(M,1+1,1)-CC(M,1,1))/DY*AR1-(CC(M,1,1)-CC(M,1-1,1))/
DY*AR2)/DT/A(I)/DY
GO TO 500
310 CC(M,1,2)=(CC(M,1,1)*A(I)+DY*(V(I,1)*CC(M,1,1)*AR12-V(I+1,1)*CC(M,
1,1)+1)*AR1+(U(I,1)*CC(M,N)-U(I,1)*CC(M,1,1))*B(I)*DY)/DT/A(I)
2/DY
3-CONST1*CC(2,1,1)*DT
1+(DIM(1)*(CC(M,1+1,1)-CC(M,1,1))/DY*AR1-(CC(M,1,1)-CC(M,1-1,1))/
DY*AR2)/DT/A(I)/DY
GO TO 500
210 IF(V(I+1,1)) 400,400,410
410 CC(M,1,2)=(CC(M,1,1)*A(I)+DY*(V(I,1)*CC(M,1,1)*AR12-V(I+1,1)*CC(
M,1,1)+1)*AR1+(U(I,1)*CC(M,N)-U(I,1)*CC(M,1,1))*B(I)*DY)/DT/A(I)
2/DY
3-CONST1*CC(2,1,1)*DT
1+(DIM(1)*(CC(M,1+1,1)-CC(M,1,1))/DY*AR1-(CC(M,1,1)-CC(M,1-1,1))/
DY*AR2)/DT/A(I)/DY
GO TO 500
400 CC(M,1,2)=(CC(M,1,1)*A(I)+DY*(V(I,1)*CC(M,1,1)*AR12-V(I+1,1)*CC(
M,1,1)+1)*AR1+(U(I,1)*CC(M,N)-U(I,1)*CC(M,1,1))*B(I)*DY)/DT/A(
21)/DY
3-CONST1*CC(2,1,1)*DT
1+(DIM(1)*(CC(M,1+1,1)-CC(M,1,1))/DY*AR1-(CC(M,1,1)-CC(M,1-1,1))/
DY*AR2)/DT/A(I)/DY
500 IF(CC(M,1,2)=0.1E-30) 600,600,100
600 CC(M,1,2)=0.0
100 CONTINUE
J=JM
DUSA=14.4776-0.3797*(J,1)+0.0043*(T(J,1)**2)
CONST1=0.0
IF(M=1) 95,95,96
95 CONST2=KK2
GO TO 97
96 CONST2=0.0
97 CONTINUE
IF(V(JM,1)) 9,10,10
9 CC(M,JM,2)=(CC(M,JM,1)*SAREA+DYSUR+(V(JM,1)*(CC(M,JM-1,1)-CC(M,JM,
1,1))*A(JM)+A(JM-1,1))/2.0+J(JM,1)*(CC(M,N)-CC(M,JM,1))*B(JM)*DYSUR
2)/DT)/SAREA/DYSUR
3-CONST1*CC(2,JM,1)*DT+CONST2*(DUSA-CC(1,JM,1))*DT
1-(DIM(1)*(CC(M,JM,1)-CC(M,JM-1,1))/DY*(A(JM)+A(JM-1,1))/2.0/SAREA/
DYSUR)*DT
GO TO 11
10 CC(M,JM,2)=(CC(M,JM,1)*SAREA+DYSUR+(U(JM,1)*(CC(M,N)-CC(M,JM,1))
+1)*B(JM)*DYSUR)/DT)/SAREA/DYSUR
3-CONST1*CC(2,JM,1)*DT+CONST2*(DUSA-CC(1,JM,1))*DT
1-(DIM(1)*(CC(M,JM,1)-CC(M,JM-1,1))/DY*(A(JM)+A(JM-1,1))/2.0/SAREA/
DYSUR)*DT
11 CONTINUE
IF(M=1) 547,547,558
547 CONST1=KK1
CONST2=KK2
GO TO 555
558 CONST1=KK1
CONST2=0.0
555 IF(V(2,1)) 12,13,13
13 CC(M,1,2)=(CC(M,1,1)*A(1)+DY/2.0*(U(1,1)*B(1)*DY/2.0*(CC(M,N)-
CC(M,1,1))*DT)/A(1)/DY*2.0
2-CONST1*CC(2,1,1)*DT
1+(DIM(1)*(CC(M,2,1)-CC(M,1,1))*A(2)+A(1))/2.0/DY)/A(1)/DY*2.0)*

```

```

107
GO TO 4
12 CCI(M,1,2)=(CCI(M,1,1)*A(1)*DY/2.0+(U(I,1)*B(1)*DY/2.0*(CCC(M,N)-
CCI(M,1,1))-V(2,1)*(A(2)+A(1))/2.0*(CCI(M,2,1)-CCI(M,1,1))*DT)/A(1)/
ZDY*2.0
2-CCNST)=CC(2,1,1)*DT
1-(DIM(1))*(CCI(M,2,1)-CCI(M,1,1)*(A(2)+A(1))/2.0/DY)/A(1)/DY*2.0)*
107
4 CONTINUE
IF(CCI(M,J,2)-0.1E-30) 54,54,55
54 CCI(M,J,2)=0.0
55 CONTINUE
IF(CCI(M,1,2)-0.1E-30) 52,52,53
52 CCI(M,1,2)=0.0
53 CONTINUE
DD 3547 J=1,JM
DOSA=14.4776-0.3579*(J,1)+0.0043*(T(J,1)**2)
IF(CCI(1,J,2)) 3699,3699,3655
3699 CCI(L,J,2)=0.0
GO TO 3547
3655 IF(CCI(1,J,2)-DOSA) 3547,3547,3548
3548 CCI(1,J,2)=DOSA
3547 CONTINUE
IF(ET-GE-180) GO TO 800
DD 65 J=JEU+JM
DOSA=14.4776-0.3579*(J,1)+0.0043*(T(J,1)**2)
65 CCI(1,J,2)=DOSA
GO TO 850
800 CONTINUE
DD 808 J=JEU+JM
DOSA=14.4776-0.3579*(J,1)+0.0043*(T(J,1)**2)
DOSA=0.8*DOSA
808 CCI(1,J,2)=DOSA
850 RETURN
END
SUBROUTINE CNMIX(MN)
COMMON T(102,2),EL(102),XL(102),A(102),TI(366),TA(366),SIGH(366)
COMMON FEF(366),WIND(366),DD(366),QI(366),QD(366),NPR
COMMON UOMAX(5),UIMAX(1),DTI,DTA,DTSIGH,DTFEE,DTWIND,DTDD,DTQI
COMMON DTQI,JP,JDUT,JIN,YSUR,YOUT,DT,DY
COMMON TSTNP,EVPCON,STDDV,SIGMAI,SIGMAO
COMMON EVAP,RAD,FAIR,PSI,DTBDY,HAFDEL,EPSEL,GJ
COMMON V(102,1),U(102,1),DTT,YROT,MM,BETA,CONST
COMMON XMIX,PHI,HCAP,KMIX,JMIX,KOMIX,QMIX,DATRAD,ATRAD(366)
COMMON AR,WINDY,B(102),S(102),EX(102),EXO(102),UOI(102,1)
COMMON QIN(460),TIN(460),QMIX(102),MIXH,DMIX,EXI(102),OXI(102),MM
COMMON DIM(366),CC(20,102,2),CCC(20,366),COUT(20,366)
COMMON NOUT,LOUT(5),ELOUT(5),TOUT(5),UOT(102,5)
COMMON SARF,A,SUPF(366),EO,E1,E2,E3,ET
COMMON DTUR,DTMIX,DD(366),BDD(366),DYSUR,AYSUR
COMMON XK <2,NLEVE(366),JEU,III,NM
JMIX=JM-0+1
NM=2
DD 1 M=1,MM
XCC=0.0
XA=0.0
JMP=JM-1
DD 2 J=JMIX+JM
XCC=CCI(M,J,2)*A(J)*DY*XCC
2 XA=XA+A(J)*DY
XCC=XCC+CCI(M,J,2)*A(J)*DY/2.0
XA=XA+A(J)*DY/2.0
DD 3 I=JMIX,JM
3 CCI(M,I,2)=XCC/XA
1 CONTINUE
IF(ET-GE-180) GO TO 10
DD 3547 J=JMIX+JM
DOSA=14.4776-0.3579*(J,1)+0.0043*(T(J,1)**2)
IF(CCI(1,J,2)) 3699,3699,3655
3699 CCI(L,J,2)=0.0
GO TO 3547
3655 IF(CCI(1,J,2)-DOSA) 3547,3547,3548
3548 CCI(L,J,2)=DOSA
3547 CONTINUE
GO TO 16
10 DD 11 J=JMIX+JM
DOSA=14.4776-0.3579*(J,1)+0.0043*(T(J,1)**2)
DOSA=0.8*DOSA
IF(CCI(1,J,2)) 12,12,14
12 CCI(1,J,2)=0.0
GO TO 11
14 IF(CCI(1,J,2)-DOSA) 11,11,15
15 CCI(1,J,2)=DOSA
11 CONTINUE
16 RETURN
END
FUNCTION SHROUTIN)
COMMON T(102,2),EL(102),XL(102),A(102),TI(366),TA(366),SIGH(366)
COMMON FEF(366),WIND(366),DD(366),QI(366),QD(366),NPR
COMMON UOMAX(5),UIMAX(1),DTI,DTA,DTSIGH,DTFEE,DTWIND,DTDD,DTQI
COMMON DTQI,JP,JDUT,JIN,YSUR,YOUT,DT,DY
COMMON TSTNP,EVPCON,STDDV,SIGMAI,SIGMAO
COMMON EVAP,RAD,FAIR,PSI,DTBDY,HAFDEL,EPSEL,GJ
COMMON V(102,1),U(102,1),DTT,YROT,MM,BETA,CONST
COMMON XMIX,PHI,HCAP,KMIX,JMIX,KOMIX,QMIX,DATRAD,ATRAD(366)
COMMON AR,WINDY,B(102),S(102),EX(102),EXO(102),UOI(102,1)
COMMON QIN(460),TIN(460),QMIX(102),MIXH,DMIX,EXI(102),OXI(102),MM
COMMON DIM(366),CC(20,102,2),CCC(20,366),COUT(20,366)
COMMON NOUT,LOUT(5),ELOUT(5),TOUT(5),UOT(102,5)
COMMON SARF,A,SUPF(366),EO,E1,E2,E3,ET
COMMON DTUR,DTMIX,DD(366),BDD(366),DYSUR,AYSUR
COMMON XK1,XK2,NLEVE(366),JEU,III,NM
F=ET+H*DATIN)
P=ET/DTTA
L=R
RR=R-FLOAT(L)
TAIR=TA(1)+RR*(TA(L+1)-TA(1))
P=ET/DTSIGH
L=P
RR=R-FLOAT(L)
PSI=SIGH(L)+RR*(SIGH(L+1)-SIGH(L))
TS=T(JP+1)
H=97.3-0.56*TS
ES=0.0418*TS-0.6216*TS+13.0068
EA=PSI*10.0418*TAIR*TAIR-0.6216*TAIR+13.0068
DE=E3-EA
P=ET/DYWIND
L=P
W=WIND(L)+(P-FLOAT(L))*WIND(L+1)-WIND(L)
WINDY=W
P=ET/DAT*AD
L=P
AR=ATRAD(L)+(P-FLOAT(L))*(ATRAD(L+1)-ATRAD(L))
RAD=1.13587E-6*(TS+273.16)**4-AR
CHI=PHI*(H*DE+HCAP*PDE)
FW=0.7338*H*0.185*W
EVAP=CHI*FW*EVPCON
CONDUC=H*EVPCON*269.1*(TS-TAIR)*FW
IF(EVAP) 5,5,6
5 EVAP=0.0
6 EVAP=EVAP+CONDUC
SHROUT=EVAP+RAD

```

```

RETURN
END
SUBROUTINE TOUT(HFATOT, FLOWOT)
COMMON T(102,2), EL(102), XL(102), A(102), TI(366), TA(366), SIGH(366)
COMMON FEE(366), WINDI(366), DD(366), QI(366), QOI(366,5), NPR
COMMON UOJAX(5), UJMAX(1), DTTI, DTTA, DTSIGH, DTFEE, DTWIND, DTDD, DTQI
COMMON DTQD, JM, JOUT, JIN, YSUR, YOUT, DT, DY
COMMON TSTOP, EVPCON, STDEEV, SIGMAI, SIGMAD
COMMON EVAP, P, AD, TAIR, PS I, DTBDY, HAFDEL, EPSIL, GJ
COMMON V(102,1), UI(102,1), DTT, YBOT, NN, BETA, CONST
COMMON XMI XC, RHO, HCAP, KMIX, JMI XB, KDMI X, QMI X, DATRAD, ATRADI(366)
COMMON AR, WINDY, B(102), SI(102), EX(102), EXO(102), UO(102,1)
COMMON QIN(460), TIN(460), QQMI X(102), MIXH, DMI X, EXI(102), DX(102), MM
COMMON DIM(366), CC(20,102,2), CCC(20,366), COUT(20,366)
COMMON NOUT, LOUT(5), ELOUT(5), TOUT(5), UOT(102,5)
COMMON SAREA, SURF(366), EO, E1, E2, E3, ET
COMMON DTDD, DTBDD, DD(366), BDD(366), DYSUR, AYSUR
COMMON XK1, XK2, NLEVE(366), JEUP, ITI, NW
T=TI
HEATOT=(JM,1)*B(JM)*UOT(JM,1)*DYSUR*(1,1)*B(1)*UOT(1,1)*DY/2.0
FLOWOT=B(JM)*UOT(JM,1)*DYSUR*(1,1)*UOT(1,1)*DY/2.0
JMM=JM-1
DO 2 J=2, JMM
HEATOT=HEATOT+UOT(J,1)*B(J)*DY*(J,1)
2 FLOWOT=FLOWOT+UOT(J,1)*B(J)*DY
IF (FLOWOT.EQ.0.0) FLOWOT=1.0
CONTINUE
RETURN
END
SUBROUTINE DTFCOIN(N)
COMMON T(102,2), EL(102), XL(102), A(102), TI(366), TA(366), SIGH(366)
COMMON FEE(366), WINDI(366), DD(366), QI(366), QOI(366,5), NPR
COMMON UOJAX(5), UJMAX(1), DTTI, DTTA, DTSIGH, DTFEE, DTWIND, DTDD, DTQI
COMMON DTQD, JM, JOUT, JIN, YSUR, YOUT, DT, DY
COMMON TSTOP, EVPCON, STDEEV, SIGMAI, SIGMAD
COMMON EVAP, P, AD, TAIR, PS I, DTBDY, HAFDEL, EPSIL, GJ
COMMON V(102,1), UI(102,1), DTT, YBOT, NN, BETA, CONST
COMMON XMI XC, RHO, HCAP, KMIX, JMI XB, KDMI X, QMI X, DATRAD, ATRADI(366)
COMMON AR, WINDY, B(102), SI(102), EX(102), EXO(102), UO(102,1)
COMMON QIN(460), TIN(460), QQMI X(102), MIXH, DMI X, EXI(102), DX(102), MM
COMMON DIM(366), CC(20,102,2), CCC(20,366), COUT(20,366)
COMMON NOUT, LOUT(5), ELOUT(5), TOUT(5), UOT(102,5)
COMMON SAREA, SURF(366), EO, E1, E2, E3, ET
COMMON DTDD, DTBDD, DD(366), BDD(366), DYSUR, AYSUR
COMMON XK1, XK2, NLEVE(366), JEUP, ITI, NW
JMM=JM-1
MM=2
DO 1 M=1, MM
XC=CC(M, JM, 1)*B(JM)*UO(JM,1)*DYSUR+CC(M,1,1)*B(1)*UO(1,1)*DY/2.0
XF=B(JM)*UO(JM,1)*DYSUR*(1,1)*UO(1,1)*DY/2.0
DO 2 J=2, JMM
XC=XC+UO(J,1)*B(J)*DY*CC(M, J, 1)
2 XF=XF+UO(J,1)*B(J)*DY
IF (XF.EQ.0.0) XF=1.0
CONTINUE
COUT(M,N)=XC/XF
1 CONTINUE
DO 16 M=1, MM
DO 15 I=1, JM
15 CC(M,1,1)=CC(M,1,2)
16 CONTINUE
RETURN
END
FUNCTION DDIN(N)
COMMON T(102,2), EL(102), XL(102), A(102), TI(366), TA(366), SIGH(366)
COMMON FEE(366), WINDI(366), DD(366), QI(366), QOI(366,5), NPR
COMMON UOJAX(5), UJMAX(1), DTTI, DTTA, DTSIGH, DTFEE, DTWIND, DTDD, DTQI
COMMON DTQD, JM, JOUT, JIN, YSUR, YOUT, DT, DY
COMMON TSTOP, EVPCON, STDEEV, SIGMAI, SIGMAD
COMMON EVAP, P, AD, TAIR, PS I, DTBDY, HAFDEL, EPSIL, GJ
COMMON V(102,1), UI(102,1), DTT, YBOT, NN, BETA, CONST
COMMON XMI XC, RHO, HCAP, KMIX, JMI XB, KDMI X, QMI X, DATRAD, ATRADI(366)
COMMON AR, WINDY, B(102), SI(102), EX(102), EXO(102), UO(102,1)
COMMON QIN(460), TIN(460), QQMI X(102), MIXH, DMI X, EXI(102), DX(102), MM
COMMON DIM(366), CC(20,102,2), CCC(20,366), COUT(20,366)
COMMON NOUT, LOUT(5), ELOUT(5), TOUT(5), UOT(102,5)
COMMON SAREA, SURF(366), EO, E1, E2, E3, ET
COMMON DTDD, DTBDD, DD(366), BDD(366), DYSUR, AYSUR
COMMON XK1, XK2, NLEVE(366), JEUP, ITI, NW
ET=DTI*FLOAT(N)
R=ET/DTQI
L=R
QOIN=QI(1)
RETURN
END
FUNCTION TTIN(N)
COMMON T(102,2), EL(102), XL(102), A(102), TI(366), TA(366), SIGH(366)
COMMON FEE(366), WINDI(366), DD(366), QI(366), QOI(366,5), NPR
COMMON UOJAX(5), UJMAX(1), DTTI, DTTA, DTSIGH, DTFEE, DTWIND, DTDD, DTQI
COMMON DTQD, JM, JOUT, JIN, YSUR, YOUT, DT, DY
COMMON TSTOP, EVPCON, STDEEV, SIGMAI, SIGMAD
COMMON EVAP, P, AD, TAIR, PS I, DTBDY, HAFDEL, EPSIL, GJ
COMMON V(102,1), UI(102,1), DTT, YBOT, NN, BETA, CONST
COMMON XMI XC, RHO, HCAP, KMIX, JMI XB, KDMI X, QMI X, DATRAD, ATRADI(366)
COMMON AR, WINDY, B(102), SI(102), EX(102), EXO(102), UO(102,1)
COMMON QIN(460), TIN(460), QQMI X(102), MIXH, DMI X, EXI(102), DX(102), MM
COMMON DIM(366), CC(20,102,2), CCC(20,366), COUT(20,366)
COMMON NOUT, LOUT(5), ELOUT(5), TOUT(5), UOT(102,5)
COMMON SAREA, SURF(366), EO, E1, E2, E3, ET
COMMON DTDD, DTBDD, DD(366), BDD(366), DYSUR, AYSUR
COMMON XK1, XK2, NLEVE(366), JEUP, ITI, NW
ET=DTI*FLOAT(N)
R=ET/DTQI
L=R
RR=R-FLOAT(L)
TTIN=TI(L)+RR*(TI(L+1)+TI(L))
RETURN
END
FUNCTION DDOIN(N)
COMMON T(102,2), EL(102), XL(102), A(102), TI(366), TA(366), SIGH(366)
COMMON FEE(366), WINDI(366), DD(366), QI(366), QOI(366,5), NPR
COMMON UOJAX(5), UJMAX(1), DTTI, DTTA, DTSIGH, DTFEE, DTWIND, DTDD, DTQI
COMMON DTQD, JM, JOUT, JIN, YSUR, YOUT, DT, DY
COMMON TSTOP, EVPCON, STDEEV, SIGMAI, SIGMAD
COMMON EVAP, P, AD, TAIR, PS I, DTBDY, HAFDEL, EPSIL, GJ
COMMON V(102,1), UI(102,1), DTT, YBOT, NN, BETA, CONST
COMMON XMI XC, RHO, HCAP, KMIX, JMI XB, KDMI X, QMI X, DATRAD, ATRADI(366)
COMMON AR, WINDY, B(102), SI(102), EX(102), EXO(102), UO(102,1)
COMMON QIN(460), TIN(460), QQMI X(102), MIXH, DMI X, EXI(102), DX(102), MM
COMMON DIM(366), CC(20,102,2), CCC(20,366), COUT(20,366)
COMMON NOUT, LOUT(5), ELOUT(5), TOUT(5), UOT(102,5)
COMMON SAREA, SURF(366), EO, E1, E2, E3, ET
COMMON DTDD, DTBDD, DD(366), BDD(366), DYSUR, AYSUR
COMMON XK1, XK2, NLEVE(366), JEUP, ITI, NW
ET=DTI*FLOAT(N)
R=ET/DTQI
L=R
NSOT=NLEVE(N)
DDC=DC(1)
REUPN
END
FUNCTION D900(N)

```











VITA

Prasert Chuaphanich

Candidate for the Degree of

Doctor of Philosophy

Thesis: QUALITY PARAMETER MODELS FOR STRATIFIED IMPOUNDMENTS

Major Field: Civil Engineering

Biographical:

Personal Data: Born in Bangkok, Thailand, August 28, 1946, the son of Mr. and Mrs. Rit Chuaphanich.

Education: Graduated from Assumption School, Bangkok, Thailand, in May, 1965; received the Bachelor of Engineering degree in Civil Engineering from Chulalongkorn University, Bangkok, Thailand, in June, 1969; received the Master of Science degree in Civil Engineering from Oklahoma State University, Stillwater, Oklahoma, in January, 1972; completed requirements for the Doctor of Philosophy degree at Oklahoma State University in May, 1975.

Professional Experience: Design Engineer, Municipal and Public Works Department, Bangkok, Thailand, June, 1969 - June, 1970; Graduate Research Assistant, Oklahoma State University, September, 1972 - May, 1975.

Membership in Professional Societies: Engineering Institute of Thailand under the patronage of His Majesty the King; Registered Professional Engineer, Thailand.

Membership in Honorary Societies: Phi Kappa Phi.